



NOAA Technical Memorandum NMFS-NWFSC-170

<https://doi.org/10.25923/x4ge-hn11>

Ecosystem Status Report of the California Current for 2020–21: A Summary of Ecosystem Indicators Compiled by the California Current Integrated Ecosystem Assessment Team (CCIEA)



September 2021

U.S. DEPARTMENT OF COMMERCE

National Oceanic and Atmospheric Administration
National Marine Fisheries Service
Northwest Fisheries Science Center

NOAA Technical Memorandum Series NMFS-NWFSC

The Northwest Fisheries Science Center of NOAA's National Marine Fisheries Service uses the NOAA Technical Memorandum NMFS-NWFSC series to issue scientific and technical publications that have received thorough internal scientific review and editing. Reviews are transparent collegial reviews, not anonymous peer reviews. Documents within this series represent sound professional work and may be referenced in the formal scientific and technical literature.

The Northwest Fisheries Science Center's NOAA Technical Memorandum series continues the NMFS-F/NWC series established in 1970 by the Northwest and Alaska Fisheries Science Center, which subsequently was divided into the Northwest Fisheries Science Center and the Alaska Fisheries Science Center. The latter uses the NOAA Technical Memorandum NMFS-AFSC series.

NOAA Technical Memorandums NMFS-NWFSC are available from the NOAA Institutional Repository, <https://repository.library.noaa.gov>.

Any mention throughout this document of trade names or commercial companies is for identification purposes only and does not imply endorsement by the National Marine Fisheries Service, NOAA.

Cover image: Scripps Institution of Oceanography (SIO) and California Cooperative Oceanic Fisheries Investigations (CalCOFI) team collecting seawater samples from the conductivity–temperature–depth (CTD) rosette during the Summer 2020 CalCOFI cruise aboard the R/V *Sally Ride*. Pictured, from left, are SIO/University of California, San Diego (UCSD) staff K. Vogel, volunteer G. Cawley, and Ph.D. student A. Schulberg. Photograph by A. Klemmedson, SIO/UCSD.

Reference this document as follows:

Harvey, C. J., N. Garfield, G. D. Williams, and N. Tolimieri, editors. 2021. Ecosystem Status Report of the California Current for 2020–21: A Summary of Ecosystem Indicators Compiled by the California Current Integrated Ecosystem Assessment Team (CCIEA). U.S. Department of Commerce, NOAA Technical Memorandum NMFS-NWFSC-170.

Reference a chapter in this document as follows:

Schroeder, I. D., A. Leising, S. Bograd, L. deWitt, N. Garfield, E. L. Hazen, D. Robinson, D. L. Rudnick, M. Jacox, J. Santora, J. Fisher, K. Jacobson, E. Norton, S. Siedlecki, I. Kaplan, C. Greene, and S. Munsch. 2021. Climate and Ocean Drivers. Pages 8–28 *in* C. J. Harvey, N. Garfield, G. D. Williams, and N. Tolimieri, editors. 2021. Ecosystem Status Report of the California Current for 2020–21: A Summary of Ecosystem Indicators Compiled by the California Current Integrated Ecosystem Assessment Team (CCIEA). U.S. Department of Commerce, NOAA Technical Memorandum NMFS-NWFSC-170.

<https://doi.org/10.25923/x4ge-hn11>



NOAA
FISHERIES

Ecosystem Status Report of the California Current for 2020–21: A Summary of Ecosystem Indicators Compiled by the California Current Integrated Ecosystem Assessment Team (CCIEA)

Edited by Chris J. Harvey,¹ Newell (Toby) Garfield,² Gregory D. Williams,^{1,3} and Nicholas Tolimieri¹

<https://doi.org/10.25923/x4ge-hn11>

September 2021

¹Conservation Biology Division
Northwest Fisheries Science Center
2725 Montlake Boulevard East
Seattle, Washington 98112

²Environmental Research Division
Southwest Fisheries Science Center
8901 La Jolla Shores Drive
La Jolla, California 92037

³Pacific States Marine Fisheries Commission
205 Southeast Spokane Street, Suite 100
Portland, Oregon 97202

U.S. DEPARTMENT OF COMMERCE

National Oceanic and Atmospheric Administration
National Marine Fisheries Service
Northwest Fisheries Science Center

Contributors

California Current Integrated Ecosystem Assessment (CCIEA) Team

Corresponding authors

Dr. Chris J. Harvey	chris.harvey@noaa.gov
Dr. Newell (Toby) Garfield	toby.garfield@noaa.gov
Mr. Gregory D. Williams	greg.williams@noaa.gov
Dr. Nicholas Tolimieri	nick.tolimieri@noaa.gov

All contributors, by affiliation

NOAA Fisheries

Northwest Fisheries Science Center (NWFSC)

Dr. Chris J. Harvey, Mr. Kelly Andrews, Ms. Katie Barnas, Dr. Brian Burke, Dr. Jason Cope, Dr. Thomas P. Good, Dr. Correigh Greene, Dr. Marie Guldin, Dr. Daniel Holland, Dr. Mary Hunsicker, Dr. Kym Jacobson, Dr. Isaac Kaplan, Ms. Su Kim, Dr. Jerry Leonard, Dr. Stephanie Moore, Dr. Stuart Munsch, Dr. Karma Norman, Dr. Jameal Samhour, Dr. Kayleigh A. Somers, Ms. Erin Steiner, Dr. Nicholas Tolimieri, Ms. Ashley Vizek, and Mr. Curt Whitmire

Southwest Fisheries Science Center (SWFSC)

Dr. Newell (Toby) Garfield, Dr. Eric Bjorkstedt, Dr. Steven Bograd, Ms. Lynn deWitt, Dr. John Field, Dr. Elliott L. Hazen, Dr. Michael Jacox, Dr. Andrew Leising, Dr. Nate Mantua, Mr. Keith Sakuma, Dr. Jarrod Santora, Dr. Cameron Speir, Dr. Andrew Thompson, Dr. Brian Wells, and Dr. Thomas Williams

Alaska Fisheries Science Center (AFSC)

Dr. Stephen Kasperski, Ms. Elizabeth Jaime, and Dr. Sharon Melin

West Coast Region (WCR)

Mr. Dan Lawson and Ms. Lauren Saez

Pacific States Marine Fisheries Commission

Ms. Amanda Phillips, Mr. Gregory D. Williams, and Ms. Margaret Williams

Humboldt State University

Ms. Roxanne Robertson

Oregon State University

Ms. Jennifer Fisher, Ms. Cheryl Morgan, Dr. Rachael Orben, Ms. Jessica Porquez, and Ms. Samantha Zeman

Scripps Institution of Oceanography

Dr. Clarissa Anderson, Dr. Melissa Carter, Dr. Daniel L. Rudnick, and Dr. Eva Ternon

University of California, Santa Cruz

Dr. Barbara Muhling, Dr. Dale Robinson, and Dr. Isaac D. Schroeder

University of Connecticut

Dr. Samantha Siedlecki

University of Washington

Ms. Mary Fisher and Dr. Emily Norton

Wellesley College

Dr. Becca Selden

Beach Watch (Greater Farallones Association)

Ms. Jan Roletto and Ms. Kirsten Lindquist

Oikonos Ecosystem Knowledge

Ms. Jessie Beck and Ms. Rozy Bathrick

Point Blue Conservation Science

Dr. Jaime Jahncke, Dr. Mike Johns, and Mr. Pete Warzybok

Wildlands Conservation Science

Mr. Morgan Ball

United States Geological Survey

Ms. Cheryl Horton

California Department of Fish and Wildlife

Ms. Christy Juhasz

California Department of Public Health

Ms. Christina Grant, Mr. Duy Trong, and Ms. Vanessa Zubkousky-White

California Office of Environmental Health Hazard Assessment

Dr. Beckye Stanton

Oregon Department of Agriculture

Mr. Alex Manderson

Oregon Department of Fish and Wildlife

Dr. Caren Braby and Mr. Matthew Hunter

Washington Department of Health

Ms. Tracie Barry and Mr. Jerry Borchert

Washington Department of Fish and Wildlife

Mr. Dan Ayres and Mr. Zachary Forster

Contents

List of Contributors.....	i
List of Figures.....	v
List of Tables.....	ix
Executive Summary.....	x
Infographic.....	xiii
1 Introduction.....	1
1.1 Ecosystem-Based Fisheries Management and Integrated Ecosystem Assessment.....	1
1.2 Notes on Interpreting Time-Series Figures.....	4
1.3 Sampling Locations.....	5
2 Climate and Ocean Drivers.....	8
2.1 Basin-Scale Indicators.....	8
2.2 Regional Upwelling Indices and Coastal Habitat Compression.....	15
2.3 Hypoxia and Ocean Acidification.....	18
3 Lower Trophic Levels and Forage.....	29
3.1 Northern and Southern Copepod Biomass Anomaly off of Newport.....	30
3.2 Krill Size off of Trinidad Head.....	30
3.3 Harmful Algal Blooms and Red Tide.....	31
3.4 Regional Forage Availability.....	33
3.4.1 Northern CCE.....	34
3.4.2 Central CCE.....	35
3.4.3 Southern CCE.....	37
3.4.4 Pyrosomes.....	39
4 Fishes.....	40
4.1 Salmon.....	40
4.1.1 Early marine abundance of juvenile salmon.....	40
4.1.2 Abundance of spawning adult salmon.....	41
4.1.3 “Stoplight charts” of salmon-related ecosystem indicator suites.....	44
4.2 Groundfish Stock Abundance, Community Structure, and Distribution.....	52
4.3 Highly Migratory Species.....	54

5	Marine Mammals and Seabirds	57
5.1	Marine Mammals	57
5.1.1	Sea lion production	57
5.1.2	Whale entanglement.....	59
5.2	Seabirds.....	60
5.2.1	Seabird population productivity	60
5.2.2	Seabird diets	62
5.2.3	Seabird mortalities.....	64
5.2.4	Seabird at-sea densities	66
6	Human Activities.....	67
6.1	Coastwide Landings and Revenue by Major Fisheries.....	67
6.2	Bottom Trawl Contact with Seafloor	70
6.3	Aquaculture and Seafood Consumption.....	73
6.4	Nonfisheries Human Activities	74
6.4.1	Commercial shipping.....	74
6.4.2	Oil and gas activity.....	75
6.4.3	Nutrient loading	76
7	Human Wellbeing.....	77
7.1	Community Social Vulnerability	77
7.2	Fishing Revenue Diversification.....	79
7.3	Revenue Consolidation.....	81
7.4	Fishery Participation Networks.....	85
8	Synthesis.....	90
	List of References.....	92

Figures

Figure ES-1. Visual summary of the status and trends of key indicators in the California Current social–ecological system during 2020.....	xiii
Figure 1-1. Loop diagram of the five progressive steps in iterations of the integrated ecosystem assessment process.....	2
Figure 1-2. Conceptual model of the California Current social–ecological system.....	3
Figure 1-3. (a) Sample time-series plot, with indicator data relative to the long-term mean and ± 1.0 SD of the full time series.....	5
Figure 1-4. Map of the CCE and sampling areas.....	6
Figure 2-1. Monthly values of the ONI, PDO, and NPGO from 1981–2021.....	9
Figure 2-2. SSTa (2020), 5-year means (2016–20), and 5-year trends (2016–20) in winter and summer	11
Figure 2-3. Time–depth temperature anomalies for hydrographic stations NH25 (Jul 1997–Oct 2020) and CalCOFI 93.30 (Jan 1997–Jul 2020).....	12
Figure 2-4. Standardized SSTa across the NE Pacific: a) Jul 2020, b) Sep 2020, c) Nov 2020, and d) Jan 2021.....	13
Figure 2-5. Area of North Pacific warm SST anomalies, 1982–2021.....	13
Figure 2-6. Early fall progression of the large marine heatwaves in 2019 and 2020.....	14
Figure 2-7. Daily 2020 estimates of vertical transport of water and nitrate from 1 Jan–31 Dec, relative to 1988–2019 climatology ± 1.0 SD, at lats 33°N, 39°N, and 45°N.....	16
Figure 2-8. Mean winter and spring Habitat Compression Index, by region, 1980–2020.....	17
Figure 2-9. Dissolved oxygen through 2020 at: 50-m depth, Station NH05, 5 nmi off Newport, and 150-m depth, CalCOFI Station 93.30, <50 km off San Diego.....	18
Figure 2-10. Dissolved oxygen observations during the summer 2020 CalCOFI survey of the Southern CCE at 50 m, 150 m, and at the bottom of the hydrographic cast.....	19
Figure 2-11. Vertical profiles of aragonite saturation at Stations NH05 and NH25 off Newport, 1999–2020.....	20
Figure 2-12. J-SCOPE forecasts of bottom DO, May–Sep 2021, averaged over all three ensemble members.....	21
Figure 2-13. J-SCOPE forecasts of bottom aragonite saturation state, Jan–Aug 2021, averaged over all three ensemble members.....	22
Figure 2-14. Anomalies of 1 Apr SWE in five freshwater ecoregions of the CCE through 2021.....	24
Figure 2-15. Mountain snowpack on 1 April 2021 at select monitoring sites, relative to 1981–2010 median value.....	25
Figure 2-16. Mean max stream temperature in Aug measured at 466 USGS gages in 6 ecoregions, 1981–2020.....	26

Figure 2-17. Anomalies of the 7-day min streamflow measured at 213 gages in 6 ecoregions, 1981–2020	27
Figure 2-18. Anomalies of the 1-day max streamflow measured at 213 gages in 6 ecoregions, 1981–2020	27
Figure 2-19. Recent (5-year) trend and average of max and min streamflow anomalies in 16 freshwater Chinook salmon ESUs in the CCE through 2020	28
Figure 3-1. Monthly northern and southern copepod biomass anomalies from Newport Hydrographic Line station NH05, 1996–2020	30
Figure 3-2. Monthly mean body length of adult <i>E. pacifica</i> krill off Trinidad Head, 2007–20	31
Figure 3-3. Monthly maximum domoic acid concentration in razor clams and Dungeness crab viscera through 2020 for WA, OR, NorCal (Del Norte to Mendocino Counties), and Central CA (Sonoma to San Luis Obispo Counties).....	32
Figure 3-4. Catch per unit effort of 9 taxa in the Northern CCE, 1998–2020	35
Figure 3-5. CPUE anomalies of 8 key forage groups in the Central CCE, 1990–2020.....	37
Figure 3-6. Mean abundance of the larvae of ten key forage groups in the Southern CCE, 1998–2020.....	38
Figure 4-1. At-sea juvenile Chinook and coho salmon catch off WA and OR in June, 1998–2020	41
Figure 4-2. Escapement anomalies of naturally produced Chinook salmon in California watersheds through 2019	42
Figure 4-3. Escapement anomalies of naturally produced Chinook salmon in Washington, Oregon, and Idaho watersheds through 2018	43
Figure 4-4. Escapement anomalies of naturally produced coho salmon through 2019	43
Figure 4-5. Observed and modeled counts of adult spring Chinook salmon and fall Chinook salmon at Bonneville Dam, by outmigration year and return year	45
Figure 4-6. Average of standardized freshwater and marine habitat condition indicators for brood years 1983–2019 for the Sacramento River and Klamath River fall runs.....	51
Figure 4-7. Locations of ports used in the availability analysis.....	53
Figure 4-8. Availability Index of biomass for selected species to ports along the U.S. West Coast, 2003–19	54
Figure 4-9. Center of gravity for 12 species of groundfish, 2003–20, calculated using VAST modeling and the West Coast Groundfish Bottom Trawl Survey	55
Figure 4-10. Recent trend and average of spawning biomass and recruitment for highly migratory species in the California Current from recent stock assessments: bluefin tuna (2018), albacore (2019), bigeye tuna (2019), and yellowfin tuna (2020)	56
Figure 5-1. California sea lion pup counts on San Miguel Island for the 1997–2020 cohorts.....	57
Figure 5-2. California sea lion pup overwinter growth rate in relation to fall–winter PDO.....	58
Figure 5-3. Confirmed numbers of whales reported as entangled in fishing gear and other sources along the U.S. West Coast, 2000–20.....	60

Figure 5-4. Standardized productivity anomalies for five seabird species breeding on SEFI through 2020.....	61
Figure 5-5. Standardized productivity anomalies for three seabird species breeding on Yaquina Head through 2020	62
Figure 5-6. Southeast Farallon Island seabird diets through 2020	63
Figure 5-7. Fork length of northern anchovy brought to rhinoceros auklet chicks at Año Neuvo Island, 1993–2020	63
Figure 5-8. Common murre chick diets at Yaquina Head through 2020.....	64
Figure 5-9. Encounter rate of bird carcasses on beaches in north-central California through 2020	65
Figure 6-1. Annual landings of U.S. West Coast commercial fisheries, including total landings across all fisheries, 1981–2020	68
Figure 6-2. Annual landings of U.S. West Coast recreational fisheries, for all recreational fisheries and salmon, 1981–2020	69
Figure 6-3. Annual revenue (ex-vessel value in 2020 dollars) of U.S. West Coast commercial fisheries, 1981–2020	69
Figure 6-4. Distance trawled by federally managed groundfish bottom trawl fisheries across the entire CCE (top: 1999–2019) and within each ecoregion (bottom: 2002–19)	71
Figure 6-5. Spatial representation of seafloor contact by bottom trawl gear from federal groundfish fisheries, calculated from annual distances trawled within each 2 × 2-km grid cell, 2002–19.....	72
Figure 6-6. Aquaculture production of shellfish and finfish in CCE waters, 1986–2019	73
Figure 6-7. Total and per capita consumption of edible and nonedible fisheries products in the USA, 1962–2019	74
Figure 6-8. Distance transited by foreign commercial shipping vessels in the CCE, 1997–2019	75
Figure 6-9. Standardized index of the sum of oil and gas production from offshore wells in California, 1974–2020.....	75
Figure 7-1. Commercial fishing reliance and social vulnerability scores as of 2018, plotted for 25 communities from WA, OR, and Northern (NCA), Central (CCA), and Southern California (SCA)	78
Figure 7-2. Commercial fishing engagement and social vulnerability scores as of 2018, plotted for 25 communities from WA, OR, NCA, CCA, and SCA.....	79
Figure 7-3. Average diversification for U.S. West Coast and Alaskan fishing vessels with over \$5K in average revenues and for vessels in the 2019 U.S. West Coast fleet with over \$5K in average revenues, grouped by state, average gross revenue class, and vessel length class	80
Figure 7-4. Trends in fishery revenue diversification in major U.S. West Coast ports by state/region: WA, OR, NCA, and SCA, 1981–2019	81

Figure 7-5. Top and middle: Theil index anomalies for all U.S. West Coast commercial fisheries plus 7 individual management groups. Bottom: Maps of 21 port groups, with bubbles proportional to Theil index values for all fisheries revenue in a given port group for each 5-yr time period.....83

Figure 7-6. Top: Port group-specific revenue by decade for landings of albacore and swordfish. Middle: Annual Theil index measures for HMS components. Bottom: Annual percent share of total coastwide HMS revenue derived from albacore and swordfish, 1980–2019 84

Figure 7-7. Fishery participation networks for IO-PAC port groups in WA based on Nov 2019–Sep 2020 landings receipts..... 86

Figure 7-8. Fishery participation networks for IO-PAC port groups in OR based on Nov 2019–Sep 2020 landings receipts.....87

Figure 7-9. Fishery participation networks for IO-PAC port groups in NCA and CCA based on Nov 2019–Sep 2020 landings receipts88

Figure 7-10. Fishery participation networks for IO-PAC port groups in SCA based on Nov 2019–Sep 2020 landings receipts 89

Tables

Table 4-1. Stoplight chart of conditions for smolt years 2017–20, and qualitative outlooks for adult returns in 2021, for coho salmon returning to coastal OR and for Chinook salmon returning to the Columbia River basin	44
Table 4-2. Table of conditions for naturally produced Central Valley fall-run Chinook salmon returning in 2021, from brood years 2016–19	46
Table 4-3. Sacramento and Klamath River fall Chinook salmon habitat indicators, definitions, and key references.....	47
Table 4-4. Stoplight chart of freshwater and marine conditions for naturally produced Sacramento River fall Chinook salmon.....	49
Table 4-5. Stoplight table of freshwater and marine conditions for naturally produced Klamath River fall Chinook salmon.....	50

Executive Summary

This document is a companion to the ecosystem status report (ESR) provided by the California Current Integrated Ecosystem Assessment team (CCIEA team) to the Pacific Fishery Management Council (PFMC) in March of 2021 (Harvey et al. 2021). The CCIEA team provides ESRs annually to PFMC, as one component of the overall CCIEA goal of providing quantitative, integrative science tools, products, and synthesis in support of a more holistic (ecosystem-based) approach to managing marine resources in the California Current.

The ESR features a suite of indicators co-developed by the CCIEA team and PFMC. An initial suite of indicators was first described by Levin and Schwing (2011), and has been refined and updated over the years to best capture the current state of the California Current ecosystem (CCE) in a way that aligns with the needs and interests of PFMC and its advisory bodies. With this context, the analyses in this document represent our best understanding of environmental, ecological, and socioeconomic conditions in this ecosystem roughly through the end of 2020. Because the time required to process data varies for different indicators, some of the resulting time series are slightly more up-to-date than others. Some indicators (snowpack, dissolved oxygen, ocean acidification, fishery landings, fishery revenue, and non-fishing human activities) have been updated since the March 2021 report to PFMC (Harvey et al. 2021) specifically for this technical memorandum.

In 2020, two distinctive sets of factors arose that had considerable influence on the CCE (Figure ES-1). One was a significant shift in two indices of large-scale ocean physics—the Pacific Decadal Oscillation (PDO) and the El Niño–Southern Oscillation (ENSO)—that have historically indicated important influence on CCE physical conditions and productivity. The other was the global COVID-19 pandemic, which drastically affected human activities along the U.S. West Coast, impacting both the fisheries and research sectors. While the system was affected by many other drivers and dynamic interactions, we emphasize these two factors at the outset because they color much of what follows in this document: the northeastern Pacific Ocean experienced major physical changes in 2020 that have ramifications for the CCE, but, due to COVID-19 restrictions, fewer research surveys were conducted in 2020, hampering our ability to explore the effects of the physical changes in real time. This adds uncertainty to our interpretations of ecological dynamics, and may also challenge our ability to distinguish how fishery catches and earnings were affected by COVID-related impacts, compared to the effects of other ecosystem drivers.

As noted, changes in physical drivers suggest that 2020 may have seen a transition toward more productive conditions in the CCE (Figure ES-1). This marks a difference from a preceding series of relatively warm and unproductive years and events, including the massive northeastern Pacific marine heatwave of 2013–16 (“the Blob”), a major El Niño event in 2015–16, further marine heatwaves in 2018 and 2019, and a minor El Niño in 2019. In 2020, climate and oceanographic signals affecting the CCE included:

- A transition from El Niño conditions and positive PDO signals to La Niña conditions and a negative PDO for the first time in many years. These conditions are generally associated with higher productivity in the CCE.

- Strong winter upwelling preceded the start of an average to above-average coastal upwelling season, providing high nutrient supply to the base of the food web.
- The second-largest marine heatwave on record since 1982 was observed in the North Pacific, but primarily remained offshore, in part because of stronger upwelling in coastal waters.
- Despite general cooling in the system and the emergence of La Niña conditions in the tropics, warmer-than-average waters persisted off Central and Southern California.
- Much of the system experienced low snowpack and widespread drought. Drought and low snow storage, especially in Oregon and California, contributed to California experiencing over four million acres burned and five of the six largest fires since 1932. Over one million acres of land burned in Oregon, approximately double the ten-year average.

Many ecological indicators in 2020 suggested that seasonal conditions in the CCE were relatively favorable for most species, although, as noted, reduced biological sampling effort due to the COVID-19 pandemic means greater uncertainty around these findings than is normally the case (Figure ES-1). Among the ecological metrics that indicated average or above-average conditions in 2020 were:

- The copepod community (the tiny, free-swimming crustaceans at the bottom of the food web) off Newport, Oregon, was characterized by a cool-water, energy-rich assemblage in the spring and summer. Densities of energy-rich copepods were among the highest ever observed.
- Several lines of evidence indicate improved production and availability of krill, a key prey for many species.
- Northern anchovy (*Engraulis mordax*) catch rates remained very high in research surveys off central and southern California.
- Abundances of seabird fledglings at the Southeast Farallon Island breeding colony, and of California sea lion (*Zalophus californianus*) pups at the San Miguel Island colony, were above average, implying good feeding conditions for many types of top predators.

However, some indicators from 2020 represented lingering signs of concern that anomalous or unproductive ecological conditions remained in the CCE (Figure ES-1). These included:

- Biological and oceanographic indicators over the past several years were generally consistent with expectations for average to below-average returns of Chinook salmon (*Oncorhynchus tshawytscha*) and coho salmon (*O. kisutch*) to several U.S. West Coast river systems in 2021.
- Pyrosomes, free-swimming colonial gelatinous animals normally found in warmer waters further to the south, were once again abundant off of Central California.
- Reports of whale entanglements in fixed fishing gear in 2020 were above average for the seventh consecutive year. The number of reports was lower than annual totals from 2014–19, although COVID-19 may have hindered our ability to track entanglements.
- Domoic acid, a toxin produced by the phytoplankton *Pseudo-nitzschia*, exceeded safety limits in Dungeness crabs (*Metacarcinus magister*) and razor clams (*Siliqua patula*) in Washington, Oregon, and California; and a major bloom of the phytoplankton *Lingulodinium polyedra* caused a record-setting and harmful “red tide” off Southern California.

Fishery landings and revenues were lower in 2020 than in 2019 (Figure ES-1). Landings and revenue were down in 2020 in nearly every management group (salmon, crab, shrimp, groundfish, etc.). The COVID-19 pandemic is one of many possible contributing factors to the reduction in fishery landings and revenue, along with ocean conditions, wildfires, and other sources of year-to-year variability. The drop in landings and revenue comes at a time when commercial fishing vessels are not highly diversified; in other words, on average, vessels depend on relatively few target species to provide the bulk of their revenues, which could leave those vessels more economically vulnerable to shocks like the disruption of COVID-19. We continue to study how commercial fishing revenue is concentrated in different ports, how vessels within ports switch back and forth among different target species, and coastal communities' overall levels of social wellbeing and vulnerability. These factors will likely influence how well fishing communities can adapt and respond to shifts in target species abundance and location resulting from year-to-year climate variability and longer-term climate change.

The sections that follow go into greater detail about the status and trends of indicators summarized here; after a short Introduction, we include sections related to Climate and Ocean Drivers, the Lower Trophic Levels and Forage, Fishes, Marine Mammals and Seabirds, Human Activities, and Human Wellbeing, followed by a brief Synthesis.

Figure ES-1 (overleaf). Visual summary of the status and trends of key indicators in the California Current social–ecological system during 2020. Graphic designed by S. Kim, NMFS/NWFSC.

2020-21 CCIEA Ecosystem Status Report Highlights

System Conditions

- Transition to La Niña conditions
- Negative Pacific Decadal Oscillation (PDO)
- Generally lead to higher productivity in the CCE

Marine Heatwave

- Second largest marine heatwave in the North Pacific, but mostly stayed offshore.

Upwelling Season

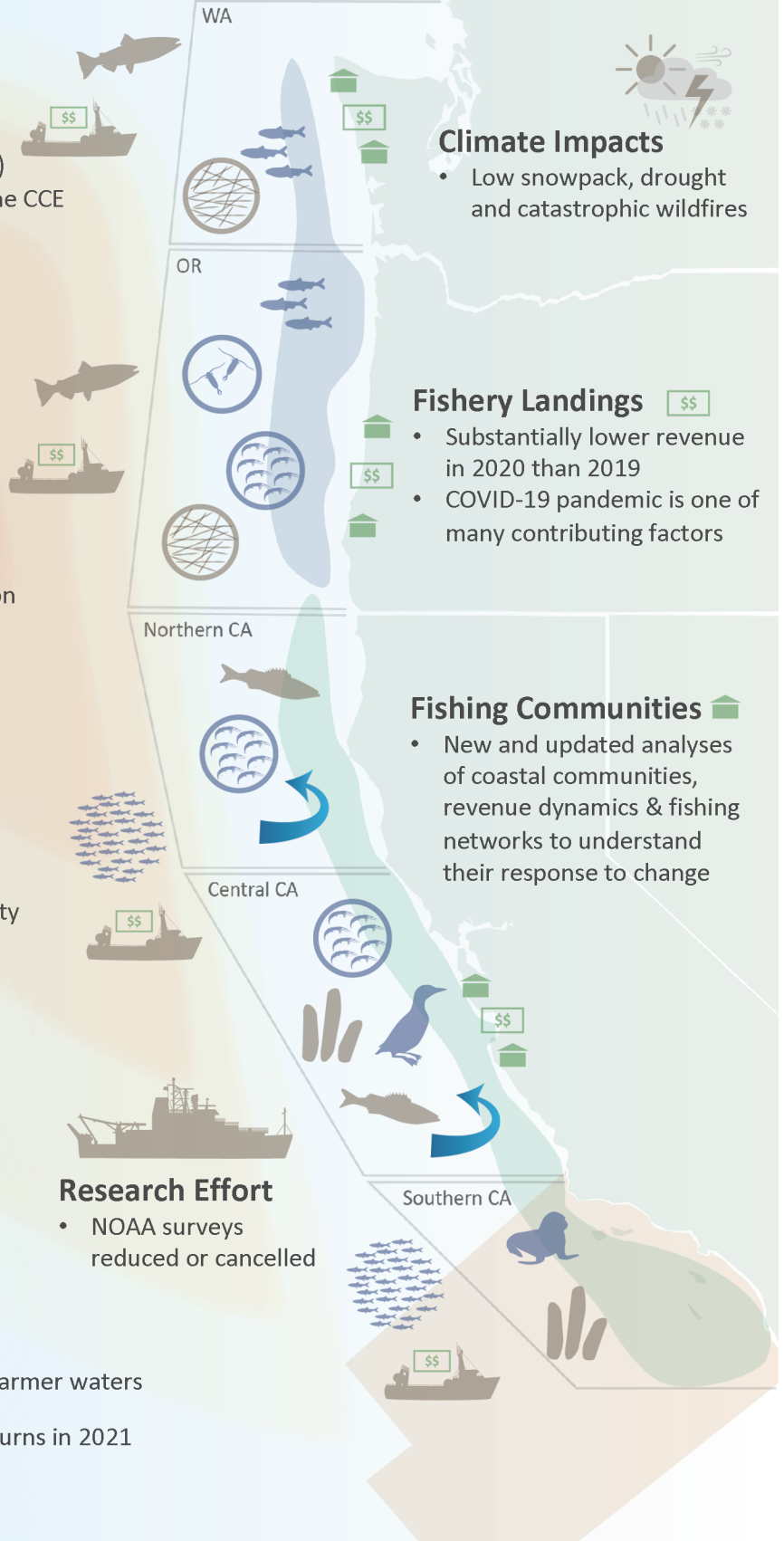
- Strong winter upwelling preceded an average to above-average upwelling season
- Good nutrient supply to the base of the food web
- Less compression of cool pelagic habitat along coastline

Favorable Ecological Conditions

-  Above-average zooplankton community
-  High abundance of anchovies
-  High production of seabird offspring
-  High production of sea lion offspring

Unfavorable Ecological Conditions

-  Widespread harmful algal blooms
-  Presence of species associated with warmer waters
-  Mixed outlooks of Chinook salmon returns in 2021



Climate Impacts

- Low snowpack, drought and catastrophic wildfires

Fishery Landings

- Substantially lower revenue in 2020 than 2019
- COVID-19 pandemic is one of many contributing factors

Fishing Communities

- New and updated analyses of coastal communities, revenue dynamics & fishing networks to understand their response to change

Research Effort

- NOAA surveys reduced or cancelled

NOTE: West Coast research efforts in 2020 were heavily impacted by the COVID-19 pandemic.

1 Introduction

Chris J. Harvey, Newell (Toby) Garfield, Gregory D. Williams, and Nicholas Tolimieri

1.1 Ecosystem-Based Fisheries Management and Integrated Ecosystem Assessment

Ecosystem-based management of fisheries and other marine resources has emerged as a priority in the United States (EPAP 1999, Fluharty et al. 2006, McFadden and Barnes 2009, NOAA 2016) and elsewhere (Browman et al. 2004, Sainsbury et al. 2014, Walther and Möllmann 2014, Long et al. 2015). NOAA's National Marine Fisheries Service (NOAA Fisheries) defines ecosystem-based fisheries management (EBFM) as “a systematic approach to fisheries management in a geographically specified area that contributes to the resilience and sustainability of the ecosystem; recognizes the physical, biological, economic, and social interactions among the affected fishery-related components of the ecosystem, including humans; and seeks to optimize benefits among a diverse set of societal goals” (NOAA 2016). This definition encompasses interactions within and among fisheries, protected species, aquaculture, habitats, and human communities that depend upon fisheries and related ecosystem services. An EBFM approach is intended to improve upon traditional fishery management practices, which primarily focus on individual fished stocks.

Successful EBFM requires considerable effort and coordination due to the formidable amount of information required and uncertainty involved. In response, scientists throughout the world have developed many frameworks for organizing science and information in order to clarify and synthesize this overwhelming volume of data into science-based guidance for policymakers. NOAA Fisheries has adopted a framework called integrated ecosystem assessment (IEA; Levin et al. 2008, Levin et al. 2009), which can be summarized in five progressive steps (Figure 1-1):

1. Identifying and scoping ecosystem goals, objectives, targets, and threats.
2. Assessing ecosystem status and trends through valid ecosystem indicators.
3. Assessing the risks of key threats and stressors to the ecosystem.
4. Analyzing management strategy alternatives and identifying potential tradeoffs.
5. Implementing selected actions, and monitoring and evaluating management success.

As shown in Figure 1-1, the IEA approach is iterative. Following the implementation of management actions, all other steps in the IEA loop must be revisited in order to ensure that: a) evolving goals and objectives are clearly identified; b) monitoring plans and indicators are appropriate for the management objectives in mind; c) existing and emerging risks are properly prioritized; and d) management actions are objectively and regularly evaluated for success. The five steps of the IEA framework, plus its iterative nature, are very similar to and compatible with the core guiding principles of the NOAA EBFM Policy (NOAA 2016, Link 2017).

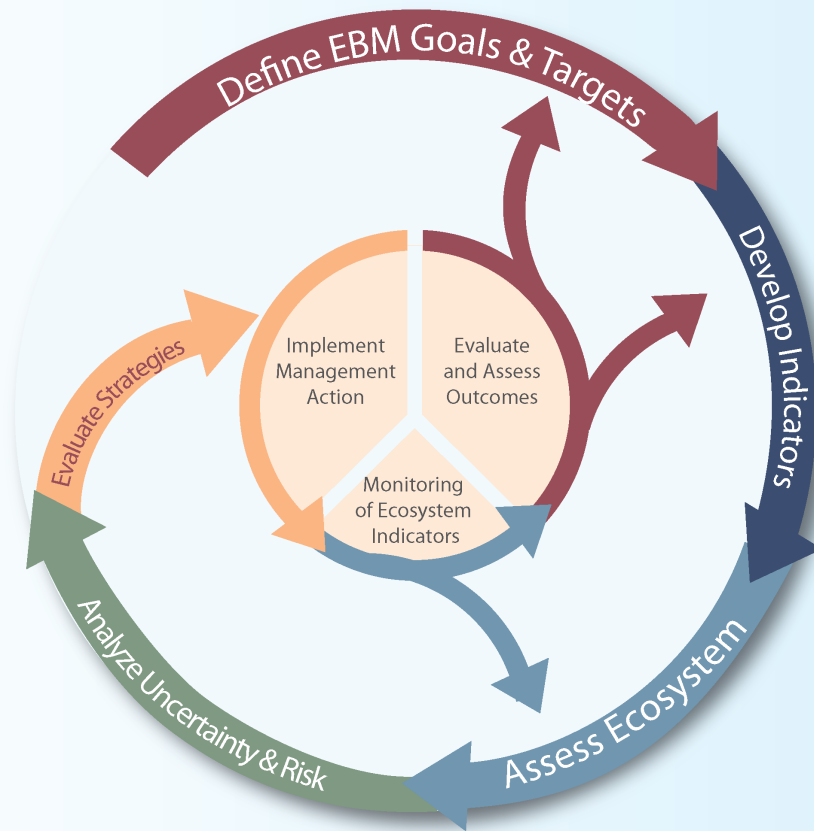


Figure 1-1. Loop diagram of the five progressive steps in iterations of the integrated ecosystem assessment (IEA) process. From Samhoury et al. (2014).

In 2009, NOAA line offices along the U.S. West Coast initiated the California Current Integrated Ecosystem Assessment (CCIEA). The CCIEA team focuses on the California Current ecosystem (CCE) along the U.S. West Coast. In keeping with the principles of ecosystem-based management, the CCIEA team regards the CCE as a dynamic, interactive, social–ecological system with multiple levels of organization and diverse goals and endpoints that are both environmental and social in nature (Figure 1-2). The challenging task of assembling and interpreting information from this broad range of disciplines, locations, and time frames engages over 50 scientists from NOAA’s Northwest and Southwest Fisheries Science Centers and other NOAA offices, as well as colleagues from other agencies, academia, and nongovernmental entities. Information on CCIEA research efforts, tools, products, publications, partnerships, and points of contact is available on the [CCIEA website](#).¹

The primary management partner of the CCIEA team to date has been the [Pacific Fishery Management Council \(PFMC\)](#),² which oversees federally managed fisheries and implementation of the Magnuson–Stevens Fishery Conservation and Management Act in the Exclusive Economic Zone off the U.S. West Coast. PFMC manages target species directly under policies outlined in its four fishery management plans (FMPs), and may incorporate nonbinding guidance from its [Fishery Ecosystem Plan \(FEP; PFMC 2013\)](#).³

¹ <https://go.usa.gov/x6Ak6>

² <https://www.pcouncil.org/>

³ <https://www.pcouncil.org/fishery-ecosystem-plan/>

INTEGRATED SOCIAL-ECOLOGICAL SYSTEM OF THE CALIFORNIA CURRENT

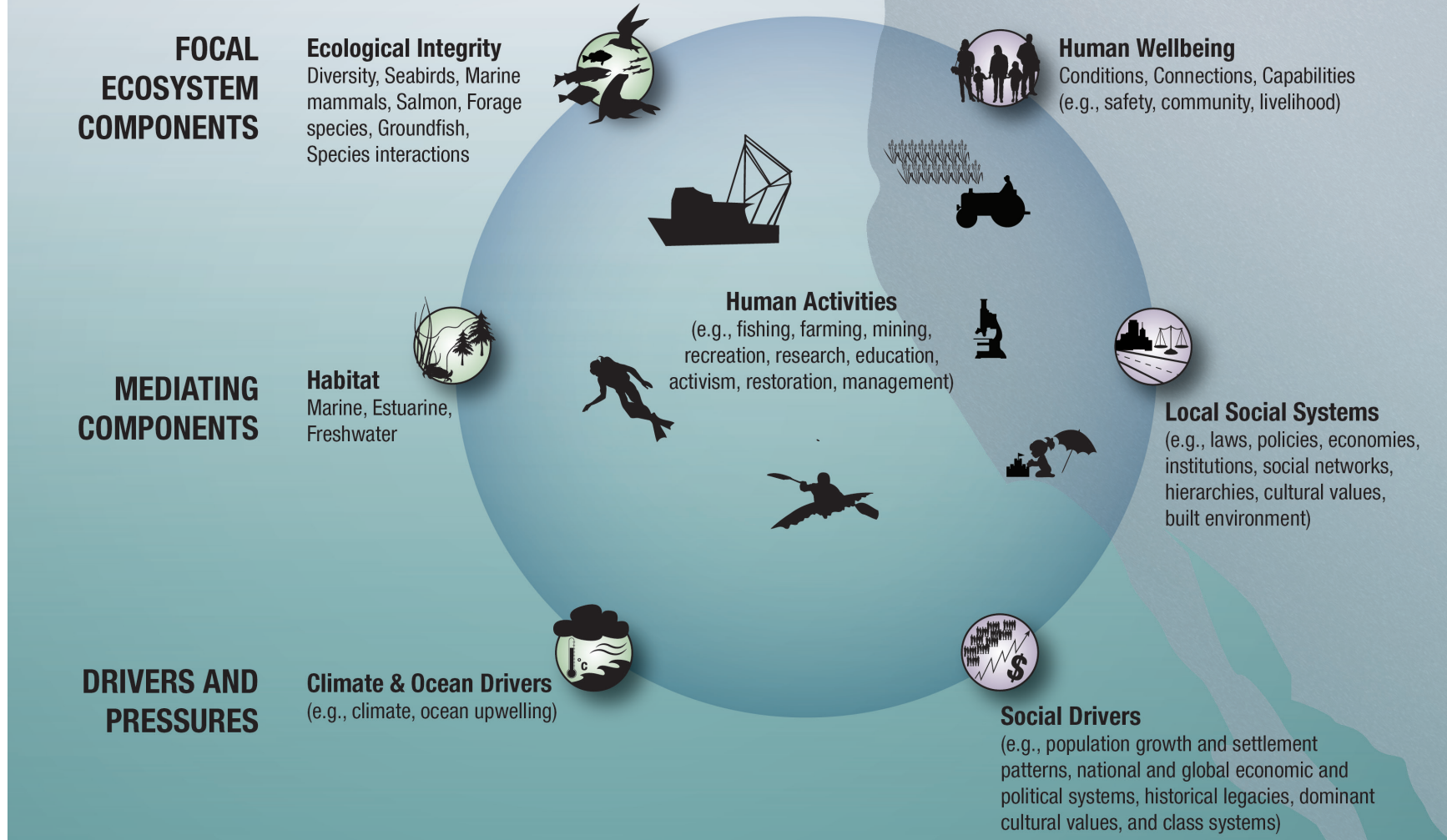


Figure 1-2. Conceptual model of the California Current social-ecological system. The model represents the complex and inextricable connections between ecological components (left) and human components (center, right). These components are arranged in three tiers: focal ecosystem components, which are often associated with broad objectives such as ecological integrity and human wellbeing; mediating components, such as habitat and local social systems; and drivers and pressures, which are generally external forces on the ecosystem. Human activities are placed at the center to emphasize their broad extent and because they are where management actions are directly implemented in order to achieve objectives elsewhere in the system. From Levin et al. (2016).

Section 1.4 of the FEP outlined a reporting process wherein the CCIEA team provides PFMC with a yearly ecosystem status report (ESR) that describes the current status and trends of ecosystem attributes of the CCE. The purpose of the ESRs is to provide PFMC with a general sense of ecosystem conditions as context for decision-making. ESRs include information on a range of attributes, including climate and oceanographic drivers, status of key species groups, fisheries-related human activities, and human wellbeing in coastal communities. ESRs track ecosystem attributes through ecosystem indicators, most of which were derived through a rigorous indicator screening process developed by Kershner et al. (2011); details of specific CCIEA indicator screening exercises are documented elsewhere (Levin and Schwing 2011, Levin et al. 2013, Harvey et al. 2014).

Since 2012, the CCIEA team has provided PFMC with nine ESRs, most recently in March 2021. The ESRs are available as online sections of [PFMC briefing books](#)⁴ for the meetings at which the CCIEA team has presented the reports (November 2012, then annually in March 2014–21), and are also available on the [CCIEA website](#).⁵ The contents of ESRs have evolved over the years through cooperation between the CCIEA team and PFMC and its advisory bodies, most notably through an [FEP initiative](#)⁶ that began in 2015 to refine the indicators in the ESRs to better reflect PFMC’s needs. For example, PFMC has requested that the annual ESRs be confined to ~20 printed pages.

This technical memorandum is a companion document to the ESR delivered by the CCIEA team to PFMC in March 2021 (Harvey et al. 2021), representing the status and trends of ecosystem indicators in the CCE through 2020 and, in some cases, early 2021. It is the fifth in an ongoing annual series of technical memorandums (beginning with Harvey et al. 2017) that will provide a more thorough ESR of the CCE than the page-limited presentation to PFMC. We will continue to provide the annual report to PFMC, and this technical memorandum series will largely be based on that report. However, as this series evolves, the technical memorandums will incorporate more indicators and analyses covering a broader range of ecosystem attributes. This is because the CCIEA team looks to support other management partners in addition to PFMC, and our goal is for our annual ESR to feature information in support of ecosystem-based management (EBM) in other sectors and services in addition to fisheries (Slater et al. 2017). The technical memorandum format enables increased information content, contributions from a broader range of authors, and value to a wider range of audiences. It is our hope that an expanded ESR will lead to greater dialogue with potential partners and stakeholders; such dialogue and engagement is at the heart of the initial step of the IEA process (Figure 1-1), and is essential to every other step in all iterations as well.

1.2 Notes on Interpreting Time-Series Figures

Throughout this report, many data figures will follow one of two common formats—time-series plots or quad plots—both illustrated with sample data in Figure 1-3; see figure caption for details. Time-series plots generally contain a single dataset (Figures 1-3a,b),

⁴ <https://www.pcouncil.org/category/briefing-book/>

⁵ <https://go.usa.gov/x6A9D>

⁶ <https://www.pcouncil.org/actions/initiative-2-coordinated-ecosystem-indicator-review/>

whereas quad plots are used to summarize the recent averages and trends for multiple time series in a single panel, as when we have time series of multiple populations that we want to compare in a simplified visual manner (Figure 1-3c). Some time-series plots now show thresholds beyond which we expect substantial changes in response variables, such as when a physiological tolerance to a physical or chemical variable is exceeded (Figure 1-3b). Where possible, we include estimates of error or uncertainty in the data. Generally, error estimates are standard deviations or standard errors in the observations.

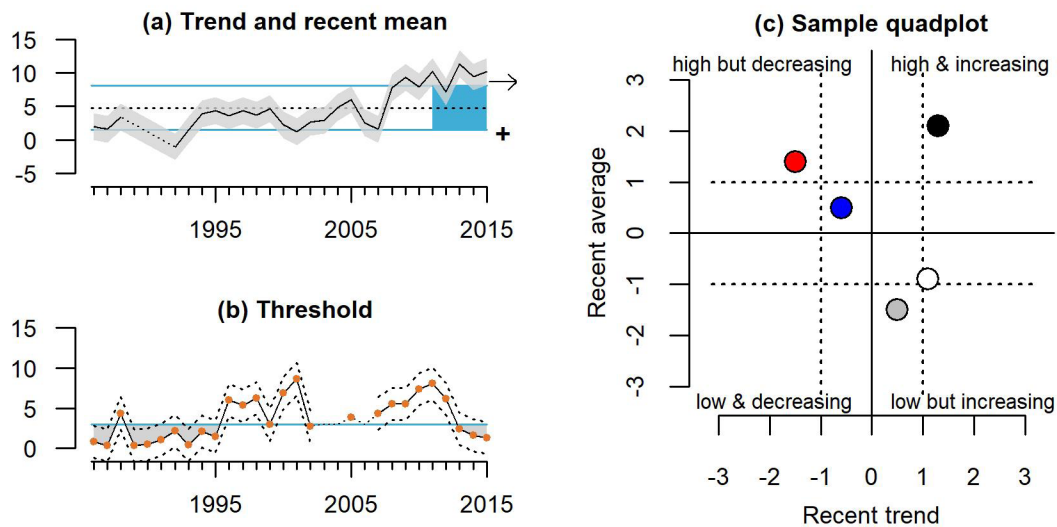


Figure 1-3. (a) Sample time-series plot, with indicator data relative to the long-term mean (black dotted horizontal line) and ± 1.0 standard deviation (SD; solid blue lines) of the full time series. Dotted black line indicates missing data, and points (when included) indicate data. Arrow at the right indicates if the trend over the evaluation period (shaded blue) is positive (\nearrow), negative (\searrow), or neutral (\rightarrow). Symbol at the lower right indicates if the recent mean was greater than (+), less than (-), or within 1.0 SD of (\cdot) the long-term mean. When possible, time series indicate observation error (gray envelope), defined for each plot (e.g., SD, standard error, or 95% confidence intervals). (b) Sample time-series plot with the indicator plotted relative to a threshold value (blue line). Dashed lines indicate upper and lower observation error, again defined for each plot. Dotted black line indicates missing data. (c) Sample quad plot. Each point represents one time series normalized by SD. The position of a point indicates if the recent trend was increasing or decreasing over the evaluation period and whether the recent mean over the evaluation period was above or below the long-term mean. Dashed lines represent ± 1.0 SD of the full time series.

1.3 Sampling Locations

Figure 1-4a shows the major headlands that demarcate potential biogeographic boundaries, in particular Cape Mendocino and Point Conception, both in California. We generally consider the region north of Cape Mendocino to be the “Northern CCE,” the region between Cape Mendocino and Point Conception the “Central CCE,” and the region south of Point Conception the “Southern CCE.” Figure 1-4a also shows sampling locations for much of the regional climate and oceanographic data presented in this report. In particular, many of the physical and chemical oceanographic data are collected on the Newport Line off Oregon and in the California Cooperative Oceanic Fisheries Investigations (CalCOFI) grid off California. Physical oceanography sampling is further complemented by basin-scale observations and models.

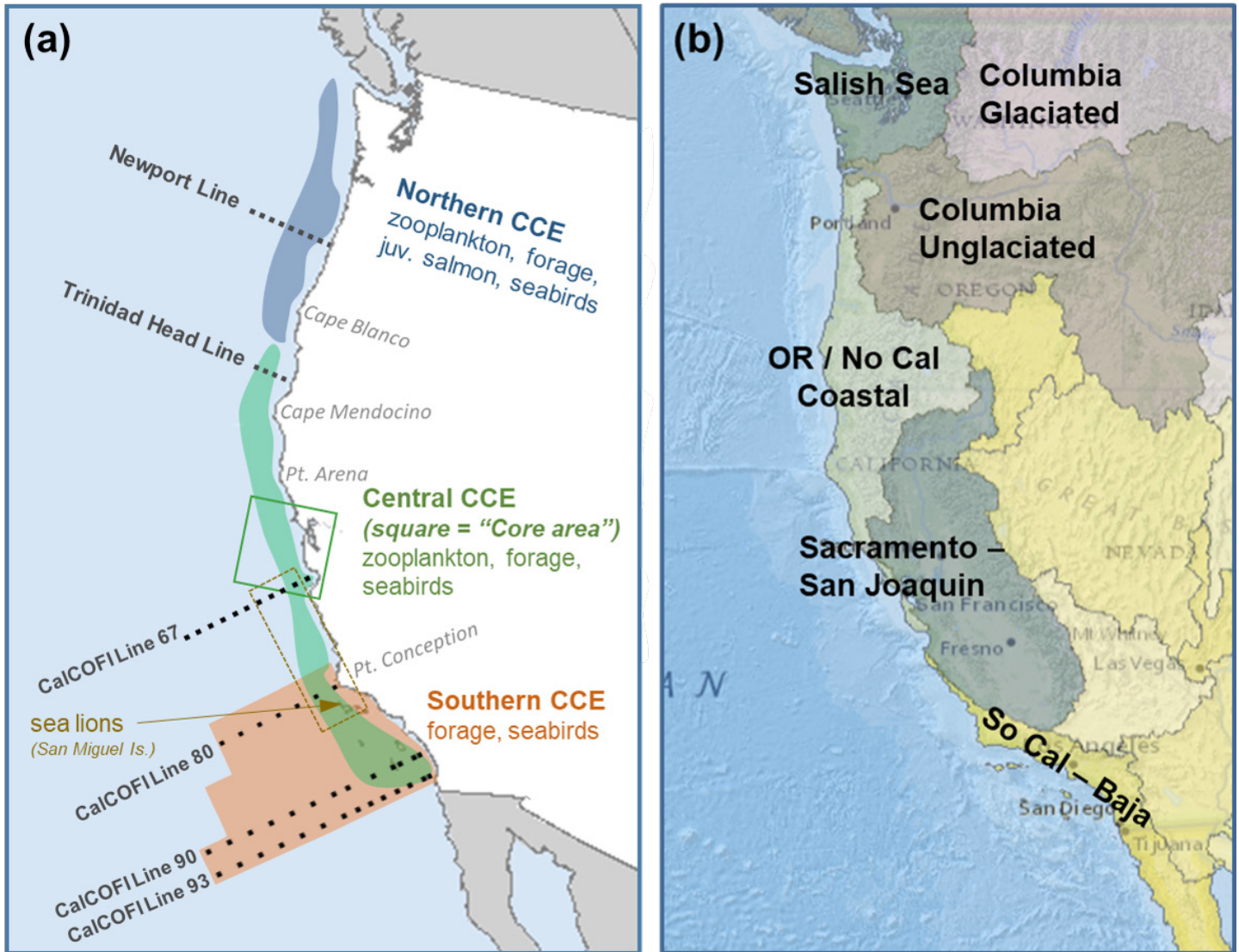


Figure 1-4. Map of the CCE and sampling areas. (a) Key geographic features, oceanographic sampling locations (dotted transect lines), and biological sampling areas (blue = Northern CCE, green = Central CCE, orange = Southern CCE). Solid box = core sampling area for forage in the central CCE. Dotted box approximates the foraging area for adult female California sea lions from the San Miguel colony. (b) Freshwater ecoregions, where snowpack and freshwater indicators are measured.

The map in Figure 1-4a also represents sampling for most biological indicators, including zooplankton, forage species, California sea lions (*Zalophus californianus*), and seabirds. Zooplankton data are primarily reported from the Newport Line off Oregon and the Trinidad Head Line off Northern California. The blue-, green-, and orange-shaded regions of coastal waters refer to the extent of major survey efforts that focus on forage species, juvenile salmon, and seabirds in shelf and slope habitats. In some cases, the surveys span both sides of the major zoogeographic boundaries of Cape Mendocino and Point Conception (especially the surveys represented by green shading), although the data we use in this report for those groups are mostly subsets drawn from areas that represent status and trends specific to the Northern, Central, and Southern CCE regions. The NOAA Fisheries

West Coast Groundfish Bottom Trawl Survey (Keller et al. 2017) occurs in roughly the same area on the shelf and upper slope (at depths of 55–1,280 m) as the blue- and green-shaded regions of Figure 1-4a, though it was not conducted in 2020 due to the COVID-19 pandemic.

Freshwater habitats worldwide can be spatially grouped into “ecoregions” according to the designations of Abell et al. (2008). The freshwater ecoregions in the CCE are shown in Figure 1-4b, and are the basis by which we summarize freshwater habitat indicators relating to streamflow, stream water temperatures, and snowpack.

2 Climate and Ocean Drivers

Isaac D. Schroeder, Andrew Leising, Steven Bograd, Lynn deWitt, Newell (Toby) Garfield, Elliott L. Hazen, Dale Robinson, Daniel L. Rudnick, Michael Jacox, Jarrod Santora, Jennifer Fisher, Kym Jacobson, Emily Norton, Samantha Siedlecki, Isaac Kaplan, Correigh Greene, and Stuart Munsch

Following the exceptionally warm and variable climate conditions of 2013–19, conditions in 2020 returned to those more favorable to higher productivity. The relatively weak 2019 El Niño shifted into the La Niña state and the positive Pacific Decadal Oscillation (PDO) became negative. These trends suggest cooler waters and higher productivity. On the other hand, the North Pacific Gyre Oscillation (NPGO) remained strongly negative, an indication of reduced transport of North Pacific gyre water into the CCE and lower productivity. The 2019 marine heatwave dissipated in the fall of 2019 and then reformed in 2020 to become the second-largest northeastern Pacific marine heatwave. However, unlike the 2013–16 event (“the Blob”), this marine heatwave remained offshore, with only limited interaction in the coastal region.

Superimposed on these large-scale climate and ocean drivers, regional indicators of upwelling, water chemistry, and stream conditions demonstrated their characteristically high spatiotemporal variability, resulting in patterns of local variation. Upwelling, especially in the Central CCE, had a strong winter pulse and then remained strong, but variable, during the spring and summer. This helped create a relatively wide band of cool coastal water. Streamflow was near average in the north and below average for California and southern Oregon.

The following subsections provide in-depth descriptions of basin-scale, regional-scale, and hydrologic indicators of climate and ocean variability in the CCE.

2.1 Basin-Scale Indicators

The CCE is driven by atmosphere–ocean energy exchanges that occur on many temporal and spatial scales. To capture large-scale variability, the CCIEA team tracks three indices: the status of the equatorial El Niño–Southern Oscillation (ENSO), described by the Oceanic Niño Index (ONI); the PDO; and the NPGO. Positive ONI and PDO values and negative NPGO values usually denote conditions that lead to low CCE productivity, whereas negative ONI and PDO values and positive NPGO values are associated with periods of high CCE productivity.

ENSO events originate in the Pacific equatorial region and impact the CCE through atmospheric teleconnection and coastally trapped waves. Atmospheric impacts occur by modifying the jet stream and storm tracks, while coastally trapped waves modify the nearshore thermocline and coastal currents, affecting transport and distribution of equatorial and subequatorial waters (and species). The ONI is related to sea surface temperature (SST) in a region of the equatorial Pacific Ocean (lat 5°N–5°S, long 120°–170°W), and is defined by a three-month running mean of SST anomalies (SSTa) in that area. A positive ONI > 0.5°C for five consecutive months indicates El Niño conditions, which usually

means more storms to the south, weaker upwelling, and lower primary productivity in the CCE. A negative ONI $< -0.5^{\circ}\text{C}$ means La Niña conditions, which usually lead to higher productivity. The PDO is derived from the SSTa distribution in the northeastern Pacific Ocean, which often persists in “regimes” that last for many years. In positive PDO regimes, coastal SSTa in the Gulf of Alaska and the CCE tends to be warmer, while in the North Pacific Subtropical Gyre it tends to be cooler. Positive PDO values are associated with lower productivity in the CCE. The NPGO is a low-frequency variation of sea surface height, indicating variations in the circulation of the North Pacific Subtropical Gyre and the Alaskan Gyre, which in turn relate to the source waters for the CCE. Positive NPGO values are associated with increased equatorward flow, along with increased surface salinities, nutrients, and chlorophyll-*a*. Negative NPGO values are associated with decreases in such values, implying less subarctic source water and generally lower productivity.

The ONI indicated that weak El Niño conditions, which had mostly persisted since late 2018, began to diminish in March 2020. ONI values were negative by June, and La Niña conditions have existed since August 2020 (Figure 2-1, top). In November, ONI dropped to -1.3°C , its lowest value since 2011. As of late April 2021, the [NOAA Climate Prediction Center](#)⁷ predicted a shift to ENSO-neutral conditions in the next month and an 80% chance of remaining in ENSO-neutral conditions through July 2021. The PDO continued a five-year trend of decreasing values since 2016 (Figure 2-1, middle), becoming increasingly negative through 2020. This was the longest string of negative values since before the Blob, and the November value (-1.12°C) was the lowest since 2013. NPGO remained in the negative state it has been in since late 2016, although the values were not as negative as the extreme lows at the end of 2019 (Figure 2-1, bottom). Collectively, the three basin-scale indices suggest a return to average or above-average conditions for productivity in the CCE in 2020.

Figure 2-2 shows the 2020 winter (top) and 2020 summer (bottom) North Pacific Ocean sea surface temperature anomalies (SSTa, left column), the most recent five-year mean SSTa (middle column), and the most recent five-year SSTa trend (right column).

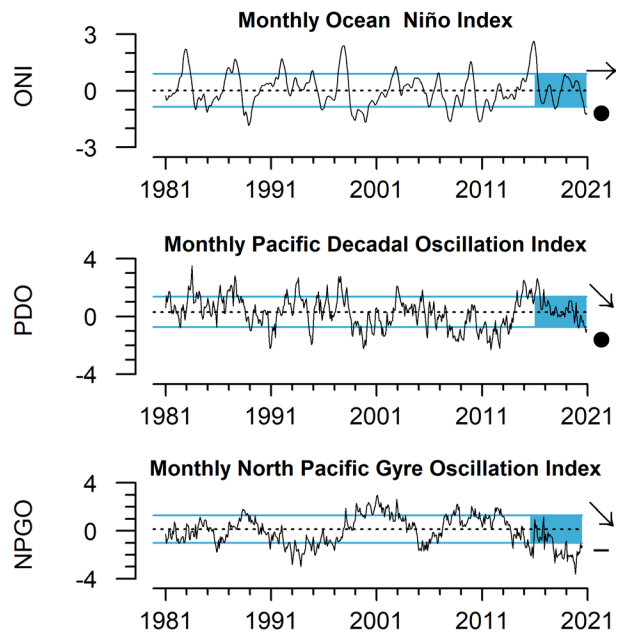


Figure 2-1. Monthly values of the ONI, PDO, and NPGO from 1981–2021. Lines, colors, and symbols as in Fig. 1-3a. ONI data are from the NOAA Climate Prediction Center,^{*} PDO data from N. Mantua (NMFS/SWFSC),[†] and NPGO data from E. Di Lorenzo (Georgia Institute of Technology).[‡]
^{*} <https://go.usa.gov/xG6QU>
[†] https://oceanview.pfeg.noaa.gov/erddap/tabledap/cciea_OC_PDO.html
[‡] <http://www.o3d.org/npgo/>.

⁷ <http://go.usa.gov/xG6QU>

SSTa are calculated relative to the 1982–2020 climatology for each grid cell. The 2020 winter SSTa was lower than the long-term average along the coastal region from the Alaska–Canada border south to San Francisco, and then slightly above the long-term average south of San Francisco (Figure 2-2, top left). Offshore, the Gulf of Alaska was warmer (~1 SD above the long-term mean) than average. The 2016–20 mean winter SSTa was very near the long-term average, except in the northern Gulf of Alaska, where the five-year mean was about 1 SD above the long-term mean (Figure 2-2, top center). The 2016–20 winter trend (Figure 2-2, top right) reflects the pattern of a strong cooling trend along the whole coastal and southern offshore region and a strong warming trend in the offshore northeastern Pacific.

The summer SSTa pattern (Figure 2-2, bottom) is different from the winter. Except for a small area off Oregon, the entire region was warmer in 2020 than the long-term mean, and the central northeastern Pacific was >2 SD above the long-term mean (Figure 2-2, bottom left). The 2016–20 summer mean was also above the long-term mean, with the northern half of the area >1 SD above the long-term mean (Figure 6, bottom center). The summer five-year trend shows cooling in the Gulf of Alaska and warming in the whole southern portion (Figure 2-2, bottom right).

Depth profiles of water temperatures in shelf waters off of Newport, Oregon, and San Diego, California (Figure 2-3), demonstrate the extent of recent warm and cool anomalies into the water column, as well as the spatial and temporal dynamics of those anomalies. The upper portion of the water column off Newport was relatively cool for much of 2020 (Figure 2-3, top). Temperatures were ~0.5°C cooler than average in the upper 50 m from winter through summer, and close to average at greater depths. The anomaly in the upper water column was the longest sustained cool period of the last five years. Temperatures off Newport switched to average or above-average in late summer, coincident with the arrival of the marine heatwave. In contrast, the Southern California Bight remained warm in 2020. At CalCOFI Station 93.30 off San Diego, warm anomalies >1°C dominated the water column in winter and spring, particularly in the upper 50 m (Figure 2-3, bottom). These anomalies were likely related to the weak El Niño in early 2020. Deeper waters shifted from warm to cool anomalies in spring. Summer and fall data are as yet unavailable from this station, but underwater glider data from nearby Line 90 (Rudnick et al. 2017) indicate warmer-than-average waters for most of 2020 (Harvey et al. 2021, Appendix D). Similarly, an underwater glider off Monterey Bay, California, recorded average or above-average temperatures down to 250 m for most of 2020 (Harvey et al. 2021, Appendix D).

There is increased recognition that marine heatwaves can have immediate short-term impacts on the ecosystem, as well as indicate stock displacements that may occur with long-term climate warming (Morgan et al. 2019, Jacox et al. 2020). For these reasons, monitoring marine heatwaves and developing robust indices of these features are important for management. Based on an analysis of SSTa from 1982–2019, a marine heatwave has the potential to cause impacts in the CCE that are comparable to those of the Blob if the anomalous feature: 1) has statistically normalized SSTa >1.29 SD (90th percentile) of the long-term SSTa time series at a location; 2) is in the top 15% of area (> ~4.25 × 10⁵ km²); 3) lasts for >5 days; and 4) comes within 500 km of the coast (Hobday et al. 2016, Leising in revision). Numerous such events have occurred in the North Pacific in recent decades, with some years experiencing multiple events, though none have matched the combined duration and intensity of the Blob.

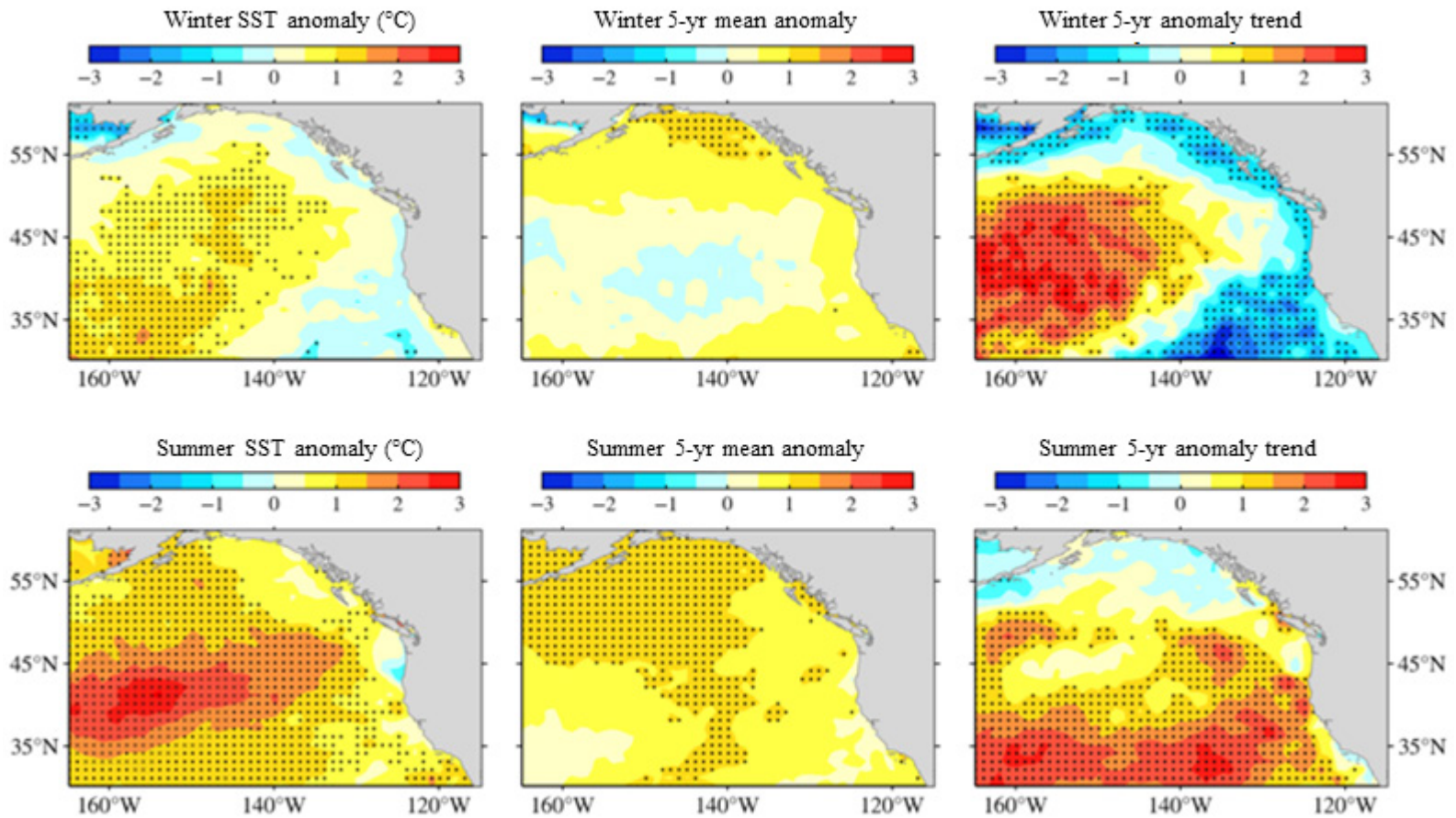


Figure 2-2. SSTa (2020, left), 5-year means (2016–20, middle), and 5-year trends (2016–20, right) in winter (Jan–Mar, top) and summer (Jul–Sep, bottom). The time series at each grid point begins in 1982. Black circles mark cells where the anomaly was >1.0 SD above the long-term mean (left, middle) or where the trend was significant (right). Black Xs mark cells where the anomaly was the largest in the time series. For the temperature 5-year means (middle) and trends (right), a given grid cell has been divided by the long-term SD, resulting in a map showing multiples of the long-term SD. SSTa maps are optimally interpolated remotely-sensed temperatures (Huang et al. 2020), which can be downloaded using ERDDAP (<https://go.usa.gov/x6scB>).

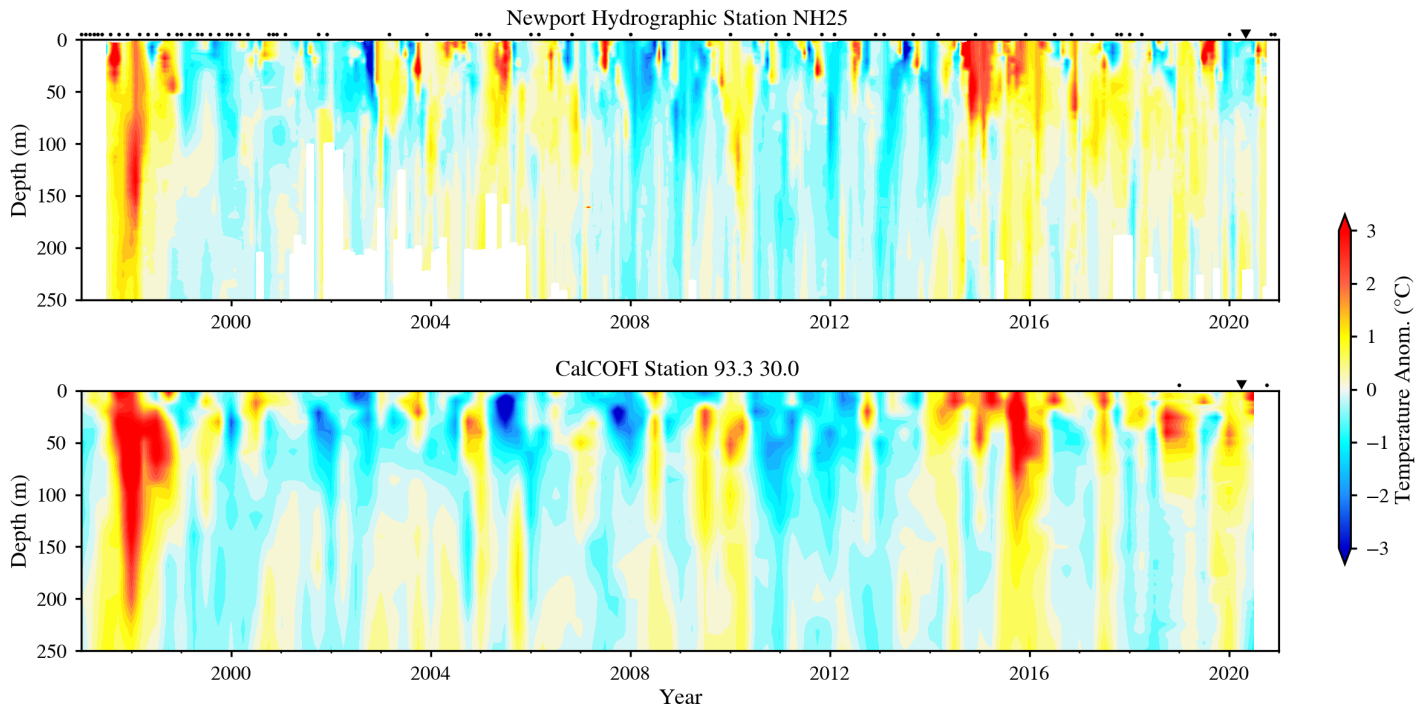


Figure 2-3. Time–depth temperature anomalies for hydrographic stations NH25 (Jul 1997–Oct 2020) and CalCOFI 93.30 (Jan 1997–Jul 2020). The NH25 (top plot) temperature anomalies are monthly means and the time interval is one month (i.e., 12 values per year). The CalCOFI (bottom plot) temperature anomalies are quarterly means and the time intervals are seasons (i.e., 4 values per year). Months or quarters not sampled are marked with a black circle along the top axis; missing samples are filled using bi-linear interpolation. Sampling missed due to COVID-19 restrictions is marked with black triangles. The spring 2020 CalCOFI temperature profile was filled using daily mean temperature data on 15 April 2020 from a data assimilative ocean model (<https://oceanmodeling.ucsc.edu/ccsirt>). For the locations of these stations, see Fig. 1-4a. Newport Hydrographic (NH) line temperature data are from J. Fisher (NMFS/NWFSC, OSU); CalCOFI hydrographic line data from <https://calcofi.org/ccdata.html>. CalCOFI data from Jan 1997–2019 are from the bottle data database, while the 2020 data are preliminary conductivity, temperature, and depth (CTD) data from the recent database.

Since the Blob ended in 2016, there have been 13 additional marine heatwaves that lasted longer than 30 days in the northeastern Pacific. A large 2019 event receded in fall into the Gulf of Alaska and reappeared in February–June 2020. This marine heatwave remained >1,500 km from the U.S. West Coast. In June 2020, a much larger marine heatwave formed (Figure 2-4), reaching its maximum extent in late September–early October 2020. The 2019 and 2020 marine heatwaves were almost as large as the Blob (Harvey et al. 2021, Appendix D).

Figure 2-5 demonstrates the relative intrusion over time of marine heatwaves with coastal waters associated with the Exclusive Economic Zone (EEZ) for the U.S. West Coast (see Figure 2-4). The Blob had high spatial overlap with the EEZ for almost a year, while the incursions in 2019 and 2020 were relatively brief (Figure 2-5). The 2020 heatwave stayed offshore until September, presumably held off by moderate-to-strong upwelling that occurred in the Central and Northern CCE for much of 2020. The heatwave lingered in coastal waters through November, particularly in the Northern CCE, then moved offshore and dissipated during the winter.

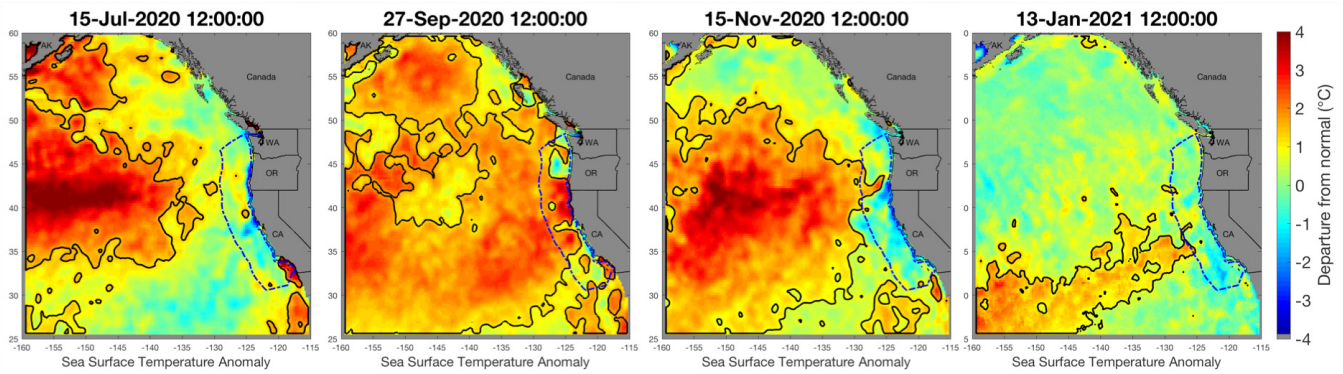


Figure 2-4. Standardized SSTa across the NE Pacific: a) Jul 2020, b) Sep 2020, c) Nov 2020, and d) Jan 2021. Dark contours outline regions that meet the criteria of a marine heatwave (see text); dashed line denotes EEZ boundary. The standardized SSTa is defined as SSTa divided by the SD of SSTa at each location calculated over 1982–2019, thus taking into account spatial variance in the normal fluctuation of SSTa. Plots created by A. Leising (NMFS/SWFSC) using SST data from NOAA’s Optimum Interpolation Sea Surface Temperature analysis (OISST; <https://www.ncdc.noaa.gov/oisst>).

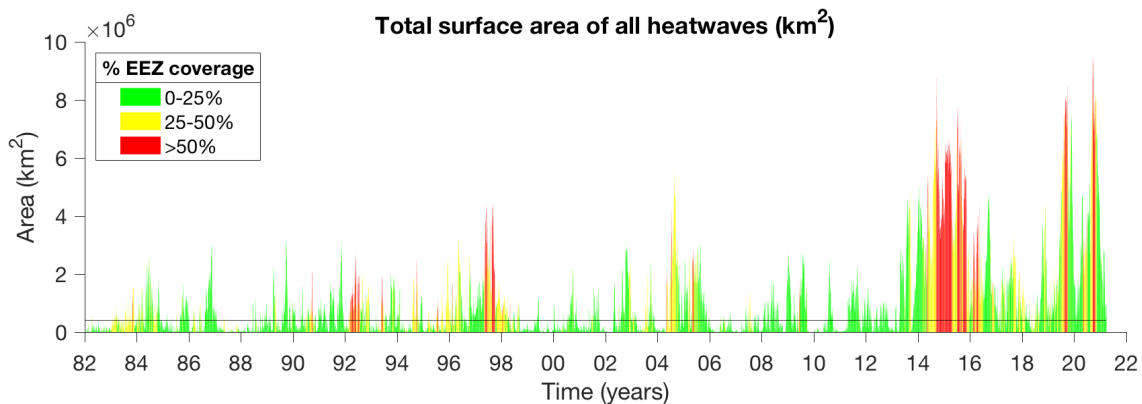


Figure 2-5. Area of North Pacific warm SST anomalies, 1982–2021. The thin horizontal line represents 400,000 km², the area threshold we use for tracking individual heatwave events over time (top 15% of heatwaves by area; Leising in revision). Color indicates the percentage of the U.S. West Coast EEZ that was covered by a given marine heatwave; for example, a tall green peak would indicate a large heatwave outside the 200-nmi EEZ; a red peak indicates a large heatwave covering most of the EEZ and more likely to have an impact on coastal ecosystems. Data courtesy of A. Leising (NMFS/SWFSC).

Although similar in their spatial and temporal patterns in terms of origination, eventual size, and intensity, there are several key differences between the second heatwave of 2020 and the 2019 heatwave. Both events reached their maximum size during late September; however, the 2019 event intersected the coast of Oregon and Washington earlier in September (Thompson et al. 2019b), whereas the 2020 event remained offshore for most parts of the U.S. West Coast until later in September, presumably due to the moderate-to-strong upwelling in summer 2020 (see Section 2.2). Another important difference between the 2019 and 2020 events relates to their spatial patterns during October. The 2019 event shrank and moved from the coast into far offshore waters, whereas the 2020 event cooled in the far offshore region while retaining a significant amount of warm water in the coastal region ~100 km from shore (Figure 2-6). The 2020 event lingered in the coastal regions, mostly off Washington

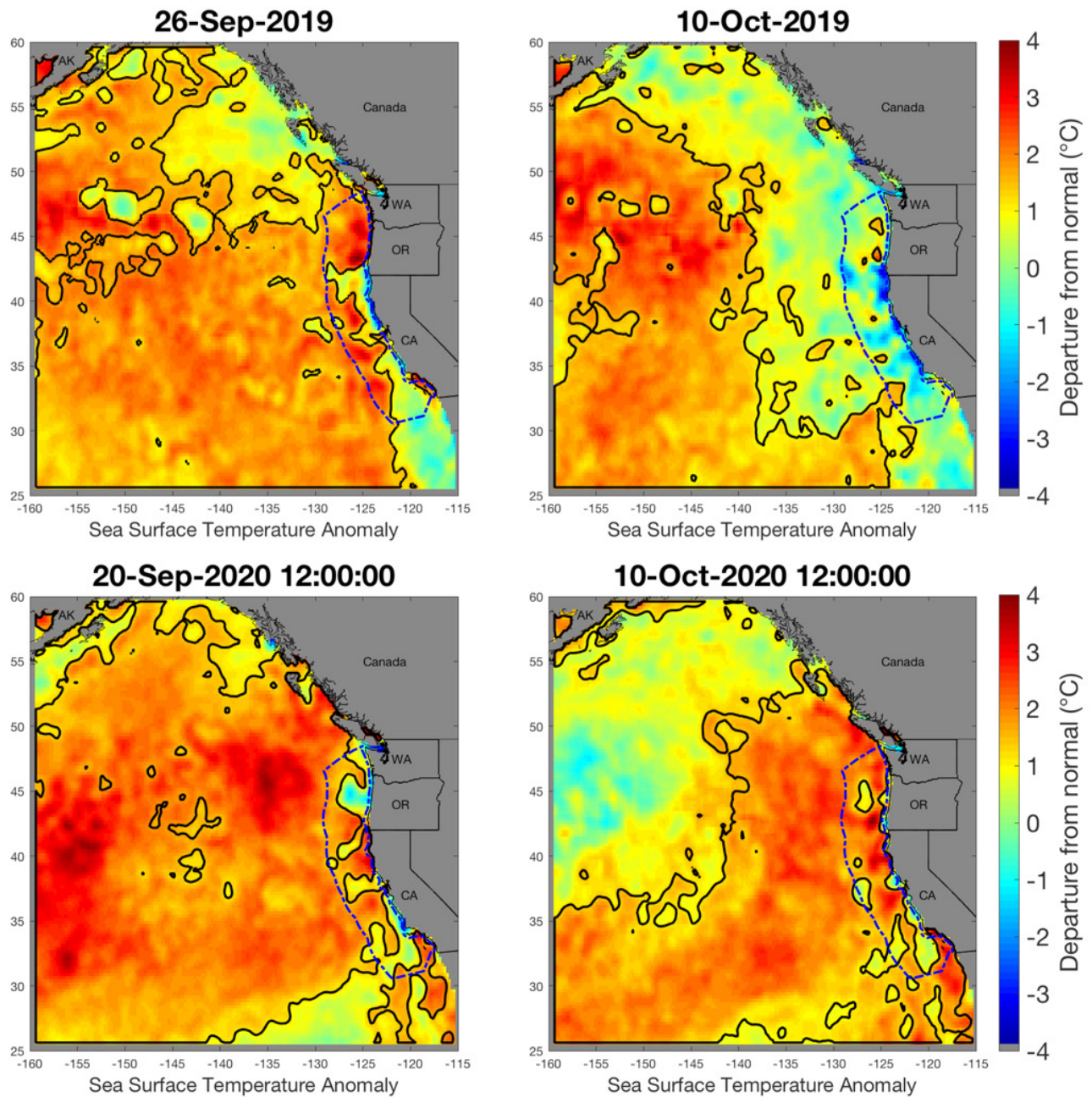


Figure 2-6. Early fall progression of the large marine heatwaves in 2019 and 2020. Dark contours outline regions that meet the criteria of a marine heatwave (see text); dashed line denotes EEZ boundary. Plots created by A. Leising (NMFS/SWFSC) using SST data from OISST (<https://www.ncdc.noaa.gov/oisst>).

and Oregon, for approximately one month longer (until mid-November) than the 2019 event. Lastly, the 2020 event had a significant amount of warming in the offshore regions of Southern California and within the Southern California Bight during most of the year, which was similar to the pattern seen during 2014 but not present during the 2019 event (Figure 2-6).

In summary, following the exceptionally warm Blob of 2013–16 and the 2015–16 El Niño, basin-scale temperatures moderated, but were still warmer than the long-term average. The weak 2018–19 El Niño, a series of short-lived marine heatwaves, and the large 2019 and 2020 marine heatwaves evidence the ongoing potential for heat storage in the central northeastern Pacific.

2.2 Regional Upwelling Indices and Coastal Habitat Compression

Seasonal cross-shore gradients in sea level atmospheric pressure produce the northerly alongshore winds that drive coastal upwelling in the CCE. Upwelling is a physical process of moving cold, nutrient-rich water from deep in the ocean to the surface, which fuels the high seasonal primary production at the base of the CCE food web. The timing, strength, and duration of upwelling vary greatly in space and time. In earlier reports, we summarized upwelling timing and intensity using the well-established Bakun Upwelling Index (BUI), estimated at three-degree latitudinal intervals along the coast. The BUI, derived from the U.S. Navy's Fleet Numerical Meteorology and Oceanography Center's sea level pressure product, provided information on the onset of upwelling-favorable winds ("spring transition"), a general indication of the strength of upwelling, relaxation events, and the end of the upwelling season at a given location. However, the BUI does not take into consideration the underlying ocean structure (e.g., ocean stratification), which can have considerable influence on the nutrient content of the upwelled water. Nor does it consider the influence of ocean circulation, which can impact upwelling. Finally, assumptions of the BUI break down off of Central and Southern California due to features of coastal geography, leading to poor wind (and therefore upwelling) estimates there. Jacox et al. (2018) developed new estimates of coastal upwelling using ocean models to improve upon the BUI by estimating the vertical transport (Cumulative Upwelling Transport Index, or CUTI) and nitrate flux (Biologically Effective Upwelling Transport Index, or BEUTI). These indices are derived from a CCE configuration of the Regional Ocean Modeling System (ROMS) model with data assimilation (Neveu et al. 2016). CUTI provides more accurate estimates of vertical transport of water, whereas BEUTI provides valuable additional information about the nature of the upwelled water (e.g., its nitrate content) that can be linked to ecological processes such as productivity (Jacox et al. 2018).

In the CCE, the timing of peak vertical flux of upwelled water (indicated by CUTI) varies by latitude, with northern latitudes having a later onset of maximum upwelling (Figure 2-7, left, shaded areas). The maximum climatological values of CUTI (Figure 2-7, left, dashed line) are at the end of April at lat 33°N (San Diego), the middle of June at lat 39°N (Point Arena, California), and the end of July at lat 45°N (Newport). Values of CUTI at Point Arena tend to be roughly a factor of two greater than at the other two latitudes. The magnitude of vertical nitrate flux (BEUTI) also varies greatly by latitude (Figure 2-7, right, shaded areas). At Point Arena, BEUTI is about an order of magnitude larger at its peak than at the other latitudes, and this much larger amount of nutrient input in upwelled water likely contributes to the high productivity of lower trophic levels in this region of the coast. At Newport, and to a lesser extent at Point Arena, downwelling occurs in the winter due to poleward-blowing winds. (Note that a negative value of BEUTI accompanying downwelling suggests removal of nitrate, but a source has not been identified.)

In 2020, Point Arena and Newport saw frequent upwelling events, with peaks ≥ 1 SD above the mean, usually followed by relaxation events (Figure 2-7, left). Upwelling events provided inputs of nitrate into the surface waters, especially the strong upwelling events in February and June at Point Arena (Figure 2-7, right). When upwelling is followed by relaxation, as occurred in 2020, the upwelled nutrients may be more likely to be retained and spur coastal production. Also, the large upwelling events in winter may have provided an early injection of nutrients before the spring transition into the productive season for the coastal food web.

The high-frequency cycling between upwelling events and relaxation or downwelling periods pictured in Figure 2-7 appears critical for the uptake of nutrients by phytoplankton and the availability of phytoplankton for higher trophic levels. These cycles, or Lasker events (Lasker 1978), create a balance of the supply of nutrients in the upwelled water, and the nutrient residence time allows for phytoplankton growth. With insufficient upwelling, there are not enough nutrients for phytoplankton growth, while with extended upwelling, the nutrients are carried out to the open ocean. Jacox et al. (2016) described the theoretical balance, while Wilkerson et al. (2006) described that an optimal window of 3–7 days of relaxation following an upwelling event was required for chlorophyll accumulation in the Central California region off Bodega Bay, California. Lasker (1978) also found cycling shifts in the Southern California phytoplankton population between dinoflagellates and diatoms, with the larger dinoflagellates providing more of the caloric requirements of first-feeding anchovy larvae.

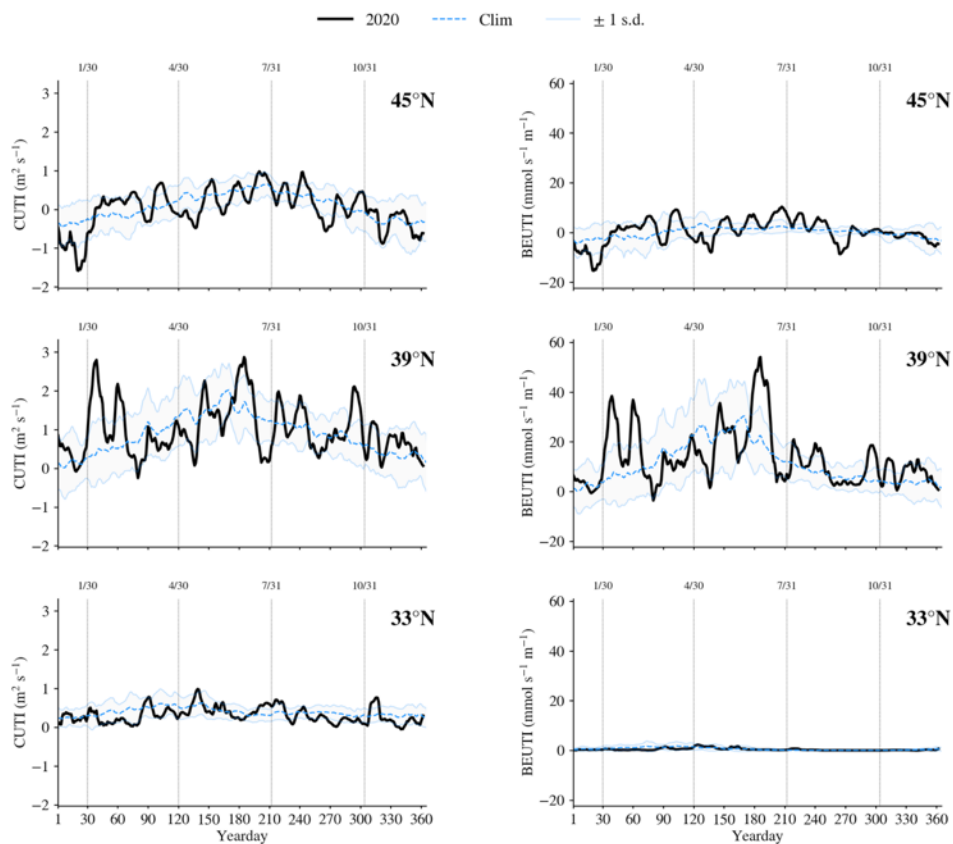


Figure 2-7. Daily 2020 estimates of vertical transport of water (CUTI, left) and nitrate (BEUTI, right) from 1 Jan–31 Dec, relative to 1988–2019 climatology (blue dashed line) ± 1.0 SD (shaded area), at lats 33°N, 39°N, and 45°N. Daily data are smoothed with a 10-day running mean. Vertical lines mark the ends of Jan, Apr, Jul, and Oct. Daily 2020 CUTI and BEUTI values are provided by M. Jacox (NMFS/SWFSC); detailed information about these indices can be found at <https://go.usa.gov/xG6Jp>.

Upwelling creates a band of relatively cool water along the coast during the spring and summer, providing suitable habitat for a diverse and productive portion of the CCE food web. A new concern that emerged in the CCE during the anomalously warm years that began with the Blob is “habitat compression.” Santora et al. (2020) used this term to denote how offshore warming during the Blob restricted the relatively cool upwelling habitat to a narrower-than-normal band along the coast in the CCE configuration of the ROMS model with data assimilation (Neveu et al. 2016). This compression of the upwelling habitat consequently altered pelagic species composition and distribution, from forage species to top predators, and likely contributed to impacts such as increased rates of whale entanglements in fixed fishing gear.

Santora et al. (2020) developed a Habitat Compression Index (HCI) to track latitudinal changes in the area of cool upwelled surface waters. They defined HCI for a region of Central California, and have since expanded it to four biogeographical provinces within the CCE: lats 48–43.5°N, 43.5–40°N, 40–35.5°N, and 35.5–30°N. HCI is defined as the fractional area of monthly averaged ROMS model temperatures at a depth of 2 m that falls below a temperature threshold. These unique temperature thresholds are defined as the spatial average of all 2-m ROMS temperatures from the coast to 75 km offshore within the latitudinal region for a given month over a climatological period of 1980–2010. Winter and spring means for all four regions are shown in Figure 2-8.

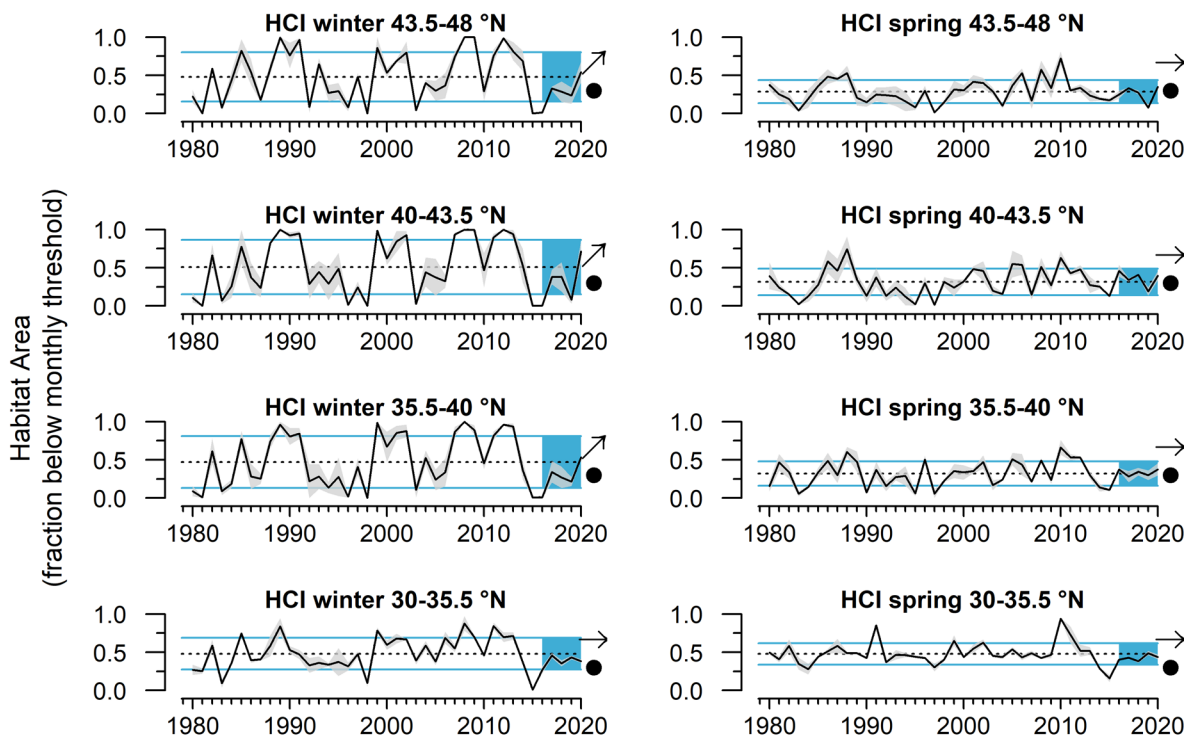


Figure 2-8. Mean winter (Jan–Mar) and spring (Apr–Jun) Habitat Compression Index (HCI), by region, 1980–2020. Error envelope indicates ± 1.0 SE. HCI estimates developed and provided by J. Santora (NMFS/SWFSC) and I. Schroeder (NMFS/SWFSC, UCSC). Lines, colors, and symbols as in Fig. 1-3a.

The most evident patterns in the seasonal means are recent positive trends in wintertime HCI in the three northerly regions, and spring 2020 means that are generally close to the long-term means in all regions (Figure 2-8). The positive winter trends from 2016–20 are due to the very low 2016 HCI, reflecting high compression of cool winter habitat in that year in all but the southernmost region. The 2020 winter means are mostly close to average, so even with the moderate-to-strong winter upwelling (Figure 2-7), HCIs remain considerably lower (more compressed) than peak values last seen before the Blob (Figure 2-8). Similarly, the spring means are close to average, an improvement over means in 2014–16 (particularly south of lat 43.5°N), but remain well below model estimates from before the Blob.

2.3 Hypoxia and Ocean Acidification

Nearshore dissolved oxygen (DO) depends on many processes, including currents, upwelling, air–sea exchange, and community-level production and respiration in the water column and benthos. DO is required for organismal respiration; low DO can compress habitat and cause stress or die-offs for sensitive species. Waters with DO levels <1.4 mL/L (2 mg/L) are considered to be hypoxic; such conditions may occur on the shelf following the onset of spring upwelling, and continue into the summer and early fall months until the fall transition mixes shelf waters. Upwelling-driven hypoxia occurs because upwelled water from deeper ocean sources tends to be low in DO, and microbial decomposition of organic matter in the summer and fall increases overall system respiration and oxygen consumption, particularly closer to the seafloor.

Low DO was a serious issue in the Northern CCE in 2020, as it has been in other recent years. Near-bottom DO at Station NH05 (5 nmi off Newport) fell below the hypoxia threshold in June–August 2020, and was similar in intensity to 2019 (Figure 2-9, top). Off San Diego at CalCOFI Station 93.30, near-bottom DO was above the hypoxia threshold in winter and summer (Figure 2-9, bottom; no spring data).

In the CalCOFI region of the Southern CCE (see Figure 1-4a), summer 2020 DO values displayed strong inshore–offshore and depth gradients, with higher values measured farther offshore and lower values measured at depth. DO concentrations were above the hypoxic threshold for all stations at depths of 50 m and 150 m (Figure 2-10, left and center). At 50 m, summer DO at stations farthest offshore was well above the hypoxia threshold, although many stations had the lowest observed summer

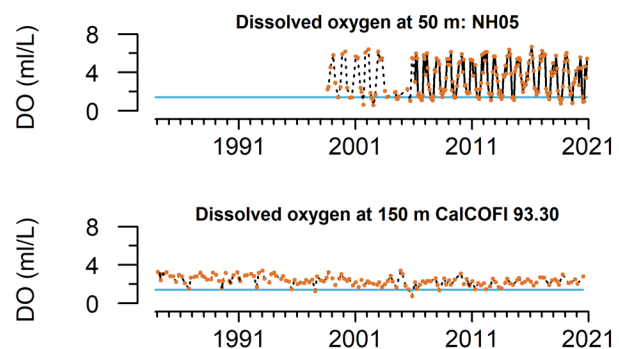


Figure 2-9. Dissolved oxygen (DO) through 2020 at: (top) 50-m depth, Station NH05, 5 nmi off Newport, and (bottom) 150-m depth, CalCOFI Station 93.30, <50 km off San Diego. Blue line is the hypoxic threshold of 1.4 mL/L DO. Dotted black line indicates missing data. Lines, colors, and symbols as in Fig. 1-3b. Newport Hydrographic (NH) Line DO data from J. Fisher (NMFS/NWFSC, OSU). CalCOFI data compiled by I. Schroeder (NMFS/SWFSC, UCSC) using CalCOFI data* from <https://calcofi.org>. * Pre-2020 CalCOFI data are from the bottle data database; 2020 data are preliminary and come from the recent CTD database.

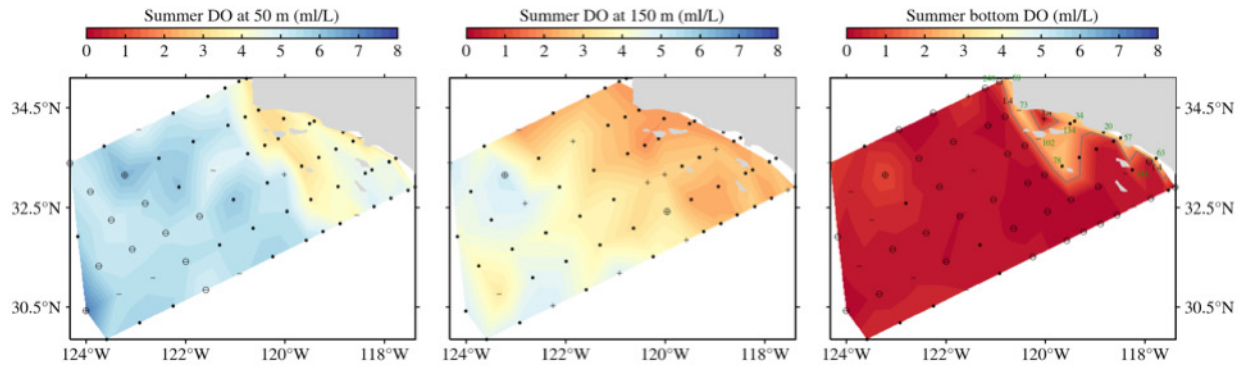


Figure 2-10. Dissolved oxygen (DO) observations during the summer 2020 CalCOFI survey of the Southern CCE at 50 m (left), 150 m (middle), and at the bottom of the hydrographic cast (right). DO was sampled at hydrographic stations (black dots). Hydrographic casts extended to the bottom or to a max depth of 500 m; only a small number of stations near shore or islands have bottom depths <500 m. These stations have the bottom depths labeled in green. Black dots are changed to either a minus (-) or a plus (+) if the measured value is less or greater than 1 SD above the long-term mean, respectively. Also, if the measured value is the smallest or largest value ever sampled since 1984, the symbol is surrounded by a black circle. The 1.4-mL/L contour level is labeled if it exists. DO data compiled by I. Schroeder (NMFS/SWFSC, UCSC) using CalCOFI data from <https://calcofi.org>.

concentrations since the time series began in 1984 (Figure 2-10). CalCOFI data are collected to 500-m depth or the bottom, whichever is shallower; in summer 2020, hypoxic conditions existed at the bottom depth for all stations except the shallower nearshore stations.

Ocean acidification (OA), caused by anthropogenically increased levels of atmospheric CO_2 entering the ocean, reduces pH and carbonate ion levels in seawater. A key indicator of OA is the aragonite saturation state, a measure of the availability of aragonite (a form of calcium carbonate). Aragonite saturation <1.0 indicates corrosive conditions that have been shown to be stressful for many CCE species, including oysters, crabs, and pteropods (Barton et al. 2012, Bednaršek et al. 2014, Marshall et al. 2017, Hodgson et al. 2018). Upwelling, which drives primary production in the CCE, also transports hypoxic, acidified waters from offshore onto the continental shelf, where increased community-level metabolic activity can further exacerbate OA (Chan et al. 2008, Feely et al. 2008). As a result, aragonite saturation levels tend to be lowest during and following upwelling in the spring and summer, and highest during the winter. Rivers in the region also tend to be undersaturated, and may contribute further to corrosivity (Feely et al. 2018).

Aragonite saturation is measured through the water column off Newport at Stations NH05 and NH25. Time series at both stations reveal the seasonal variability of the depth of the corrosive waters. Generally, at NH05, the waters from about 15 m to the bottom become corrosive in summer and fall, and the entire water column is above the saturation value in winter and into spring. Offshore, at NH25, waters below about 140 m remain corrosive year-round, and the annual variability is between ~50–140 m (Figure 2-11).

More of the water column was undersaturated in 2020 (i.e., aragonite saturation state <1.0) during peak periods of corrosivity than in 2019 (Figure 2-11). The corrosive water on the shelf at NH05 is largely driven by seasonal upwelling, where upwards of 80% of the water

column becomes corrosive each summer. In 2020, the corrosive water came within ~5 m of the surface, the shallowest level of this isocline of the entire time series. A brief winter spike in corrosivity in early 2020 can also be seen (recall that there was strong winter upwelling in 2020). While the offshore station over the slope at NH25 is slightly influenced by seasonal upwelling and downwelling, a much larger portion of the water column remains undersaturated throughout the year (Figure 2-11). As with Station NH05, the aragonite saturation horizon at NH25 reached a shallower depth in 2020 than in 2019, although it was not unusual relative to long-term observations.

Seasonal forecasts for dissolved oxygen and aragonite saturation are available for a portion of the CCE, and provide projections for conditions in spring and summer of

2021. The forecasting system was originally developed at the University of Washington Joint Institute for the Study of the Atmosphere and Ocean (JISAO), and the model system is called J-SCOPE (JISAO's Seasonal Coastal Ocean Prediction of the Ecosystem).⁸ J-SCOPE provides short-term skilled forecasts of ocean conditions off Washington and Oregon based on dynamically downscaled 6- to 9-month forecasts from the global-scale NOAA Climate Forecast System model. J-SCOPE forecasts have been extended to include seasonal predictions of habitat quality for sardines (Kaplan et al. 2016, Siedlecki et al. 2016). Each January and April, the J-SCOPE modelers produce an ensemble of three forecasts that project ocean conditions through September and include variables like temperature, DO, chlorophyll, aragonite saturation state (OA), and sardine habitat, in addition to other dynamics such as the timing and intensity of upwelling.

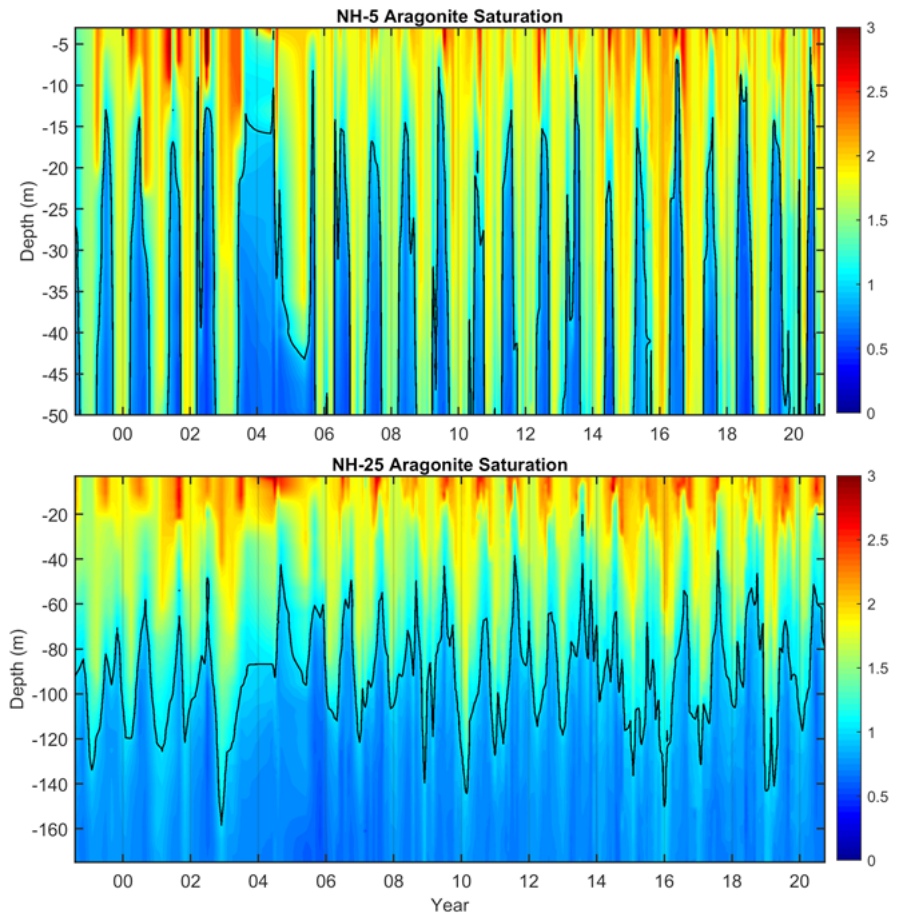


Figure 2-11. Vertical profiles of aragonite saturation at Stations NH05 and NH25 off Newport, 1999–2020. Black line indicates the depth at which aragonite saturation state = 1.0, considered a biological threshold below which seawater can be especially corrosive to shell-forming organisms. Stations NH05 and NH25 are 5 and 25 nmi offshore, respectively. Aragonite saturation state data provided by J. Fisher (NMFS/NWFSC, OSU).

⁸ <http://www.nanoos.org/products/j-scope>

According to the January J-SCOPE ensemble forecast of the 2021 summer upwelling season (May–August):

- Sea surface temperatures of coastal waters in the Northern CCE are forecast to be near the average of recent years until late summer (July–August), when they become warmer; these warm anomalies do not extend to subsurface habitats, which are forecast to be slightly cooler than average.
- Dissolved oxygen on the bottom is forecast to be lower than previous years on average over the entire Washington and Oregon continental shelves early and into the upwelling season, with the Oregon shelf trending toward near-average values later in the upwelling season.
- Hypoxia ($DO < 2 \text{ mg/L}$) is forecast to be prominent over much of the Washington and all of the Oregon shelf as early as May and spreading to nearly all of Washington’s shelf by July (Figure 2-12)—earlier than average for recent years.
- Aragonite saturation at the bottom is expected to decrease over the course of the spring and summer, with most of the bottom waters in the region undersaturated (i.e., more corrosive), except for some isolated coastal locations in Washington (Figure 2-13). Surface waters are expected to increase over the spring and into the upwelling season (May–June), with saturation maximized in midsummer (July–August).

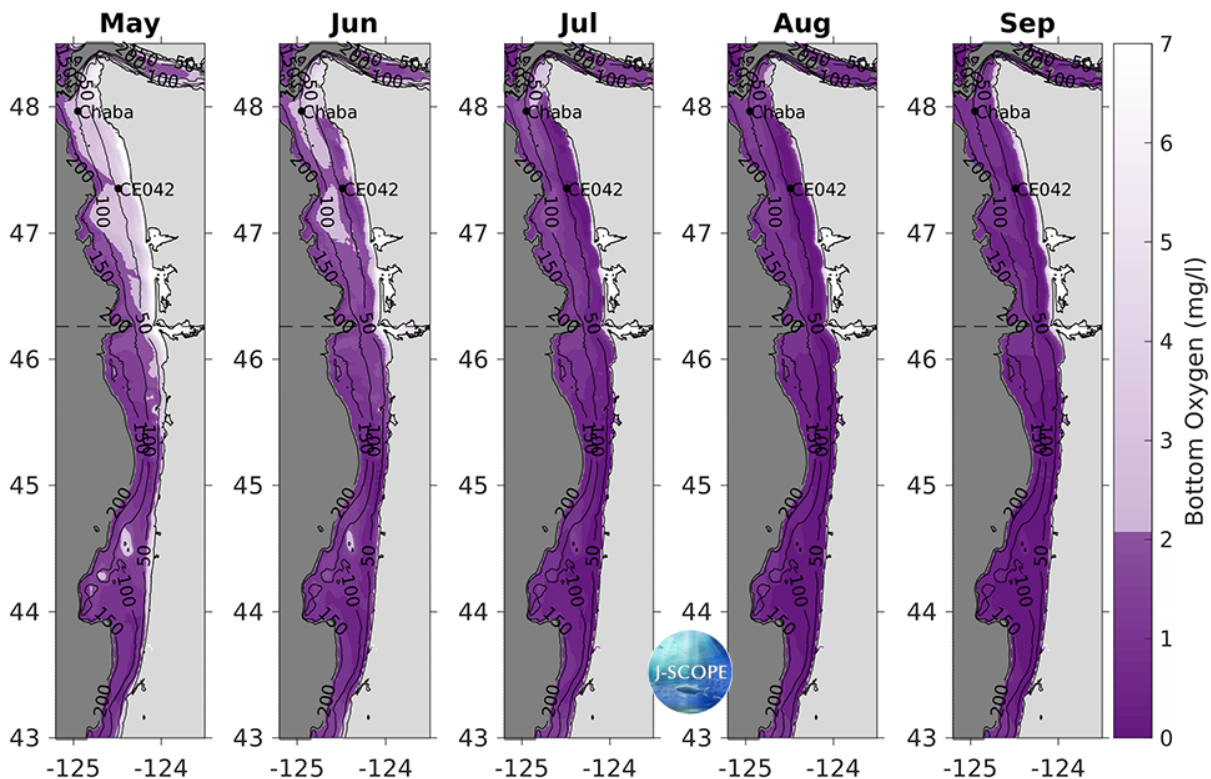


Figure 2-12. J-SCOPE forecasts of bottom DO, May–Sep 2021, averaged over all three ensemble members. Hypoxia ($O_2 < 2 \text{ mg/L}$) is shown in dark purple, offshore areas dark gray, and land light gray. The black horizontal dashed line indicates the boundary between WA and OR waters. Black contours indicate bathymetry on the shelf. J-SCOPE ensemble forecast maps provided by the J-SCOPE team, <http://www.nanoos.org/products/j-scope/forecasts.php>.

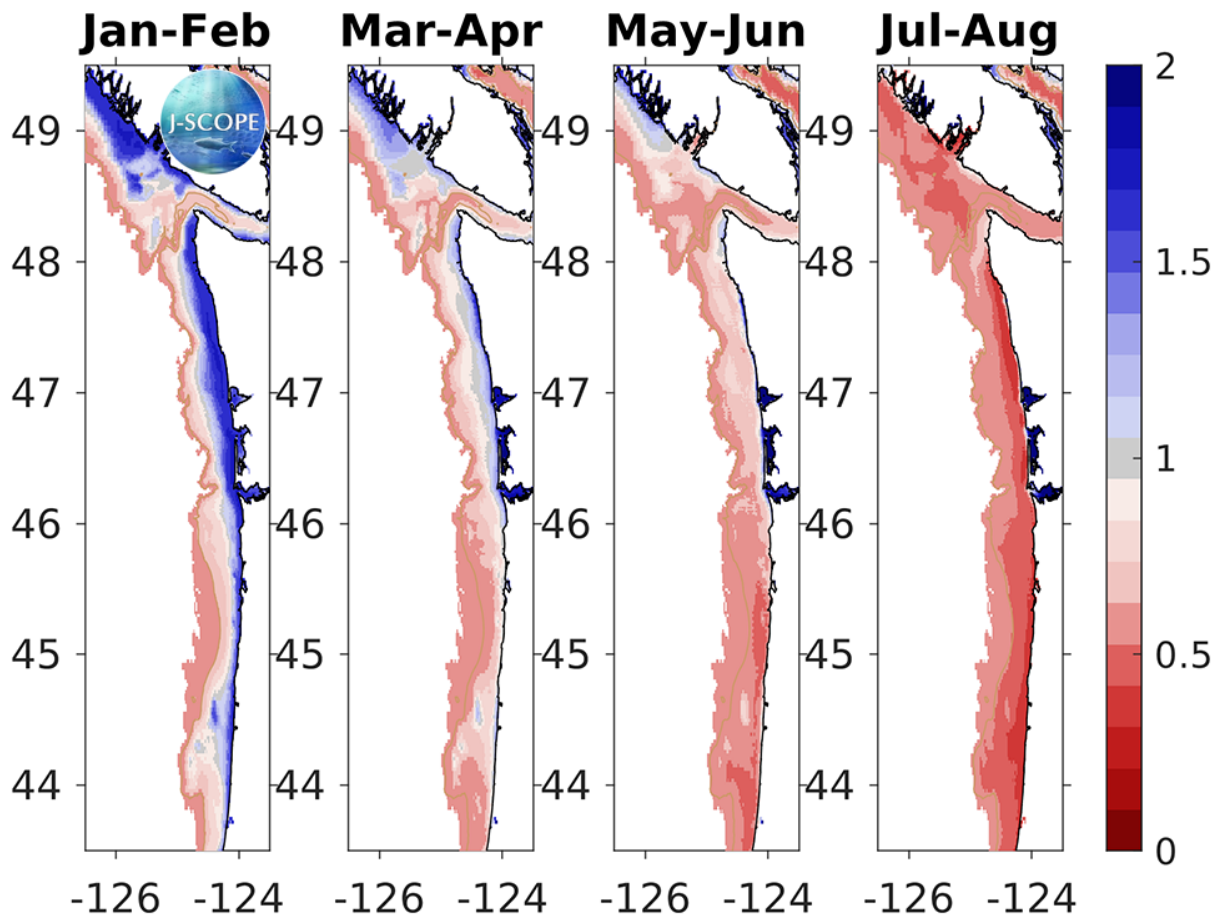


Figure 2-13. J-SCOPE forecasts of bottom aragonite saturation state (Ω), Jan–Aug 2021, averaged over all three ensemble members. For reference, $\Omega = 1$ is broadly considered the boundary between undersaturated and saturated conditions, but stressful conditions for juvenile oysters begin to occur before the waters become undersaturated ($\Omega \leq 1.3$). The 200-m isobath is outlined by the beige contour line. J-SCOPE ensemble forecast maps provided by the J-SCOPE team, <http://www.nanoos.org/products/j-scope/forecasts.php>.

- Chlorophyll-*a* concentrations are forecast to be lower than average early in the upwelling season over the Washington and Oregon shelves, but near or slightly lower later in the upwelling season. However, chlorophyll-*a* concentration will be higher than average near the mouths of the Strait of Juan de Fuca and the Columbia River, both during and later in the upwelling season.
- Recently developed models now provide environmentally driven seasonal forecasts for Pacific hake (*Merluccius productus*) occurrence and distribution over the model region.

The detailed forecasts for temperatures, chlorophyll, and sardines can be viewed at the J-SCOPE website. Additional forecasts for Dungeness crab (*Metacarcinus magister*) will be available in future years, and similar types of seasonal forecasts at the spatial scale of the full California Current are expected in the future as well. By making these forecasts available to PFMC and other partners, we hope to provide useful, skilled forecast information to assist with decision-making prior to the periods at which most productivity and harvest is occurring in key fishery sectors.

2.4 Hydrologic Indicators

Freshwater habitat conditions are critical for salmon and other anadromous species, and for estuaries that support many marine species. Indicators are reported based on a hierarchical spatial framework and are summarized by freshwater ecoregion (Figure 1-4b, as derived from Abell et al. (2008) and [Freshwater Ecoregions of the World](http://www.feow.org)⁹) or, where possible, by salmon evolutionarily significant units (ESUs, sensu Waples 1995). Within ecoregions, we summarized data by Chinook salmon ESUs. Status and trends for all freshwater indicators are estimated using space–time models (Lindgren and Rue 2015), which account for temporal and spatial autocorrelation.

The freshwater indicators presented here focus on salmon habitat conditions as related to snowpack, streamflow, and temperature. Snow-water equivalent (SWE) is the total water content in snowpack, which provides a steady source of cool, fresh water that is vital for salmon in the warm summer months (Munsch et al. 2019). Maximum streamflows in winter and spring are important for habitat formation, and in California can be important for removing a polychaete worm that is the obligate host of the salmon parasites *Ceratonova shasta* and *Parvicapsula minibicornis* (Alexander et al. 2014, True et al. 2017); however, extreme discharge relative to historic averages can potentially cause scouring of eggs from salmon redds (DeVries 1997), thereby reducing abundance and productivity (Greene et al. 2005, Zimmerman et al. 2015). Below-average minimum streamflows in summer and fall can restrict habitat for instream juveniles and migrating adults (Bradford and Heinonen 2008), and high summer water temperatures can cause impaired physiology and increased mortality for both juveniles (Marine and Cech 2004, Richter and Kolmes 2005) and returning adults (Jeffries et al. 2012). All freshwater indicators are influenced by climate and weather patterns, and intensifying climate change is expected to exacerbate high temperatures, low SWEs, and extreme flow events.

On 1 April 2021, SWEs in the northern ecoregions (Salish Sea/WA Coast, Columbia Glaciated, Columbia Unglaciated) were higher than or close to long-term means (Figure 2-14). However, SWEs in the southern ecoregions (OR/NorCal Coast, Sacramento/San Joaquin, SoCal Bight) were below average in 2021, with SWE in Sacramento/San Joaquin ~1 SD below average for the second year in a row. Due to COVID-19, ampling was down about 30% in Sacramento/San Joaquin, increasing the variability. In other areas, sampling reduction was small and appears not to have had much effect on SWE data quality.

The map in Figure 2-15 shows that SWE measured on 1 April 2021 varied considerably by ecoregion; stations in much of Washington, northern Idaho, and northern Oregon exceeded the long-term median, whereas most stations in California, central and southern Oregon, and southwestern Idaho were at or below the long-term median (Figure 2-15).

⁹ <http://www.feow.org>

Moderate to severe droughts were forecast for Northern California, Oregon, and parts of Washington in April 2020. These intensified to severe–extreme conditions in summer and triggered catastrophic wildfires throughout the West. The [NOAA Drought Monitor](#)¹⁰ for 11 May 2021 reveals that most of the western United States is in moderate to exceptional drought, with an outlook of continued drought through 31 July 2021. The low SWE, early melt, drought, low fuel moisture, and other conditions suggest above-normal wildland fire potential for central Washington and Oregon, eastern (Sierra) California, and the California coastal region from San Francisco Bay to the U.S.–Mexico border by July.¹¹

Mean maximum stream temperatures in August were determined from 446 U.S. Geological Survey (USGS) gages with temperature monitoring capability. While these gages did not necessarily operate simultaneously throughout the period of record, at least two gages provided data each year in all ecoregions. Stream temperature records are limited in California, so the Sacramento/San Joaquin and SoCal Bight ecoregions were combined. Maximum temperatures exhibit strong ecoregional differences (for example, Salish Sea/WA Coast streams are much cooler on average than California streams). The most recent five years have been marked by largely average values regionwide (Figure 2-16). One exception is Salish Sea/WA Coast, which experienced above-average temperatures for much of the period of 2014–19 before returning close to average in 2020. Another exception is that August stream temperatures from coastal Oregon and in California increased in 2020 compared to 2019, and were comparable to the marine heatwave years of 2014–15.

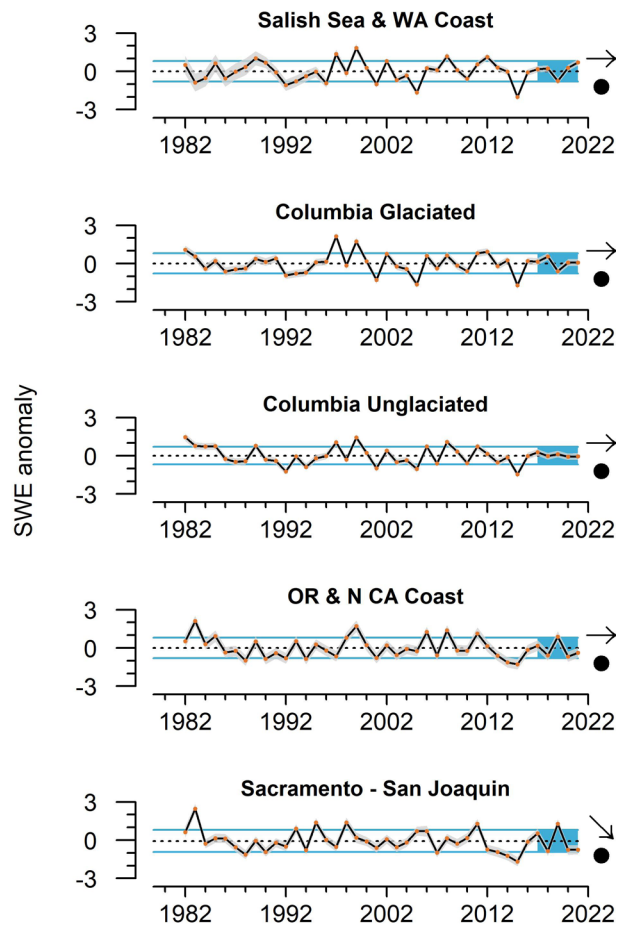


Figure 2-14. Anomalies of 1 Apr SWE in five freshwater ecoregions of the CCE through 2021. Ecoregions as in Fig. 1-4a. Error envelopes represent 2.5% and 97.5% upper and lower credible intervals. Symbols to the right follow those in Fig. 1-3a, but were evaluated based on whether the credible interval overlapped zero (slope of the 5-year trend) or the long-term mean (5-year mean). SWE data derived from the CA Department of Water Resources snow survey (<http://cdec.water.ca.gov/>) and the Natural Resources Conservation Service’s SNOTEL sites in WA, OR, CA, and ID (<http://www.wcc.nrcs.usda.gov/snow/>); data analysis and plotting by S. Munsch (NMFS/NWFSC, Ocean Associates, Inc.).

¹⁰ <https://www.cpc.ncep.noaa.gov/products/Drought>

¹¹ https://www.predictiveservices.nifc.gov/outlooks/monthly_seasonal_outlook.pdf

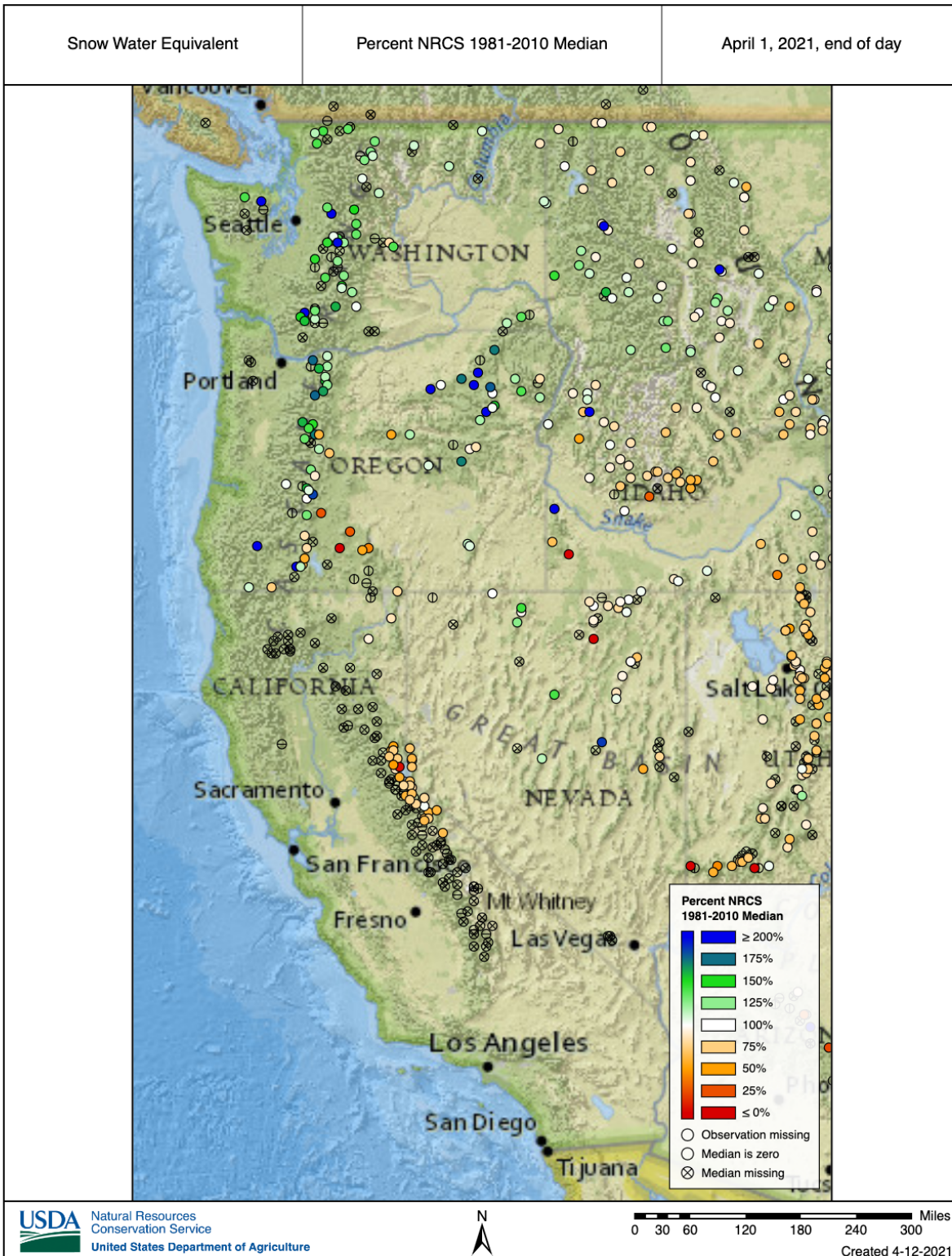


Figure 2-15. Mountain snowpack on 1 April 2021 at select monitoring sites, relative to 1981–2010 median value. Open circles are stations that either lack current data or long-term median data. Snowpack data were obtained from interactive map products produced by the Natural Resources Conservation Service (NRCS), presented as SWE percentile compared to period of record: https://www.wcc.nrcs.usda.gov/snow/snow_map.html.

Streamflow indicators are derived from active USGS stream gages with records of at least 30 years' duration. We use standardized anomalies of streamflow time series from 213 individual gages. Daily means were used to calculate annual one-day maximum and seven-day minimum flows, corresponding to flow parameters to which salmon populations are most sensitive. Across ecoregions of the California Current, both minimum and maximum streamflow anomalies have exhibited some variability in the most recent five years, although generally not outside of historical ranges. Minimum stream flows have exhibited fairly consistent patterns across all ecoregions, and were close to long-term means in 2020 (Figure 2-17). Sacramento/San Joaquin exhibited a slight decline compared to 2019, while Salish Sea/WA Coast returned close to average in 2020 after several years of below-average minimum flows.

Because high rates of winter flow are generally beneficial for juvenile salmon in southerly ecoregions, the low winter values in both 2018 and 2020 in southern ESUs suggest worsening conditions for egg and alevin incubation. Maximum flows in 2020 declined in several of the California Current's ecoregions relative to 2019 (Figure 2-18). In Sacramento/San Joaquin, maximum flows were even lower than in the Blob year of 2015, and the OR/NorCal Coast ecoregion also experienced maximum flows that were well below average.

Variability across basins exists within each ecoregion. To capture this, we also summarized streamflows at the finer scale of individual Chinook salmon ESUs. These results are presented in quad plots, showing flow anomalies and 95% credible intervals to indicate which ESUs had significant trends from 2016–20, or short-term averages that differed from the long-term means. Significance is associated with credible intervals that do not overlap with zero on one or both axes; these credible intervals take into account

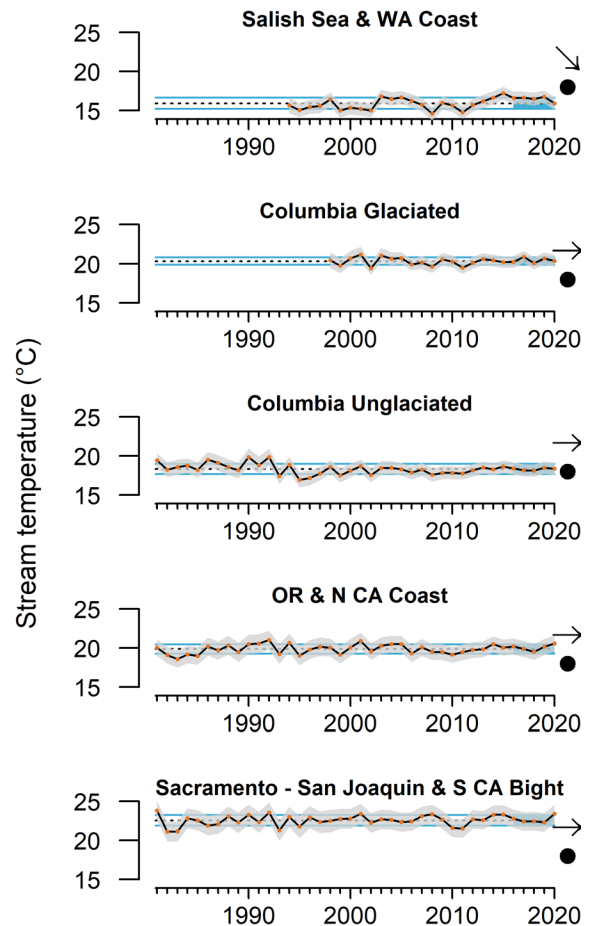


Figure 2-16. Mean max stream temperature in Aug measured at 466 USGS gages in 6 ecoregions (Sacramento/San Joaquin and SoCal Bight combined), 1981–2020. Gages include both regulated (subject to hydropower operations) and unregulated systems, although trends were similar when these systems were examined separately. Error envelopes represent 2.5% and 97.5% upper and lower credible intervals. Symbols to the right follow those in Fig. 1-3a, but were evaluated based on whether the credible interval overlapped zero (slope of the 5-year trend) or the long-term mean (5-year mean). Stream temperature data provided by USGS (<http://waterdata.usgs.gov/nwis/sw>); data analysis and plotting by S. Munsch (NMFS/NWFSC, Ocean Associates, Inc.).

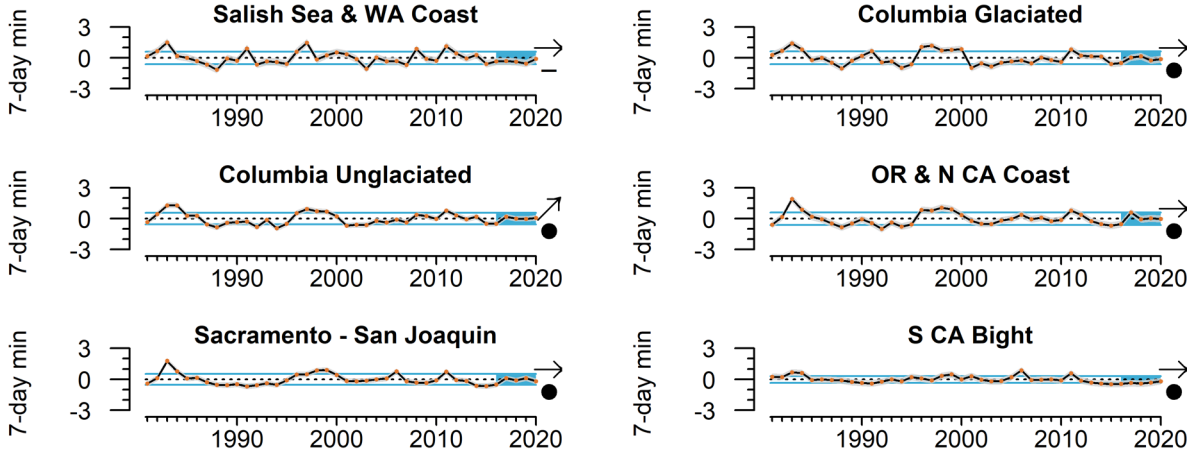


Figure 2-17. Anomalies of the 7-day minimum streamflow measured at 213 gages in 6 ecoregions, 1981–2020. Gages include both regulated (subject to hydropower operations) and unregulated systems, although trends were similar when these systems were examined separately. Error envelopes represent 2.5% and 97.5% upper and lower credible intervals. Symbols to the right follow those in Fig. 1-3a, but were evaluated based on whether the credible interval overlapped zero (slope of the 5-year trend) or the long-term mean (5-year mean). Minimum streamflow data provided by USGS (<http://waterdata.usgs.gov/nwis/sw>); data analysis and plotting by S. Munsch (NMFS/NWFSC, Ocean Associates, Inc.).

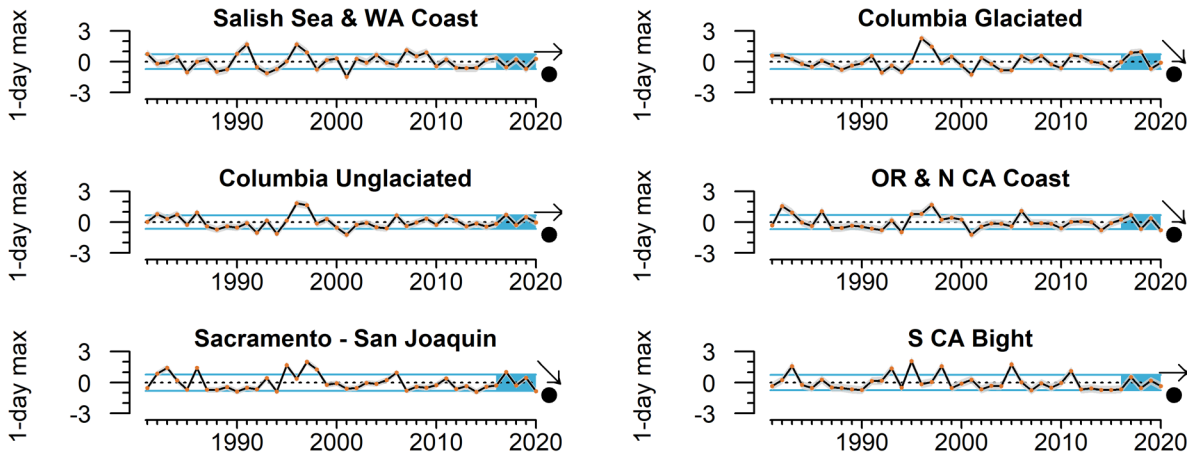


Figure 2-18. Anomalies of the 1-day maximum streamflow measured at 213 gages in 6 ecoregions, 1981–2020. Gages include both regulated (subject to hydropower operations) and unregulated systems, although trends were similar when these systems were examined separately. Error envelopes represent 2.5% and 97.5% upper and lower credible intervals. Symbols to the right follow those in Fig. 1-3a, but were evaluated based on whether the credible interval overlapped zero (slope of the 5-year trend) or the long-term mean (5-year mean). Maximum streamflow data provided by USGS (<http://waterdata.usgs.gov/nwis/sw>); data analysis and plotting by S. Munsch (NMFS/NWFSC, Ocean Associates, Inc.).

spatial correlations between different gages within a given ESU. With the exception of two ESUs in the Columbia River system, maximum flows had either declining or nonsignificant trends from 2016–20; in general, maximum flows were close to or above average during that period (Figure 2-19, left). Because high winter maximum flows are generally beneficial for juvenile salmon in southerly populations, the negative winter trends in southern ecoregions, driven by low values in 2018 and 2020, suggest worsening recent conditions for egg and alevin incubation. Minimum flows were generally close to long-term averages, but some ESUs experienced increasing minimum flows over the past five years, including the Snake River fall and both Central Valley ESUs (Figure 2-19, right). Minimum flows in the Washington Coast and Lower Columbia River ESUs have been below average in recent years. Time series summarized in these quad plots can be found in Harvey et al. (2021), Appendix F.

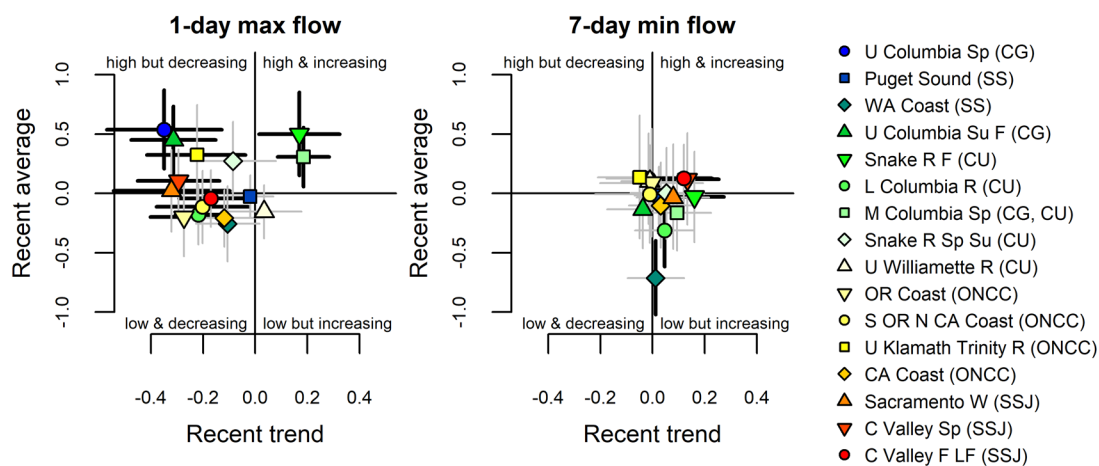


Figure 2-19. Recent (5-year) trend and average of maximum and minimum streamflow anomalies in 16 freshwater Chinook salmon ESUs in the CCE through 2020. ESU symbols are color-coded from north (blue) to south (red). Error bars represent 2.5% and 97.5% upper and lower credible intervals. Gray error bars overlap zero, while heavy black error bars differ from zero. Abbreviations in the legend refer to the ESU’s freshwater ecoregion shown in Fig. 1-4b (CG = Columbia Glaciated, SS = Salish Sea, CU = Columbia Unglaciated, ONCC = OR/NorCal Coast, SSJ = Sacramento/San Joaquin). Lines and symbols as in Fig. 1-3c. Max/min streamflow data provided by USGS (<http://waterdata.usgs.gov/nwis/sw>); data analysis and plotting by S. Munsch (NMFS/NWFSC, Ocean Associates, Inc.).

3 Lower Trophic Levels and Forage

Jennifer Fisher, Kym Jacobson, Samantha Zeman, Eric Bjorkstedt, Roxanne Robertson, Cheryl Morgan, Brian Burke, John Field, Jarrod Santora, Keith Sakuma, Andrew Thompson, Stephanie Moore, Clarissa Anderson, Eva Ternon, Melissa Carter, Tracie Barry, Matthew Hunter, Caren Braby, Jerry Borchert, Alex Manderson, Christy Juhasz, Christina Grant, Duy Trong, Vanessa Zubkousky-White, Beckye Stanton, Zachary Forster, Dan Ayres, and Gregory D. Williams

The CCIEA team examines many indicators related to the ecological integrity of the CCE, particularly the abundance and condition of key species, the dynamics of community structure, and ecological interactions. Lower trophic level species—phytoplankton, zooplankton, and small, schooling invertebrates and fishes—form essential links between climate, physics, and biogeochemistry (described in the previous section) and higher consumers such as larger fishes, seabirds, marine mammals, and people (described in sections that follow). Oceanographic processes also drive production of phytoplankton species that can produce toxins; excessive blooms of these species can have negative effects on species and people. This section of the report focuses on indicators related to these lower trophic level processes. It includes information on zooplankton, harmful algal blooms (HABs), and forage dynamics. Here, “forage” refers to the representative species and age groups of small pelagic fishes and invertebrates that are sampled by regional cruises (Figure 1-4a). We consider catch data from these regional cruises to be indicators of relative forage community composition, availability, and variability, not indices of absolute abundance of coastal pelagic species (CPS) that are targeted by commercial fisheries. Absolute abundance estimates of fish populations come from PMFC adopted stock assessments (e.g., PFMC 2019a) and comprehensive monitoring programs, rather than from these regional cruises that were designed for other purposes, as are outlined later in this section.

Between 2014 and 2016, many ecological metrics indicated conditions of poor productivity at lower trophic levels and poor foraging conditions for many predators. A notable exception was that anchovy increased dramatically in 2016, resulting in improved forage conditions for predators that feed on anchovy (e.g., sea lions). In 2017–18, there were some signs that indicator species abundance, condition, and composition were returning to more average conditions, although there were many exceptions that implied residual effects of the anomalous warming events. In 2019, ecological indicators implied average to above-average productivity in the Northern and Southern portions of the CCE, but average to below-average conditions in the Central CCE. The mid-2019 marine heatwave may have affected portions of the system later in the year, but we have relatively little ecological data to demonstrate impacts (Harvey et al. 2020).

Biological and ecological survey data suggest average to above-average feeding conditions in 2020 in much of the CCE, although the detailed sections below should be interpreted with care: survey effort was reduced in 2020 due to COVID-19, and many samples have yet to be processed.

3.1 Northern and Southern Copepod Biomass Anomaly off of Newport

Copepod biomass anomalies recorded off of Newport represent interannual variation for two groups of copepod taxa: “northern copepods,” which are cold-water species rich in wax esters and fatty acids that appear to be essential for pelagic fishes, and “southern copepods,” warm-water species that are smaller and have lower fat content and nutritional quality. In summer, northern copepods usually dominate the coastal zooplankton community observed along the Newport Hydrographic Line (Figure 1-4a), while southern copepods dominate during winter. However, delayed upwelling, El Niño events, and positive PDO regimes can disrupt these seasonal patterns, leading to lower biomass of northern copepods and higher biomass of southern copepods (Keister et al. 2011, Fisher et al. 2015). Positive biomass anomalies of northern copepods correlate with stronger returns of Chinook salmon to Bonneville Dam and coho salmon to coastal Oregon (Peterson et al. 2014).

In 2020, northern copepods continued an overall increasing trend following extremely low biomass during the Blob. They were >1 SD above the mean in spring/summer 2020, before returning to neutral in the fall (Figure 3-1, top). The spring/summer anomaly was among the highest of the time series. Southern copepods were below average for much of 2020, continuing a decline since the Blob (Figure 3-1, bottom). These values suggest above-average feeding conditions for pelagic fishes off central Oregon in 2020, with late spring/summer copepod ratios the most favorable since before the Blob and in nearly a decade. The biweekly survey that collects these data lost only two sampling dates due to COVID-19, both in spring.

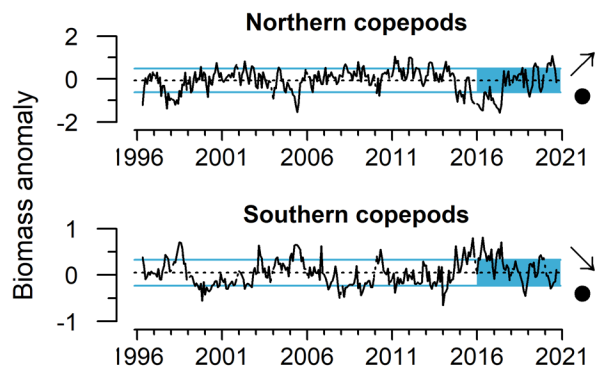


Figure 3-1. Monthly northern (top) and southern (bottom) copepod biomass anomalies from Newport Hydrographic Line station NH05, 1996–2020. Lines, colors, and symbols as in Fig. 1-3a. Copepod biomass anomaly data provided by J. Fisher (NMFS/NWFSC, OSU).

3.2 Krill Size off of Trinidad Head

Krill are among the most important prey for fishes, mammals, and seabirds in the CCE. Two species of particular importance are *Thysanoessa spinifera* and *Euphausia pacifica*. *E. pacifica* has been sampled multiple times per season off of Trinidad Head, California (Figure 1-4a), since late 2007. Mean length of adult *E. pacifica* is one indicator of krill as a resource for predators. *E. pacifica* length cycles from short individuals in winter that grow into longer individuals by summer. *E. pacifica* lengths in spring and summer 2020 were above average (Figure 3-2), and much greater than in 2019, when krill growth may have been negatively affected by El Niño conditions in the winter months early that year. The overall trend for krill lengths has been increasing since the decline in size observed at the onset of the Blob. COVID-19 led to some cancelled cruises and delayed sample processing at

Trinidad Head, but the 2020 data are from stations that are highly representative of *E. pacifica* lengths in the region (Robertson and Bjorkstedt 2020). A spring survey that has previously produced estimates of krill biomass and distribution off Oregon and Washington since 2011 (Brodeur et al. 2019) was cancelled in 2020 due to COVID-19.

3.3 Harmful Algal Blooms and Red Tide

Harmful algal blooms (HABs) of diatoms in the genus *Pseudo-nitzschia* have been of concern along the U.S. West Coast in recent years. Certain species of *Pseudo-nitzschia* produce the toxin domoic acid, which can accumulate in filter feeders and extend through food webs to cause harmful or lethal effects on people, marine mammals, and seabirds (Lefebvre et al. 2002, McCabe et al. 2016). Because domoic acid can cause amnesic shellfish poisoning in humans, fisheries that target shellfish (including razor clam [*Siliqua patula*], Dungeness crab, rock crab [*Cancer* spp.], and spiny lobster [*Panulirus interruptus*]) are closed, or operate under a health advisory in the recreational sector, when concentrations exceed regulatory thresholds for human consumption. Domoic acid regulatory thresholds are currently set by the U.S. Food and Drug Administration (FDA); federal action levels for domoic acid levels are >20 parts per million (ppm) for all fish, with the exception of ≥30 ppm for crab viscera. Extremely toxic HABs of *Pseudo-nitzschia* are influenced by ocean conditions and have been documented in 1991, 1998–99, 2002–03, 2005–06, and 2015–19. In the Northern CCE, they have been found to coincide with or closely follow El Niño events or positive PDO regimes, and to track regional anomalies in southern copepod species (McCabe et al. 2016, McKibben et al. 2017). Fishery closures may result in tens of millions of dollars in lost revenue and a range of sociocultural impacts in coastal economies (Dyson and Huppert 2010, NMFS 2016, Ritzman et al. 2018), and can also cause “spillover” of fishing effort into other fisheries (Fisher et al. 2021). The largest and most toxic HAB of *Pseudo-nitzschia* ever recorded on the U.S. West Coast coincided with the Blob and caused the longest-lasting and most geographically widespread fisheries closures on record (McCabe et al. 2016, Moore et al. 2019).

In 2020, exceedances of domoic acid—detected in razor clams and crabs from Northern California to the Canadian border (Figure 3-3)—caused protracted fishery closures and delays for much of the U.S. West Coast, many of which continued into early 2021. Washington shellfish fisheries experienced impacts for the first time in several years, as a rapid rise of domoic acid closed recreational and tribal razor clam harvests in October 2020. In Oregon, a statewide razor clam closure begun in the winter of 2019 was gradually lifted for northern (January), central (February), and southern Oregon beaches (August), before closing again over the course of the fall of 2020. The razor clam fishery remained closed in Northern California, as it has been since 2016. Many crab fishery seasons were shortened, due in part to domoic acid but also to meat quality and to reducing risk of

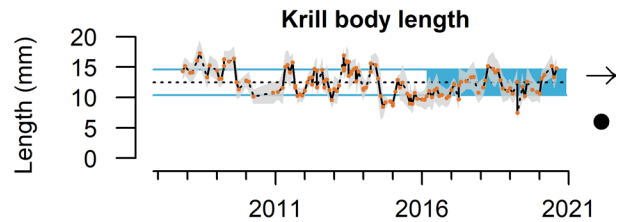


Figure 3-2. Monthly mean body length (mm) of adult *E. pacifica* krill off Trinidad Head, 2007–20. Gray shaded envelope indicates ± 1.0 SD. Lines, colors, and symbols as in Fig. 1-3a. Krill data provided by R. Robertson (Cooperative Institute for Marine Ecosystems and Climate [CIMEC] at Humboldt State University [HSU]) and E. Bjorkstedt (NMFS/SWFSC, HSU).

whale entanglement in crab gear. Domoic acid led to closure of Northern California rock crab fisheries throughout 2020. In Oregon, precautionary concerns over domoic acid levels in Washington crabs caused delayed opening of the Oregon Dungeness crab fishery from Cape Falcon, Oregon, to the Oregon–Washington border for all of December 2020. Domoic acid also led to closures of commercial, recreational, and tribal Dungeness crab fisheries in Washington for parts of November and December 2020. These delays extended into 2021 for recreational and nontribal harvest; when the Washington nontribal commercial sector eventually opened in February 2021, crabs caught from the Columbia River to Point Chehalis, Washington, were required to be eviscerated. Details of the causes, locations, and timings of delays and closures are provided in Harvey et al. (2021), Appendix E.

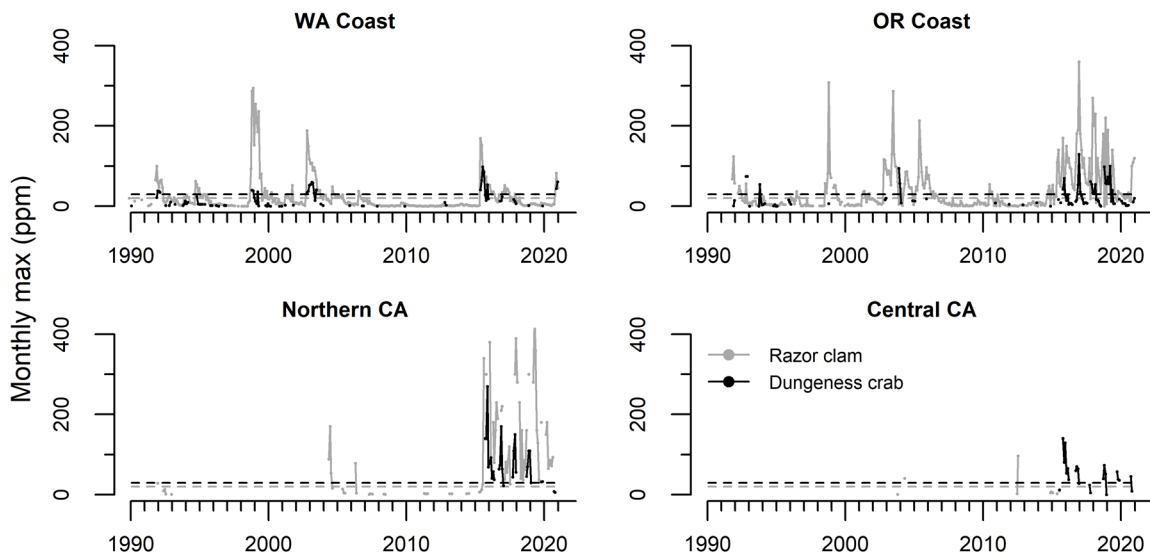


Figure 3-3. Monthly maximum domoic acid concentration (ppm) in razor clams (gray) and Dungeness crab viscera (black) through 2020 for WA, OR, Northern CA (Del Norte to Mendocino Counties), and Central CA (Sonoma to San Luis Obispo Counties). Horizontal dashed lines are the management thresholds of 20 ppm (clams in gray) and 30 ppm (crab viscera in black). WA data provided by the WA State Department of Health, OR data from the OR Department of Agriculture, and CA data from the CA Department of Public Health.

Farther south, a major red tide event affected the coast of the Southern CCE in the spring of 2020. The event was caused by an incredibly dense and prolonged bloom of the dinoflagellate *Lingulodinium polyedra* that extended from Los Angeles to central Baja California, Mexico, coloring the water a deep red–brown and producing spectacular nighttime bioluminescence. Cell numbers at the Scripps Pier (La Jolla, California) were the highest ever recorded at 9 million cells/L (the previous maximum was just under 1.5 million cells/L), and chlorophyll was also the highest recorded (1,083 $\mu\text{g/L}$) since monitoring began in 1983. Conditions thought to have led to the development of the bloom included unusually high precipitation (200–400% above normal) in March–April 2020, low wind that contributed to stratification, and seasonal warming of waters. These factors were superimposed on a backdrop of anomalously warm water temperatures in the region since 2015, further promoting growth and contributing to water column stratification, which is favorable for proliferation of *L. polyedra*.

Occasional blooms of *L. polyedra* lasting one week to one month are not unusual in California and generally do not cause harm, but this bloom had significant ecological and human health impacts. In early May, after a month of sustained cell concentrations above 1 million cells/L, a widespread stranding of fishes (e.g., bass, sardines, rockfish, and rays) and invertebrates (e.g., snails, sea hares, sand dollars, mussels, sea pansy, octopus, and lobster) occurred on beaches throughout Orange and San Diego Counties. In addition, anecdotal reports from surfers and beachgoers claimed respiratory irritation from sea spray emerging near red tide water. Hypoxia and anoxia were reported at Scripps Pier for several days in early May (J. Smith, Scripps Institution of Oceanography, preliminary data) and likely contributed to the die-offs. Bacterial degradation of the large amount of organic matter at the end-stage of the bloom depleted oxygen to levels expected to cause lethal effects in marine organisms due to hypoxia and produced hydrogen sulfide. This effect was amplified in semi-enclosed bays and lagoons with little exchange with the ocean and reduced mixing with the atmosphere. However, local research aquaria at Scripps Institution of Oceanography (SIO), the University of California, San Diego (UCSD), and SWFSC, which all use seawater from Scripps Pier, also experienced a nearly complete loss of all vertebrate and invertebrate specimens—including in tanks with additional aeration systems, suggesting that die offs may have been due to more than hypoxia.

A toxin associated with *L. polyedra*, yessotoxin (YTX), is known to occasionally cause harm in other parts of the world and may also have played a role in the die-offs. Preliminary analysis of particulate, dissolved, and aerosol samples collected during the 2020 bloom detected YTX in particulate and dissolved samples, with the highest concentrations (1.44–1.89 ng/L) measured near the end of the bloom, after the highest cell abundances of *L. polyedra* (E. Ternon and M. Carter, unpublished data). YTX was also detected in the aerosols at various time points throughout the bloom. Concentrations were low but detectable (≤ 1.13 pg/m³), though particularly high on 30 April (13.02 pg/m³; E. Ternon, unpublished data). This is the first-ever report of YTX in aerosols during an *L. polyedra* bloom, and suggests that up to 13 pg of YTX could have been inhaled by an adult within 2 hours (breathing 0.5 m³ per hour). Given the low toxicity of YTX reported so far on human cell lines, it is still not clear whether YTX or some other compound(s) are responsible for the reported respiratory symptoms of 25% of 872 respondents to a survey conducted by Surfrider, the Southern California Coastal Ocean Observing System (SCCOOS), and Surfline. While the timing of high in-water YTX coincides with the earliest reports of dead animals on beaches, YTX levels measured thus far are not significant enough to be the culprit for the massive die-offs. A preliminary analysis of aerosol samples showed that sulfur compounds (most likely sulfolipids) are being transferred from the cells to the aerosols. Ongoing isolation and characterization of these compounds should provide more insight into the cytotoxicity. In addition, sulfur gas precursors and the role of bacteria in the degradation and toxicity of the bloom are under investigation.

3.4 Regional Forage Availability

This section describes trends in pelagic forage community composition and availability, typically based on spring/summer research surveys that have been conducted independently in three different regions (see Figure 1-4a) for decades. However, our ability to understand forage community dynamics in 2020 was impacted by COVID-19, which disrupted the regional forage surveys and sample processing. Fewer samples were collected in 2020,

particularly in spring, adding uncertainty to this year's indicators and interpretations. COVID-19 disruptions also affected how we analyze and present data in this report: the three regional surveys use different methods (e.g., gear selectivity, timing, frequency, and survey objectives); thus, the amplitudes of a given species' time series from a particular region are not necessarily comparable to that species' time series from the other regions. We have addressed this issue in recent reports with multivariate analyses to compare the timing and nature of forage community shifts across the three regions (Thompson et al. 2019a, Harvey et al. 2020). However, we are unable to do so this year due to COVID-driven data limitations.

Below, we present forage species time series from each region that we believe to be most representative of times and locations that were surveyed in 2020, along with explanations of methodological changes to ensure comparability of 2020 data with data from earlier years. We encourage interpreting these data with care, given the added uncertainty associated with COVID-driven changes in methodology.

3.4.1 Northern CCE

Forage assemblage data from the Northern CCE come from a NOAA survey off Washington and Oregon (see Figure 1-4a) called the Juvenile Salmon and Ocean Ecosystem Survey (JSOES). JSOES uses a horizontal trawl at 10 m to target juvenile salmon (*Oncorhynchus* spp.), and also catches pelagic fishes, squid, and gelatinous zooplankton (Brodeur et al. 2005, Morgan et al. 2019). Because JSOES is a daytime survey that employs a near-surface trawl, it is not suitable for effective quantitative monitoring of pelagic species that undergo diel vertical migration (DVM) or that tend to be deeper in the water column. Thus, to avoid sampling bias, we focused on surface-oriented or non-DVM species such as salmon, market squid (*Doryteuthis opalescens*), and gelatinous zooplankton. We excluded data from midwater and DVM species such as sardine, anchovy, whitebait smelt (*Allosmerus elongatus*), jack mackerel (*Trachurus symmetricus*) and Pacific herring (*Clupea pallasii*).

The 2020 JSOES cruise was completed on time (late June) and all stations were sampled as planned; the major COVID-19 impacts on JSOES were delays in sample processing. Thus, no special statistical approaches were used to compare 2020 JSOES catches to prior years' catches. One striking observation in the 2020 JSOES data was unprecedentedly large catches of pelagic juvenile sablefish (*Anoplopoma fimbria*), a commercially valuable groundfish species (Figure 3-4). Catches of juvenile chum salmon (*Oncorhynchus keta*) dropped to >1 SD below the long-term mean in 2020, while juvenile sockeye salmon (*O. nerka*) catches were average; both had nonsignificant five-year trends (Figure 3-4). Catches of market squid in 2020 remained above average, and high catches from 2018 to 2020 contributed to an increasing recent trend of market squid in the JSOES time series. Water jelly (*Aequorea* spp.) were 1 SD above the mean in 2020, although they were down from peaks in 2015–16 associated with the Blob. Catches of *Chrysaora fuscescens* jellyfish (sea nettles) increased back to near-average values since the lows in 2015–16. Moon jellies (*Aurelia labiata*) also showed an increasing trend and were well above long-term averages in 2020. In contrast, catches of Pacific pompano (*Peprilus simillimus*) and egg yolk jelly (*Phacellophora camtschatica*), which peaked during the Blob in 2015 and 2016, declined in 2020 to within

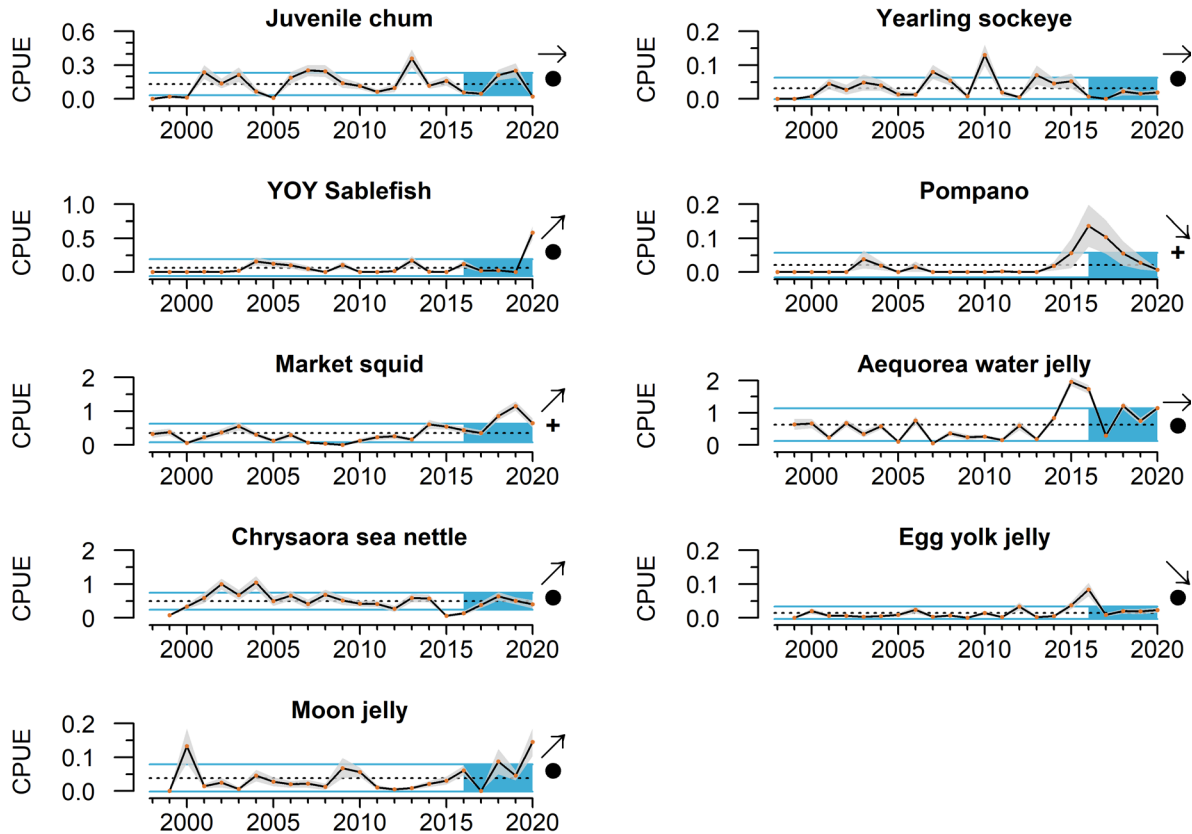


Figure 3-4. Catch per unit effort (CPUE = $\text{Log}_{10}(\text{no}/(\text{km} + 1))$) of 9 taxa in the Northern CCE, 1998–2020. Lines, colors, and symbols as in Fig. 1-3a. Pelagic forage data from the Northern CCE provided by B. Burke (NMFS/NWFSC) and C. Morgan (NMFS/NWFSC, OSU). Data derived from surface trawls taken in June during JSOES (<https://www.fisheries.noaa.gov/west-coast/science-data/ocean-indicator-ancillary-data-and-future-research-directions>).

long-term averages. Finally, the main targets of the JSOES survey are juvenile Chinook and coho salmon; as noted in *Fishes* (Figure 4-1), catches of juvenile subyearling Chinook salmon in 2020 were ~1 SD above average, of juvenile yearling Chinook salmon ~1 SD below average, and of juvenile coho salmon close to average.

3.4.2 Central CCE

Forage data for the Central CCE are from the “core area” (centered on Monterey Bay) of the NOAA Rockfish Recruitment and Ecosystem Assessment Survey (RREAS; see Figure 1-4a), a springtime midwater trawl survey that targets pelagic young-of-the-year (YOY) rockfishes (*Sebastes* spp.), but also samples other YOY and adult forage species, market squid, adult krill, and gelatinous zooplankton (Sakuma et al. 2016).

Because of COVID-19, different statistical approaches were required to compare 2020 RREAS results from results in previous years. Effort for the RREAS was considerably reduced as a result of the COVID-19 pandemic (15 hauls in 2020 for the core area, compared to a long-term average of >60 per year from 1990 to 2019). Because the survey was

conducted on a chartered fishing vessel rather than the normal survey vessel, the timing and spatial distribution of effort was also anomalous, with more trawls conducted in shelf habitat relative to offshore habitat, and all hauls conducted later than usual (mid- to late June, rather than a broader May–mid-June time period). As initial evaluations using average log-transformed catch rates indicated substantial bias for many taxa (particularly those with strong inshore or offshore habitat associations), abundance indices were instead developed using a delta-generalized linear model to explicitly account for spatial and temporal sampling covariates, consistent with the approach typically used to develop prerecruit indices of rockfish and other groundfish for stock assessments (e.g., Ralston et al. 2013). The best candidate models (including error distributions) were determined based on the Akaike information criterion, and uncertainty was estimated by running the model in a Bayesian framework with vague priors and computing 95% credible intervals using the package `rstanarm` in R. The resulting indices were $\log(x + 1)$ transformed, and standardized anomalies (z-scores, with transformed uncertainty estimates) are presented in this report, consistent with how these indicators have been reported in prior years. Comparisons with past indices indicated that the previous methods of reporting (average of log-transformed indices) yielded highly comparable and unbiased results relative to the model-based approach for the historical time series, but that approach would have led to substantial bias if applied to the sparse 2020 data. Although uncertainty was considerably greater for most taxa (particularly less-abundant taxa) due to the small number of trawls conducted in 2020, comparisons of catch rates with seabird diets indicated comparable relative abundance levels for several key forage species (YOY rockfish and northern anchovy), as has been reported previously in the literature for this region.

As shown in Figure 3-5, catches of adult anchovy were well above average in 2020 at the 15 sampled stations. Anchovy catches at these stations have been well above average since 2018, and have an increasing trend over the past five years. In contrast, juvenile rockfish catches continued a recent decline and were 1 SD below average. Among other species, all groups shown in Figure 3-5 had average to below-average catches in 2020, although many estimates had greater uncertainty than in previous years—especially myctophids, YOY Pacific hake, and octopus. YOY Pacific hake, YOY sanddabs (*Citharichthys* spp.), YOY rockfish, octopus, and krill all had decreasing trends over the past five years. The relative abundance of market squid, a highly important forage species and commercial fishery target, was below average in 2020, following a multi-year trend during which abundance was generally well above average levels.

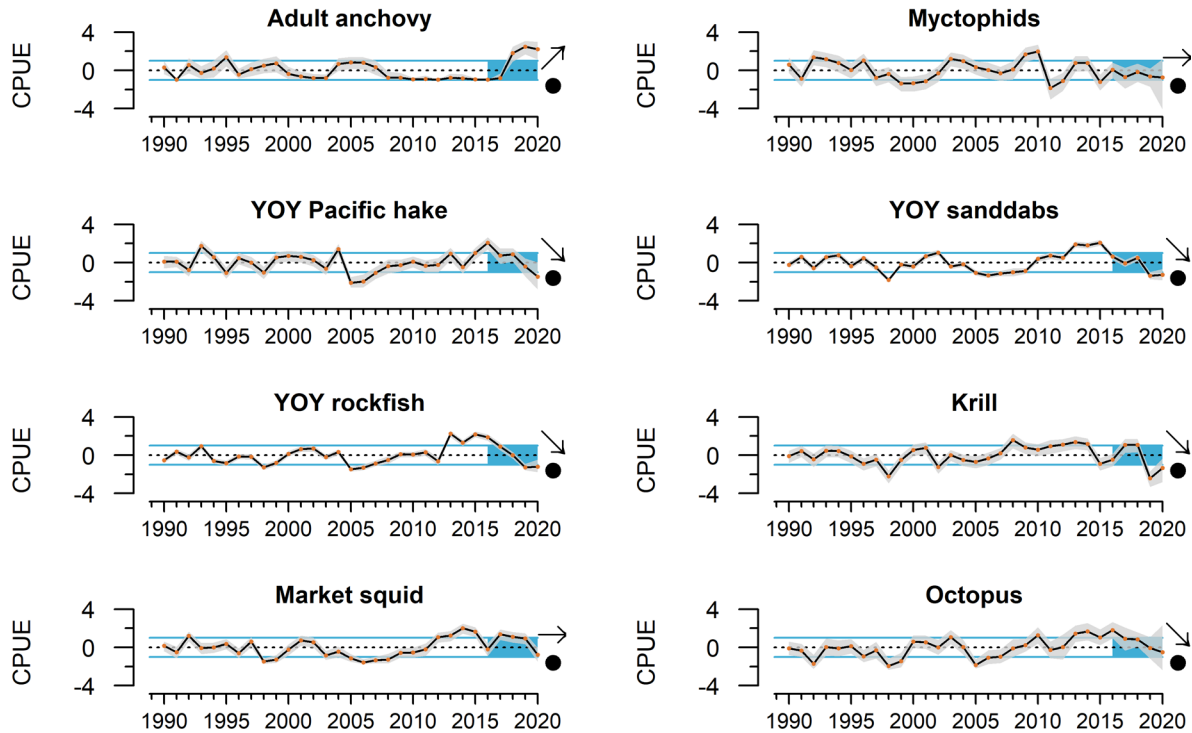


Figure 3-5. CPUE (Δ -glmm index and 95% CL) anomalies of 8 key forage groups in the Central CCE, 1990–2020. Lines, colors, and symbols as in Fig. 1-3a. Pelagic forage data from the Central CCE provided by J. Field and K. Sakuma (NMFS/SWFSC), from the SWFSC Rockfish Recruitment and Ecosystem Assessment Survey (<https://go.usa.gov/xGMfR>).

3.4.3 Southern CCE

Forage indicators for the Southern CCE usually come from CalCOFI larval fish surveys conducted in the spring (March–May) across all core stations of the CalCOFI survey (see Figure 1-4a). However, in 2020 the spring larval survey was canceled due to COVID-19. Therefore, we instead show data from the winter (January–February) CalCOFI larval cruise, which was completed in 2020 prior to the restrictions on survey operations due to the COVID-19 pandemic. The winter cruise is the seasonal cruise with the greatest similarity in larval community composition to the spring cruise, although some key species, including anchovy, likely have peak spawning somewhat later in the year and may be underrepresented in the winter data.

The seasonal CalCOFI surveys collect a variety of fish and invertebrate larvae (most <5 days old) from several taxonomic and functional groups, captured via oblique vertical tows of fine-mesh Bongo nets to 212 m depth (McClatchie 2014). Larval biomass is assumed to correlate with regional abundance of mature forage fish (Moser and Watson 2006). Data in Figure 3-6 represent winter cruise samples processed from CalCOFI transect lines 80 (off of Point Conception) and 90 (off of Dana Point, California; Figure 1-4a), which generally are representative of the Southern California Bight area because they are typically exposed to the main water masses found in the region (the California Current, the California Undercurrent, the central Pacific Ocean waters, and coastal upwelled waters; Roemmich and McGowan 1995).

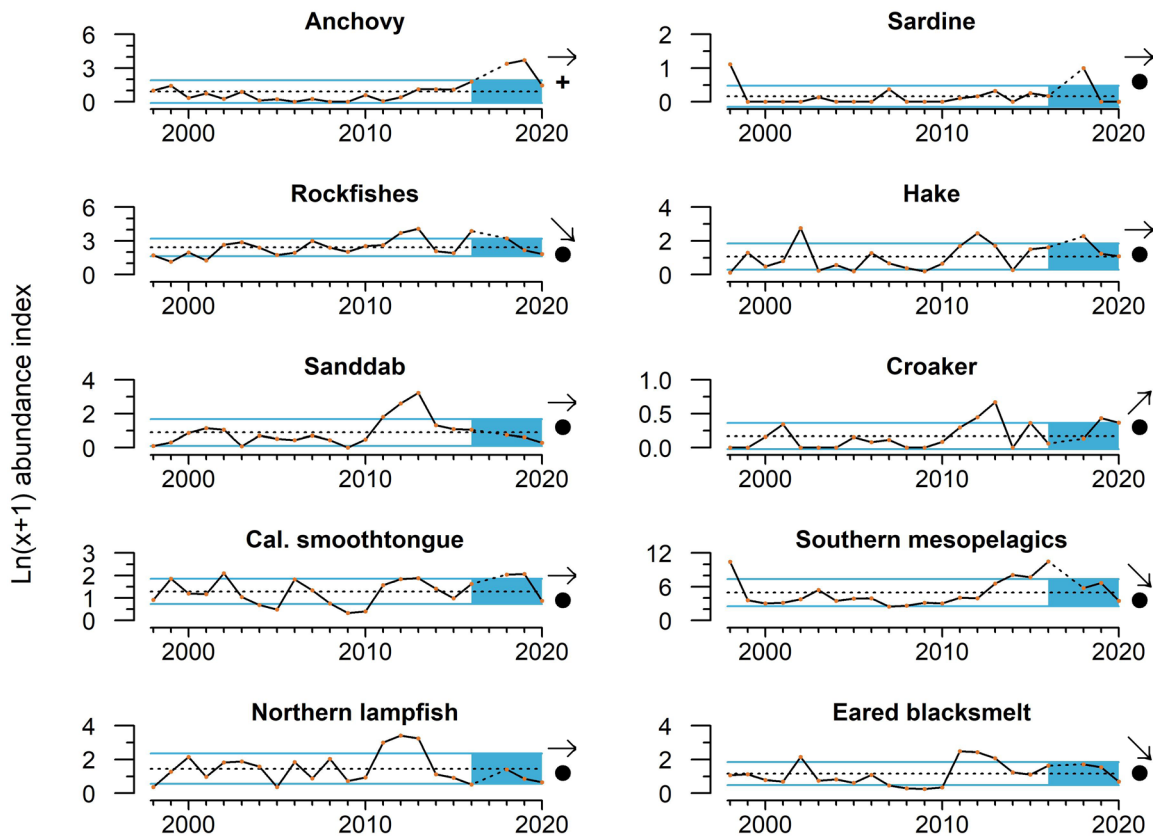


Figure 3-6. Mean abundance ($\ln(x + 1)$) of the larvae of ten key forage groups in the Southern CCE, 1998–2020. Lines, colors, and symbols as in Fig. 1-3a. Pelagic forage data from the Southern CCE provided by A. Thompson (NMFS/SWFSC), derived from winter CalCOFI surveys (<http://calcofi.org/>).

The southern forage community appeared to experience a shift from winter 2019 to winter 2020. Larval anchovy decreased from 2019 to 2020, but were still above the long-term average (Figure 3-6). Southern mesopelagic fishes also decreased from 2019 to 2020. Rockfishes were uncommon in 2020, as were larval flatfishes and sardines (Figure 3-6). Other noteworthy observations from the 2020 winter survey include the continued low abundance of northern lampfish (*Stenobranchius leucopsarus*), a mesopelagic species common north of Southern California which has been scarce since 2013 (Figure 3-6). Another mesopelagic, eared blacksmelt (*Lipolagus ochotensis*), has declined over the past five years, while larval croakers (family Sciaenidae) have increased.

In past reports (e.g., Harvey et al. 2020), we used multivariate cluster analysis methods described in Thompson et al. (2019a) to discern if forage communities within each region underwent considerable changes in composition over time, and if the timing of major changes is synchronized across regions of the CCE and linked to major events. The Southern CCE winter forage community is the only time series we have updated through 2020 with this approach as of this report, and the analysis indicates that there was a significant shift from 2019 to 2020 (data not shown), mostly driven by the decreases in southern mesopelagic larvae and larval anchovy shown in Figure 3-6. We will resume including those analyses in future reports, although it is likely that 2020 forage community data will be difficult to incorporate from either the Central CCE or Southern CCE due to the considerable disruptions caused by COVID-19.

3.4.4 Pyrosomes

Though not shown in Figure 3-5, pyrosomes (*Pyrosoma atlanticum*) were once again prevalent in the Central CCE in 2020, occurring in abundance in almost every RREAS tow, but trends have not yet been quantified due to likely sampling biases associated with 2020 survey conditions. Pyrosomes were also observed further north at Trinidad Head (R. Robertson and E. Bjorkstedt, unpublished data), and smaller individuals began to show up in Newport Line plankton samples (J. Fisher, unpublished data) and on Oregon beaches in late 2020, possibly after being forced north by seasonal currents and winter storms. Pyrosomes are pelagic tunicates associated with relatively warm water. They are known to have a subtropical distribution, and historically have been observed on occasion in Southern and Central California waters. Over the past several years they have been far more abundant in CCE waters; this increase has been attributed to the Blob, when anomalously warm ocean conditions may have favored pyrosome feeding and reproduction. They were abundant in survey catches from California to Washington in 2016–18, but had contracted to mostly Central and Southern California stations in 2019 (Miller et al. 2019). Pyrosomes are aggregate filter feeders that consume pico- and microplankton, and in some areas have been shown to cause depletion of chlorophyll-*a* standing stocks. Mass occurrences of pelagic tunicates have impacts on human activities, damaging fishing nets and clogging cooling-water intakes of coastal hydropower facilities.

4 Fishes

Brian Burke, Cheryl Morgan, Katie Barnas, Margaret Williams, Thomas Williams, Brian Wells, Nate Mantua, Correigh Greene, Stuart Munsch, Nicholas Tolimieri, Becca Selden, Jameal Samhouri, Jason Cope, and Barbara Muhling

This chapter focuses on status and trend indicators related to the abundance, condition, and distribution of fish species that are important components of U.S. West Coast fisheries. In particular, it focuses on four groups (Coastal Pelagic Species, Salmon, Groundfish, and Highly Migratory Species) that are managed by NOAA Fisheries and PFMC. Management of these major groups is outlined in the four FMPs overseen by PFMC.¹² These indicators are intended to provide ecosystem context to support the decision-making process outlined in the FMPs.

4.1 Salmon

Salmon indicators in this chapter are for Chinook and coho salmon, the two salmon species of greatest importance in PFMC's salmon FMP. This section is divided into three parts: indicators of abundance of juvenile Chinook and coho salmon during their early marine phase; indicators of abundance of adult Chinook and coho salmon on natural area spawning grounds; and suites of physical and biological indicators arrayed in regional "stoplight" tables, which may provide a general qualitative outlook of how many adults are likely to return to spawning areas in 2021.

4.1.1 Early marine abundance of juvenile salmon

We evaluate the time series of juvenile salmon catches from the JSOES cruise, a surface trawl survey conducted in the Northern CCE in ocean waters off Oregon and Washington each June (see Figure 1-4a). This is the same survey that generated the forage assembly data for the Northern CCE shown in Figure 3-4. Despite restrictions related to the COVID-19 pandemic, JSOES was able to sample all of its stations in 2020. Annual catches of juvenile coho and Chinook salmon in this region can serve as indicators of salmon survival during their first few weeks at sea, which is a critical window for the productivity of salmon populations (e.g., Miller et al. 2013).

Juvenile subyearling Chinook salmon catches in the JSOES cruise were higher in 2020 than in the previous two years, and were greater than average but slightly less than 1 SD above the time-series average (Figure 4-1). Juvenile yearling Chinook salmon catches declined in 2020 relative to 2019, and were ~1 SD below average. Yearling coho salmon catches were similar to 2019, and were within 1 SD of the time-series average (Figure 4-1). Preliminary analyses suggest 2020 body condition indices (length-to-weight ratios) were good for yearling coho and interior spring and interior fall Chinook (C. Morgan, preliminary data). As noted previously (see Figure 3-4), catches of juvenile chum salmon at JSOES stations dropped to >1 SD below the long-term mean in 2020, while juvenile sockeye salmon catches were average; both had nonsignificant five-year trends.

¹² Available at <https://www.pccouncil.org/fishery-management-plans/>

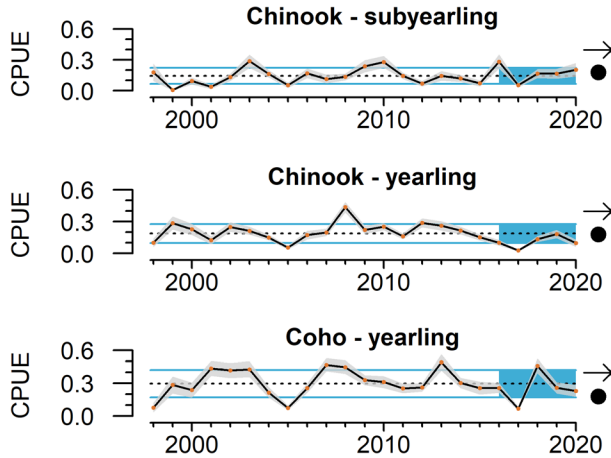


Figure 4-1. At-sea juvenile Chinook and coho salmon catch ($\text{Log}_{10}(\text{no}/(\text{km} + 1))$) off WA and OR in June, 1998–2020. Lines, colors, and symbols as in Fig. 1-3a. Data for at-sea juvenile salmon provided by B. Burke (NMFS/NWFSC), with additional calculations by C. Morgan (OSU/CIMRS). Data derived from surface trawls taken during JSOES cruises.

4.1.2 Abundance of spawning adult salmon

For indicators of the abundance and reproductive potential of naturally spawning Chinook and coho salmon populations, we compare the trends in spawning escapement throughout the CCE to evaluate the coherence in production dynamics, and also to get a more complete perspective of their status across the greater portion of their range. When available, we use escapement time series back to the 1970s; however, some populations have shorter time series (for example, Central Valley spring-run Chinook salmon starts in 1995, Central Valley winter-run Chinook salmon starts in 2001, and Lower Columbia River coho salmon starts in 2002). Time series are generally updated through 2018 or 2019, although California Coast Chinook salmon have not been updated since 2015. Data are expressed as escapement anomalies relative to the long-term mean of the available time series. Recent averages and trends are evaluated for the most-recent 10-year period of the time series in order to capture population dynamics across multiple generations, given the spatial segregation of successive year classes of salmon.

We must stress the importance of evaluating these escapement anomalies in the proper context. The time series means and standard deviations, as well as the recent averages and trends, are based solely on the data shown in the plots and may not be directly relatable to conservation and management goals specific to those populations. For example, a given year may have an escapement anomaly that is >1 SD above zero, meaning that the escapement was well above the time-series average. However, that above-average escapement may still be well below historic escapement levels or population recovery goals if a population is severely depressed. In future years we hope to relate salmon escapements to abundance goals within the recovery plan frameworks, where appropriate. This is challenging in many cases because, while we aggregate escapement indicators at the ESU level, many recovery goals are quantified at finer levels (e.g., populations returning to discrete tributaries), and recovery is not necessarily established by meeting abundance quotas.

Escapements of California Chinook salmon to natural spawning areas in 2010–19 were mostly within ± 1 SD of long-term means (Figure 4-2), though 2019 escapements were among the lowest on record in several ESUs (Southern Oregon/Northern California Coast; Klamath River fall-run; Central Valley winter-run). California escapement trends over the

past decade were neutral for most ESUs except for decreasing trends in Klamath River fall-run and California Coast Chinook salmon, though those trends mask increases followed by declines during that time period. As the California Coast ESU data have not been updated since 2015, Figure 4-2 may not be representative of recent escapement for that ESU.

In the Pacific Northwest, the most recent escapement data are currently available through 2018. Most mean escapement patterns in the past decade were within ± 1 SD of average (Figure 4-3); the exception was above-average Snake River fall-run Chinook salmon, due to escapements in 2009–16 that were above the time-series average. Escapement trends for northwest stocks over the past decade were mostly neutral, but Upper Willamette River Chinook salmon had a positive trend while Snake River spring/summer-run Chinook salmon had a negative trend.

Natural spawning area escapement data for coho salmon ESUs are current through 2019 (2018 for Southern Oregon/Northern California Coast; Figure 4-4). Ten-year means for these four ESUs are within ± 1 SD of the time-series averages. Recent observations range from slightly above the time-series average (Southern Oregon/Northern California Coast coho salmon in 2018) to well below average (California Coast coho salmon in 2019). The trend over the most recent ten years of data was negative for Oregon Coast coho salmon, following declines from relative peaks in 2010, 2011, and 2014; other ESUs shown had nonsignificant trends but general interannual variability.

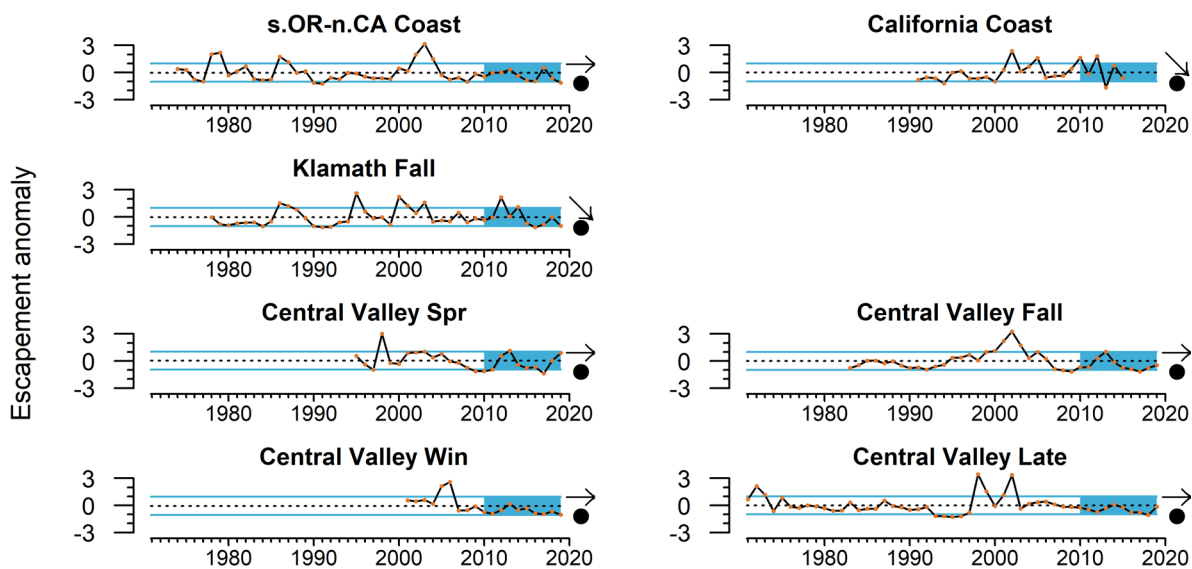


Figure 4-2. Escapement anomalies of naturally produced Chinook salmon in California watersheds through 2019. Lines and symbols as in Fig. 1-3a. Chinook salmon escapement data derived from California Department of Fish and Wildlife,^{*} PFMC pre-season reports,[†] and NWFSC’s Salmon Population Summary Database,[‡] with data provided directly from Streamnet’s Coordinated Assessments Database,^{**} Oregon Department of Fish and Wildlife, and U.S. Fish and Wildlife Service.
^{*} <https://wildlife.ca.gov/Conservation/Fishes/Chinook-Salmon>
[†] <https://www.pcouncil.org/salmon-management-documents/#safe>
[‡] <https://www.webapps.nwfsc.noaa.gov/sps>
^{**} <https://cax.streamnet.org>

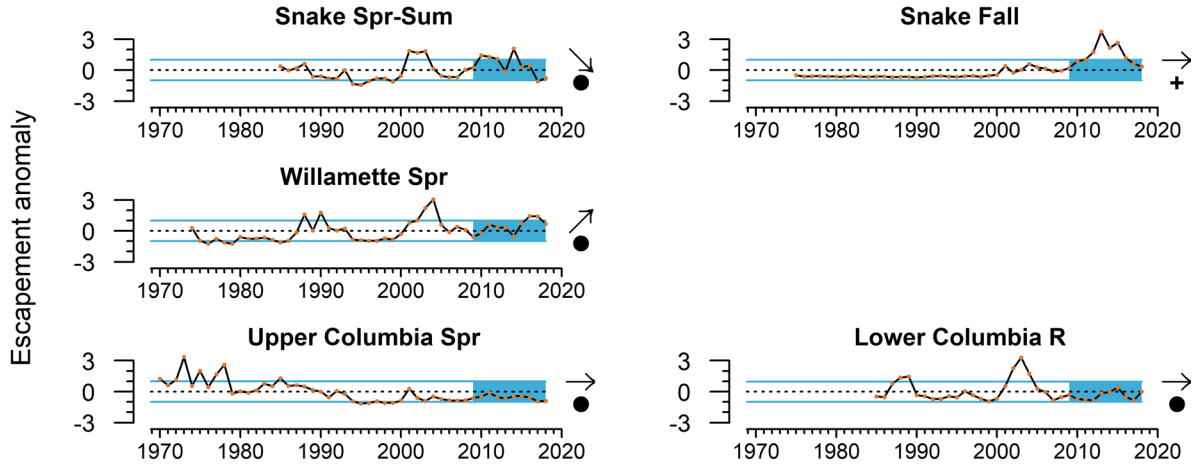


Figure 4-3. Escapement anomalies of naturally produced Chinook salmon in Washington, Oregon, and Idaho watersheds through 2018. Lines and symbols as in Fig. 1-3a. Chinook salmon escapement data were derived from PFMC pre-season reports* and NWFSC’s Salmon Population Summary Database,† with data provided directly from the Nez Perce Tribe, the Yakama Nation Tribe, and from Streamnet’s Coordinated Assessments Database,‡ with data provided by the Oregon Department of Fish and Wildlife, Washington Department of Fish and Wildlife, Idaho Department of Fish and Game, Confederated Tribes and Bands of the Colville Reservation, Shoshone–Bannock Tribes, Confederated Tribes of the Umatilla Indian Reservation, and the U.S. Fish and Wildlife Service.
 * <https://www.pcouncil.org/salmon-management-documents/#safe>
 † <https://www.webapps.nwfsc.noaa.gov/sps>
 ‡ <https://cax.streamnet.org>

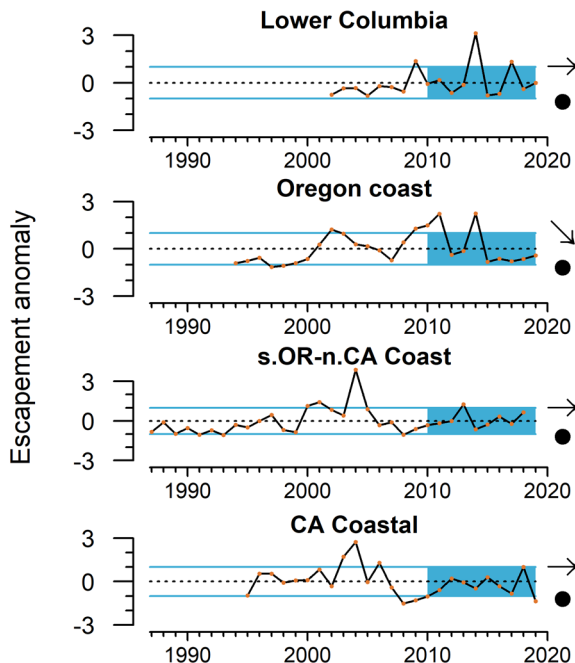


Figure 4-4. Escapement anomalies of naturally produced coho salmon through 2019. Lines and symbols as in Fig. 1-3a. Coho salmon escapement data compiled from the California Department of Fish and Wildlife,* PFMC pre-season reports,† and Streamnet’s Coordinated Assessments Database,‡ with data provided by the Oregon Department of Fish and Wildlife and Washington Department of Fish and Wildlife.
 * <https://wildlife.ca.gov/Conservation/Fishes/Coho-Salmon>
 † <https://www.pcouncil.org/salmon-management-documents/#safe>
 ‡ <https://cax.streamnet.org>

4.1.3 “Stoplight charts” of salmon-related ecosystem indicator suites

Long-term associations between oceanographic conditions, food web structure, and salmon productivity (Burke et al. 2013, Peterson et al. 2014) support projections of returns of Chinook salmon to Bonneville Dam and smolt-to-adult survival of Oregon Production Index area coho salmon. The suite of indicators is depicted in the “stoplight chart” in Table 4-1, and includes many indicators (PDO, ONI, SSTa, deep temperature, copepod biomass anomalies, juvenile salmon catch) shown elsewhere in this report. In Table 4-1, green circles represent indicator values that rank among the top third of all observations for a given time series, dating from 1998–2020; yellow squares represent values ranking in the middle third of all observations; and red triangles represent values in the lowest third. For coho salmon returning to the Oregon Production Index area in 2021, ecosystem indicators for the dominant smolt year (2020) suggest a mix of good, intermediate, and poor relative conditions. For Chinook salmon returning to the Columbia River basin in 2021, indicators for the dominant smolt year (2019) mostly reflect a mix of intermediate and poor conditions.

Table 4-1. Stoplight chart of conditions for smolt years 2017–20, and qualitative outlooks for adult returns in 2021, for coho salmon returning to coastal OR and for Chinook salmon returning to the Columbia River basin. Green circles rank in the top third of all years examined (“good”), yellow squares rank in the middle third of all years examined (“intermediate”), and red diamonds rank in the bottom third of all years examined (“poor”) for a given indicator. Courtesy of B. Burke and K. Jacobson (NMFS/NWFSC) and J. Fisher, C. Morgan, and S. Zeman (OSU/CIMRS).

Scale of indicators	Smolt year				Adult return outlook, 2021	
	2017	2018	2019	2020	Coho	Chinook
Basin scale						
PDO (May–Sep)	■	■	◆	■	■	◆
ONI (Jan–Jun)	■	●	◆	◆	◆	◆
Local and regional						
SST anomalies	■	■	◆	■	■	◆
Deep-water temperature	◆	◆	◆	◆	◆	◆
Deep-water salinity	■	●	■	◆	◆	■
Copepod biodiversity	◆	■	■	●	●	■
Northern copepod anomaly	◆	■	●	●	●	●
Biological spring transition	◆	◆	■	●	●	■
Winter ichthyoplankton biomass	■	■	◆	●	●	◆
Winter ichthyoplankton community	◆	◆	◆	■	■	◆
Juvenile Chinook salmon catch (Jun)	◆	■	■	■	■	■
Juvenile coho salmon catch (Jun)	◆	●	■	■	■	■

A more robust quantitative analysis of Chinook salmon outlooks based on Table 4-1 uses an expanded set of ocean indicators plus principal components analysis and dynamic linear modeling to produce salmon forecasts (methods in Burke et al. 2013). The principal components analysis essentially is used for weighted averaging of the ocean indicators, reducing the total number of indicators while retaining the bulk of the information from them. The dynamic linear modeling technique relates salmon returns to the principal components of the indicator data, and the approach used here also incorporates dynamic

information from sibling regression modeling. The model fits well to data for spring and fall Chinook salmon at the broad scale of returns to Bonneville Dam (Figure 4-5). Model outputs with 95% confidence intervals estimate 2021 Bonneville counts of spring Chinook salmon that are similar to the poor counts in 2019 and 2020 (Figure 4-5, top), while the outlook is for a decrease in fall Chinook at Bonneville in 2021 relative to 2020 (Figure 4-5, bottom). In past years, a similar model was run for coho salmon returns to the Oregon Production Index area, but that model has proven unreliable and will not be included in the report until further study is done to improve it. Although these analyses represent a general description of ocean conditions related to multiple populations in the Columbia Basin, we must acknowledge that the importance of any particular indicator will vary among salmon species and runs (Burke et al. 2013).

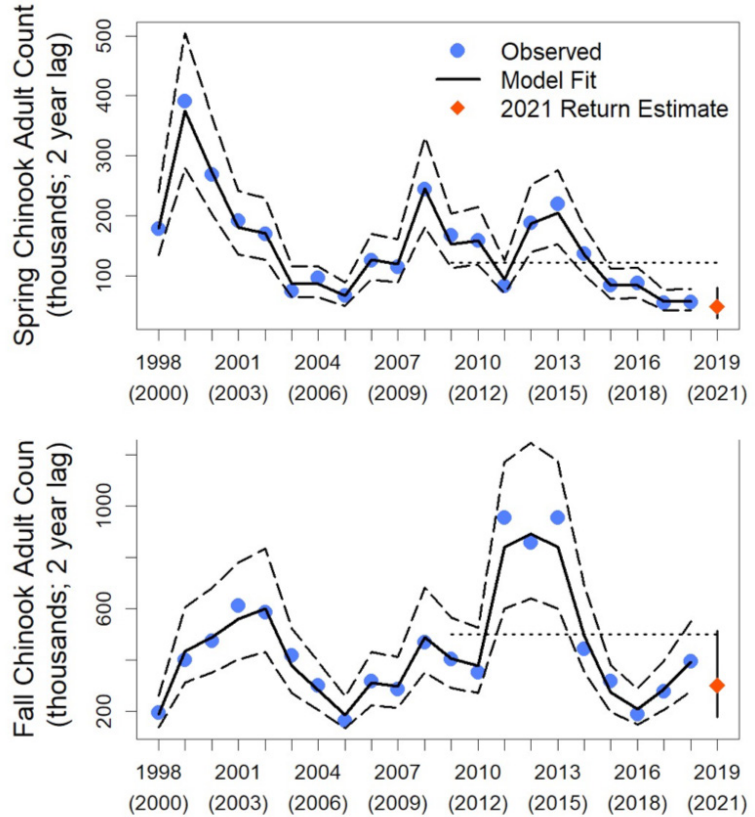


Figure 4-5. Observed and modeled counts of adult spring Chinook salmon (top) and fall Chinook salmon (bottom) at Bonneville Dam, by outmigration year and return year (in parentheses). In each plot, the dark line represents the model fit and dashed lines represent 95% confidence intervals. Outlooks for return year 2021 are in red, and were estimated with a Dynamic Linear Model, with log of sibling counts and first principal component of ocean indicators as predictor variables. Courtesy of B. Burke (NMFS/NWFSC).

In last year's report (Harvey et al. 2020), we introduced a stoplight-style indicator-based outlook for Central Valley fall Chinook salmon in California, based on work by Friedman et al. (2019). They found that Central Valley fall Chinook salmon returns correlated with natural-area spawning escapement of parent generations; fall egg incubation temperature and February streamflow in the Sacramento River; and a marine predation index based on the abundance and diet of common murrets (*Uria aalge*) at Southeast Farallon Island. For adult salmon returning in 2021, signals are mixed, both within and across age classes. The dominant age class (age-3, from the 2018 brood year) experienced unfavorable parent escapement and egg incubation temperature, but favorable winter flows for newly hatched juveniles (Table 4-2). Age-4 fish are the progeny of a very low escapement year (2017), and experienced both poor egg incubation temperature in the 2017–18 winter and very low streamflow for juveniles. Age-5 fish (produced in 2016) have mixed signals thanks to better juvenile flow regimes.

Reflecting discussions with PFMC’s Scientific and Statistical Committee (SSC) Ecosystem Subcommittee in September 2020, we emphasize that the stoplight chart in Table 4-2 is strictly qualitative and contextual decision-support information. The qualitative categories (e.g., terms like “poor” or “very poor” in color in the table cells) are based on expert opinion of how a given environmental indicator value relates to quantitative functions describing the relationship between the indicator and estimated life-stage specific survival (from Figure 5 in Friedman et al. 2019), or of how total escapement of a parent generation to the natural spawning area relates to the conservation objective of a combined natural + hatchery escapement of 122,000 to 180,000 fish (PFMC 2016). For example, in Table 4-2, February flows rated “very low” were near the low end of the range of observed values reported by Friedman et al. (2019) from 1982–2016, and are consistent with ~25% outmigrant survival, while the flows rated “high” or “very high” were consistent with ~50% to ~90% outmigrant survival (see Friedman et al. 2019, Figure 5). Egg incubation temperatures in Table 4-2 were consistent with egg-to-fry survival ranging from ~50% (which we rated as “suboptimal”) to ~33% (“poor”). The CCIEA team will work to refine these qualitative categories for future reports so that their basis is more explicit. The qualitative nature of this stoplight chart is in part due to the fact that some of the parameters used by Friedman et al. (2019) were estimated using information from both natural- and hatchery-origin fish, and while it is reasonable to assume that true parameter values would be similar, given correlations between natural and hatchery escapements, additional data specific to natural-origin fish are likely necessary in order to improve model fits, evaluate other potential covariates, and support adequate testing of model predictive skill.

Table 4-2. Table of conditions for naturally produced Central Valley fall-run Chinook salmon returning in 2021, from brood years 2016–19. Indicators reflect each cohort’s parent generation escapement, egg incubation temperature, flow during juvenile stream residence, and seabird predation in the early marine phase. Shading indicates age-3 Chinook salmon, the dominant age class returning to the Central Valley. Courtesy of N. Mantua (NMFS/SWFSC). Note: *cfs* = cubic feet per second.

Spawning escapement (t = 0)	Incubation temperature, Oct–Dec (t = 0)	February median flow (t + 1)	Seabird Marine Predation Index (t + 1)	Chinook age, fall 2021
2016: 56,000 (low)	11.8°C (poor)	48,200 cfs (very high)	Near average	5
2017: 18,000 (very low)	11.8°C (poor)	5,525 cfs (very low)	Near average	4
2018: 72,000 (low)	11.7°C (poor)	21,700 cfs (high)	Near average	3
2019: 120,400 (met goal)	11.2°C (suboptimal)	6,030 cfs (very low)	Near average	2

PFMC’s Habitat Committee (HC), Salmon Technical Team (STT), and others (including CCIEA scientists) have begun developing more comprehensive, habitat-based stoplight charts for Sacramento River fall and Klamath River fall Chinook salmon, both of which were the focus of formal rebuilding plans for brood years 2012–14, following recent determinations of overfishing (PFMC 2019b, 2019c). Many potential habitat issues were highlighted for Sacramento and Klamath River fall Chinook salmon runs in the rebuilding plans, and

HC advocated an indicator-based approach to address this challenge. The goals for this approach were to: 1) illustrate multiple habitat factors in years that triggered the rebuilding plan, 2) document how habitat impacts will remain in years after the rebuilding plan, 3) identify potential cumulative effects of multiple habitat stressors, and 4) identify potential avenues for Council engagement related to management actions that influence indicators.

After reviews by multiple scientists and members of various advisory bodies, HC developed a suite of 22 stoplight indicators for Sacramento River fall Chinook salmon and 17 stoplight indicators for Klamath River fall Chinook salmon (Table 4-3). Some of these indicators are featured in time-series plots elsewhere in this report. The chosen indicators either have been shown in previous studies, or were proposed in the rebuilding plans, to be strongly related to life stage-specific Chinook salmon productivity, and published studies helped determine the expected directional effect of indicators (positive or negative) on stock productivity (Table 4-3).

The chosen indicators can be divided into five general categories (Table 4-3). Four of the five categories align with the simpler stoplight chart for Central Valley fall Chinook salmon shown in Table 4-2: *Adult spawners*, *Incubation and emergence*, *Freshwater/delta residence conditions*, and *Marine residence conditions* (for the first year of marine residence). The fifth category of indicators, *Hatchery releases*, expands the scope relative to the simple stoplight chart (Table 4-2) that focuses only on naturally produced fish. These stoplight charts also share qualities with the stoplight chart developed for Columbia River basin Chinook salmon and Oregon Production Index area coho salmon (Table 4-1) by including regional and basin-scale oceanographic indicators as part of the Marine residence conditions.

Table 4-3. Sacramento and Klamath River fall Chinook salmon habitat indicators, definitions, and key references. *Months* indicates the time period for which indicators were summarized, *Effect* is the predicted direction of the indicator's effect on productivity, and *Stock* indicates whether indicators were summarized by Sacramento (S) or Klamath (K) River runs. Table developed and provided by C. Greene (NMFS/NWFSC) and S. Munsch (NMFS/NWFSC, Ocean Associates, Inc.).

Life stage-specific indicator	Abbrev.	Months	Effect	Stock	Citation
Adult spawners					
Fall-run spawners	Spawners		+	S, K	Friedman et al. 2019
Fall closures of Delta Cross Channel	CChannel.F	Sep–Oct	+	S	Rebuilding plan
Fall low flows	Flows.F	Sep–Oct	+	S, K	Strange 2012
Fall temperatures in mainstem	Temp.F	Sep–Oct	–	S, K	Fitzgerald et al. 2021
Incubation and emergence					
Fall–winter low flows in tributaries	Flows.W	Oct–Dec	+	S, K	Jager et al. 1997
Egg–fry temperatures	Temp.W	Oct–Dec	–	S, K	Friedman et al. 2019
Egg–fry productivity	FW.surv		+	S, K	Hall et al. 2018
Freshwater/delta residence conditions					
Winter–spring flows	Flows.S	Dec–May	+	S, K	Friedman et al. 2019
Delta outflow index	Delta	Apr–Jul	+	S	Reis et al. 2019
Seven-day flow variation (SD)	SDFlow.S	Dec–May	–	S, K	Munsch et al. 2020
Maximum flushing flows	Max.flow	Nov–Mar	+	K	Jordan et al. 2012
Total annual precipitation	Precip	Annual	+	S, K	Munsch et al. 2019
Spring temperatures	Temp.S	Apr–Jul	–	S, K	Munsch et al. 2019
Spring closures of Delta Cross Channel	CChannel.S	Feb–Jul	+	S	Perry et al. 2013
Days Yolo bypass was accessible	Yolo	Dec–May	+	S	Limm and Marchetti 2009

Table 4-3 (continued). Sacramento and Klamath River fall Chinook salmon habitat indicators, definitions, and key references.

Life stage-specific indicator	Abbrev.	Months	Effect	Stock	Citation
Marine residence conditions					
Coastal sea surface temperature	SSTarc	Mar–May	–	S, K	Wells et al. 2008
North Pacific High	NPH	Mar–May	–	S, K	Wells et al. 2008
North Pacific Gyre Oscillation	NPGO	Mar–May	+	S, K	Wells et al. 2008
Marine Predation Index	Predation		–	S	Friedman et al. 2019
Hatchery releases					
Release number	Releases		+	S, K	Sturrock et al. 2019
Prop net pen releases	Net.pen		+	S, K	Sturrock et al. 2019
Release timing relative to spring transition	FW.Timing	Jan–Aug	+	S, K	Satterthwaite et al. 2014
Release timing relative to peak spring flow	Mar.Timing	Jan–Aug	+	S, K	Sykes et al. 2009

The Sacramento River Fall Chinook habitat stoplight chart is shown in Table 4-4 and spans brood years 1983–2019, which includes the brood years defined by the rebuilding plan (2012–14). Indicators were standardized and tabulated using a similar approach to Table 4-1 and Peterson et al. (2014), whereby red represents relatively poor conditions (indicator value for that year ranks among the bottom 33% of all scores), yellow represents average conditions, and green represents beneficial conditions (indicator value ranks among the top 33% of all scores). Overall, the suite of indicators has been highly variable. During the brood years defined by the rebuilding plan (2012–14) and since then (Table 4-4, bottom), the four habitat indicators for adult spawners were mixed. In years since, these indicators have generally worsened, though they were mixed for the 2020 outmigration year (i.e., fish from brood year 2019). For incubation and emergence, the three habitat indicators declined over the three brood years defined by the rebuilding plan. In years since, habitat indicators of incubation conditions have generally improved, and conditions were mixed for the 2020 outmigration year. For the freshwater/delta residence conditions, habitat conditions were generally poor over the three brood years of the rebuilding plan; they have generally improved since then, although they were poorer for the 2020 outmigration year than in 2019, due to poor flows and high temperatures. Hatchery release indicators were mixed in the three rebuilding plan brood years, and have remained mixed since then. Marine residence condition indicators were generally below average for the brood years in the rebuilding plan, although they improved somewhat in the 2014 brood year. Since then, these indicators have generally worsened. Habitat conditions for the 2020 outmigration year showed some improvement compared to the previous four years, but were nonetheless mixed.

The Klamath River fall Chinook salmon habitat stoplight chart is in Table 4-5. As with the Sacramento River chart, the indicator suite as a whole was highly variable during the 1983–2019 brood years. Habitat indicators for adult spawners were mixed during the three brood years of the rebuilding plan (2012–14), and worsened in the brood years since (Table 4-5, bottom). For incubation and emergence, the three indicators generally declined over the three brood years defined by the rebuilding plan. In years since, habitat indicators for incubation conditions have been mixed. Freshwater residence conditions were mixed for the three brood years defined by the rebuilding plan, and have remained mixed since then. Hatchery release indicators were mixed in the three rebuilding plan brood years, but have been relatively poor since then

Table 4-4. Stoplight chart of freshwater and marine conditions for naturally produced Sacramento River fall Chinook salmon. Values are standardized for the given indicator time series. Green cells represent values ranked in the upper third of all years (“good”), yellow cells rank in the middle third of all years (“average”), and red cells rank in the bottom third of all years (“poor”) for a given indicator. The rebuilding plan period, encompassing brood years 2012–14, is outlined with a bold box. Table developed and provided by C. Greene (NMFS/NWFSC) and S. Munsch (NMFS/NWFSC, Ocean Associates, Inc.).

Brood year	Freshwater conditions													Marine conditions								
	Adult spawners			Incubation			Freshwater/delta residence						Hatchery releases		Marine residence							
	Spawners	CChannel.F	Flows.F	Temp.F	Flows.W	Temp.W	FW.surv	Flows.S	Delta	SDFlow.S	Precip	Temp.S	CChannel.S	Yolo	Releases	Net.pen	FW.timing	Mar.timing	SSTarc	NPH	NPGO	Predation
1983	-0.54	-0.48	2.96	0.82	1.92	2.68	n/a	0.56	-0.47	0.91	2.10	0.05	0.06	0.60	-1.30	-0.58	0.61	-0.39	-0.31	0.99	0.95	0.11
1984	-0.20	-0.48	3.44	-0.32	2.31	1.50	n/a	-0.60	-0.82	-0.94	0.24	-0.97	-0.82	-0.74	0.49	-0.81	0.58	1.35	0.35	-0.57	0.24	2.91
1985	0.50	-0.09	0.74	n/a	0.88	0.89	n/a	0.48	1.18	1.54	-0.74	0.33	-0.35	0.58	0.34	-1.16	1.02	1.52	-0.39	-0.13	-0.65	0.42
1986	0.55	1.07	-0.53	0.15	-0.76	-0.28	n/a	-0.73	-0.73	-1.09	0.91	-0.57	-1.04	-0.74	-0.05	-1.06	0.53	-0.17	-0.28	0.19	0.34	2.91
1987	0.28	0.23	0.33	0.15	0.49	0.17	n/a	-0.65	-0.86	-0.85	-1.33	0.11	-2.46	-0.74	-0.27	-0.98	-0.11	0.17	0.06	0.75	1.44	0.41
1988	0.45	-0.48	-0.86	1.58	-1.40	0.01	n/a	-0.68	-0.50	-0.66	-0.83	-0.01	-2.19	-0.55	-1.88	-1.29	1.12	1.72	-0.06	-0.33	0.76	2.91
1989	-0.12	-0.48	-0.64	-1.75	-0.93	0.05	n/a	-1.04	-0.89	-1.42	-0.14	0.05	-2.86	-0.74	-0.12	0.18	-1.39	-0.59	-0.04	0.64	0.26	-0.42
1990	-0.66	-0.48	0.79	1.58	-1.03	-0.58	n/a	-1.06	-0.75	-1.06	-0.92	1.52	-2.39	-0.74	0.37	-0.14	-0.32	0.79	0.11	0.74	-0.36	-0.23
1991	-0.52	-0.48	-1.07	-0.32	-1.33	-1.76	n/a	-0.84	-0.84	-0.40	-0.96	-0.97	-1.05	-0.74	0.82	-1.28	-0.34	-0.64	-0.49	-0.64	-1.35	0.40
1992	-1.07	-0.48	-1.04	-1.27	-0.96	-1.03	n/a	0.57	0.23	0.96	-0.88	1.35	0.04	0.38	-1.34	-1.26	0.32	-0.37	-0.45	1.74	-1.20	0.27
1993	-0.28	-0.23	-1.47	-1.75	-1.74	-0.44	n/a	-1.00	-0.80	-1.37	0.95	-0.12	-0.17	-0.74	-0.64	-1.06	1.25	-1.77	-0.36	0.96	-1.20	0.16
1994	-0.05	-0.48	0.20	-0.80	0.04	0.36	n/a	1.74	2.71	1.43	-1.09	1.86	0.22	2.28	-0.25	-1.07	1.02	0.52	-0.18	0.05	-1.79	-0.40
1995	0.74	-0.20	-0.76	-0.32	-1.11	-1.33	n/a	0.58	0.65	0.38	2.03	-0.18	0.53	1.02	0.41	-1.11	-3.52	-2.60	-0.66	1.00	-0.95	-0.68
1996	0.81	-0.48	0.25	0.15	-0.14	-1.19	n/a	0.65	-0.48	1.33	0.59	-0.29	0.52	1.12	-1.15	-1.20	1.09	0.07	-0.52	0.94	-0.67	-0.17
1997	0.87	0.36	0.47	2.05	0.32	-0.60	n/a	2.04	1.45	1.19	0.60	2.26	0.75	1.70	1.01	-0.58	0.20	0.61	-0.20	0.84	0.56	-0.38
1998	0.28	4.72	0.28	0.15	-0.43	0.09	n/a	0.87	0.16	0.45	1.92	1.35	0.68	0.67	-0.84	-1.17	0.07	-0.39	0.90	-0.46	1.74	0.37
1999	1.17	-0.48	1.14	1.10	1.33	0.36	n/a	0.53	0.27	0.88	-0.15	-0.12	-0.05	0.31	-1.07	-1.19	-0.01	-1.25	0.23	-1.04	2.25	-0.11
2000	1.21	1.60	0.57	0.15	0.73	-0.09	n/a	-0.74	-0.62	-0.67	0.05	-0.40	-0.25	-0.74	-0.06	0.00	-0.19	-0.71	0.33	0.09	2.18	0.08
2001	1.69	-0.10	0.09	0.63	0.53	-0.30	n/a	-0.26	-0.65	-0.09	-1.03	-0.46	0.58	-0.58	-0.90	-0.71	-0.24	-0.76	0.34	-0.37	1.30	-0.10
2002	1.99	-0.19	-0.60	-0.80	0.26	-0.07	n/a	0.92	-0.29	0.74	-0.42	0.28	0.55	-0.29	1.12	0.57	-1.06	1.20	-0.34	0.00	1.17	-0.29
2003	1.36	-0.48	-0.34	0.63	0.22	0.17	-0.83	0.63	-0.18	0.95	0.30	-0.52	0.68	0.09	0.29	0.21	-0.11	-1.15	-0.40	0.13	0.24	-0.61
2004	0.48	-0.48	0.04	2.29	0.42	-0.49	-0.40	0.09	0.09	0.14	-0.28	0.90	0.63	-0.61	0.92	0.89	-1.44	-0.02	-0.64	0.12	-1.32	-1.31
2005	0.53	-0.48	0.17	0.63	-0.49	-0.39	-0.38	2.21	2.55	1.10	0.37	-0.86	0.70	2.44	1.32	0.75	-0.73	-0.56	0.17	0.49	-0.47	-1.26
2006	0.42	-0.48	0.39	0.15	0.78	0.62	-0.68	-0.82	-0.73	-1.14	1.32	-0.46	0.34	-0.74	1.23	0.99	0.02	-1.72	0.49	0.27	0.13	-0.95
2007	-0.88	-0.48	0.17	-0.04	0.54	-0.41	-0.06	-0.71	-0.77	-0.64	-1.07	-0.01	0.35	-0.74	1.32	1.20	0.30	1.01	0.78	-0.41	1.50	-0.81
2008	-1.37	-0.48	-0.34	-0.51	0.44	-1.01	-0.45	-0.83	-0.60	-0.49	-0.92	-0.35	0.28	-0.74	0.80	0.98	0.53	1.08	0.67	-0.98	0.43	-0.59
2009	-2.17	-0.10	-0.93	-0.51	-1.27	-0.23	1.13	-0.32	-0.46	-0.10	-0.61	1.75	0.39	-0.61	0.87	0.84	0.73	-0.10	0.18	-0.09	1.57	-0.51
2010	-0.55	-0.29	-0.64	-0.42	-1.00	0.44	1.21	0.57	1.22	0.72	-0.01	2.14	0.75	0.48	1.17	0.90	0.22	0.07	0.25	-0.45	1.06	-0.65
2011	-0.74	0.49	0.09	-0.04	0.27	1.14	-0.31	-0.87	-0.48	-1.13	0.76	0.33	0.67	-0.74	1.18	0.53	0.30	1.45	0.58	-0.88	1.56	-0.39
2012	0.21	-0.48	0.57	n/a	2.11	0.49	-0.01	-0.54	-0.75	-0.27	-0.79	-1.20	0.66	-0.39	0.32	0.13	-2.83	-0.02	0.21	-0.33	0.66	0.02
2013	0.97	0.80	-0.20	-0.42	0.69	0.38	0.13	-1.22	-0.82	-1.26	-0.51	-1.48	0.48	-0.74	0.31	1.51	0.53	1.30	-0.81	-0.23	-0.28	0.49
2014	0.23	-0.29	-0.85	-1.37	-1.25	-2.82	-1.38	-0.78	-0.88	-0.03	-1.26	-1.14	0.52	-0.71	-0.21	0.68	0.48	-0.44	-1.32	0.32	-1.16	0.87
2015	-0.80	-0.39	-1.18	-0.61	-0.34	-0.58	0.26	-0.16	-0.12	0.58	-0.72	-0.97	0.44	-0.32	0.69	0.40	0.20	0.34	-1.12	0.09	-0.20	-0.51
2016	-1.15	-0.48	-1.37	-1.56	-0.84	0.86	2.82	2.21	1.80	1.47	0.14	-0.91	0.75	2.70	-0.92	-0.01	0.58	-0.47	-0.50	0.23	-0.49	n/a
2017	-2.59	2.00	0.21	-0.51	0.25	0.86	-0.65	-1.01	-0.27	-1.10	1.92	-1.03	0.67	-0.61	-0.26	1.10	-0.14	-0.49	-0.62	-0.10	-2.01	n/a
2018	-0.85	-0.48	0.23	0.25	0.61	0.98	-0.41	1.17	1.41	1.54	-0.66	-0.35	0.75	0.64	-0.78	0.90	0.68	0.79	-0.84	0.29	-2.09	n/a
2019	-0.20	-0.19	-0.36	-0.51	-0.62	1.55	n/a	-0.97	1.05	-1.59	1.08	-0.91	0.64	-0.74	-2.92	2.62	0.04	0.61	-0.39	0.33	-1.57	n/a

(though data are unavailable for the 2020 outmigration year as of this report). Marine residence condition indicators were generally below average for brood years in the rebuilding plan, although they improved somewhat for the 2014 brood year. Since then, these indicators have generally worsened, with some improvement for the 2020 outmigration year (brood year 2019).

Table 4-5. Stoplight table of freshwater and marine conditions for naturally produced Klamath River fall Chinook salmon. Values are standardized for the given indicator time series. Green cells represent values ranked in the upper third of all years (“good”), yellow cells rank in the middle third of all years (“average”), and red cells rank in the bottom third of all years (“poor”) for a given indicator. The rebuilding plan period, encompassing brood years 2012–14, is outlined with a bold box. Table developed and provided by C. Greene (NMFS/NWFSC) and S. Munsch (NMFS/NWFSC, Ocean Associates, Inc.).

Brood year	Freshwater conditions											Marine conditions					
	Adult spawners			Incubation			Freshwater residence			Hatchery releases			Marine residence				
	Spawners	Flows.F	Temp.F	Flows.W	Temp.W	FW.surv	Flows.S	SDFlow.S	Precip	Temp.S	Max.flows	Releases	FW.timing	Mar.timing	SSTarc	NPH	NPGO
1983	-0.66	1.23	n/a	2.87	n/a	n/a	1.6	1.02	-1.24	-0.66	0.99	-0.31	2.11	0.66	-0.31	0.99	0.95
1984	-0.95	1.94	n/a	1.89	n/a	n/a	0.0	-0.08	-1.04	0.23	0.42	-1.27	0.49	1.72	0.35	-0.57	0.24
1985	-0.49	1.18	n/a	-0.38	n/a	n/a	0.9	2.41	-0.55	0.24	0.35	2.93	1.49	1.72	-0.39	-0.13	-0.65
1986	1.16	1.12	n/a	0.23	n/a	n/a	-0.5	-0.58	0.69	0.83	1.62	2.50	1.51	0.39	-0.28	0.19	0.34
1987	1.26	1.13	n/a	0.52	n/a	n/a	-0.7	-0.57	1.22	1.12	-0.73	-0.59	-1.03	0.24	0.06	0.75	1.44
1988	1.13	-0.24	n/a	-0.07	n/a	n/a	0.2	0.25	-0.36	-0.35	-0.84	2.58	0.49	0.87	-0.06	-0.33	0.76
1989	0.49	1.17	n/a	-0.60	n/a	n/a	-0.7	-0.62	0.46	1.32	0.82	0.21	-0.69	-0.08	-0.04	0.64	0.26
1990	-1.36	-0.24	n/a	0.40	n/a	n/a	-1.1	-1.01	-0.93	0.71	-0.73	-0.73	1.23	1.53	0.11	0.74	-0.36
1991	-1.50	-1.65	n/a	-0.67	n/a	n/a	-1.2	-0.98	2.49	1.37	-0.95	-0.39	0.86	1.03	-0.49	-0.64	-1.35
1992	-1.80	-3.12	n/a	-0.96	n/a	n/a	0.7	0.45	-1.02	-0.50	-1.30	-0.43	1.32	0.05	-0.45	1.74	-1.20
1993	-0.67	1.22	n/a	-0.44	n/a	n/a	-1.2	-1.16	1.00	1.73	1.06	-0.98	0.49	-2.89	-0.36	0.96	-1.20
1994	-0.50	-0.85	n/a	-0.35	n/a	n/a	1.6	2.07	-0.44	-0.20	-1.20	0.12	1.03	0.31	-0.18	0.05	-1.79
1995	1.35	1.22	n/a	-0.55	n/a	n/a	-1.7	-1.76	0.76	-1.37	0.57	0.15	-0.18	-0.24	-0.66	1.00	-0.95
1996	1.00	0.50	n/a	0.41	n/a	n/a	n/a	n/a	-0.18	-2.24	1.35	0.31	-0.21	-0.06	-0.52	0.94	-0.67
1997	-1.10	-0.23	n/a	0.30	n/a	n/a	2.0	1.69	-0.89	-1.22	2.91	-0.08	-0.30	-0.14	-0.27	0.84	0.56
1998	0.02	1.40	n/a	0.51	n/a	n/a	1.4	0.70	-1.91	-1.01	0.56	-0.24	0.66	-0.19	0.90	-0.46	1.74
1999	-0.84	1.13	n/a	0.82	n/a	n/a	0.2	0.05	-0.15	-0.37	0.65	0.12	0.92	-0.69	0.23	-1.04	2.25
2000	1.32	0.04	n/a	0.64	n/a	n/a	-1.2	-1.34	-0.36	1.66	-0.31	0.10	-0.27	-0.58	0.33	0.09	2.18
2001	1.10	-0.27	-0.79	0.00	-1.20	-1.00	-0.1	-0.07	0.38	0.42	-1.02	0.12	-0.67	-0.51	0.34	-0.37	1.30
2002	0.87	-1.53	-0.47	-0.23	0.51	-1.69	0.4	0.37	0.22	-1.19	-0.79	0.26	0.27	1.35	-0.34	0.00	1.17
2003	1.13	0.50	-1.91	-0.59	-2.34	-1.60	0.00	0.06	0.52	0.09	-0.53	0.13	0.32	-1.03	-0.40	0.13	0.24
2004	-0.19	-0.79	0.19	-0.10	0.38	-1.03	-0.29	-0.45	-0.42	-0.18	-0.54	0.25	-1.63	-0.32	-0.64	0.12	-1.32
2005	-0.47	0.44	0.26	-0.19	0.34	2.18	1.86	1.96	-0.18	-1.78	1.14	0.61	-0.95	-0.32	0.17	0.49	-0.47
2006	-0.56	-0.46	0.38	-0.36	0.33	-0.79	-0.29	-0.36	-0.41	-0.10	1.14	0.29	-0.04	-1.80	0.49	0.27	0.13
2007	0.58	-0.24	0.52	0.11	0.44	1.19	-0.22	-0.70	-0.79	0.43	-0.57	0.24	-1.74	0.98	0.78	-0.41	1.50
2008	-0.36	-0.29	2.83	0.31	0.50	-0.02	-0.64	-0.61	0.04	0.88	-0.73	-0.30	0.15	0.87	0.67	-0.98	0.43
2009	0.17	-0.42	0.03	-0.50	0.50	0.00	-0.13	-0.55	-1.50	0.26	-1.10	-0.12	-2.73	-1.09	0.18	-0.09	1.57
2010	0.02	-0.27	0.26	-0.45	0.25	0.31	0.70	-0.04	-1.39	-0.69	-1.07	-0.28	0.04	-0.58	0.25	-0.45	1.06
2011	0.19	-0.29	-0.22	0.16	0.46	-0.46	-0.12	0.12	-0.21	0.04	-0.18	0.07	-0.21	1.19	0.58	-0.88	1.56
2012	1.77	-0.33	-0.45	-0.14	0.08	0.75	-0.61	-0.49	0.00	-0.46	-0.58	-0.31	-0.89	-0.29	0.21	-0.33	0.66
2013	0.91	-0.39	0.68	-0.35	0.76	0.39	-1.14	-0.74	0.93	0.59	-0.95	0.00	-0.13	0.61	-0.81	-0.23	-0.28
2014	0.87	-0.39	-0.16	-0.70	-0.17	-0.21	-0.70	-0.13	2.50	0.71	-1.08	-0.58	-0.47	-0.98	-1.32	0.32	-1.16
2015	-0.21	-0.51	-0.20	-0.46	0.08	0.96	0.49	0.74	1.65	-0.40	-0.76	-0.45	0.24	0.16	-1.12	0.09	-0.20
2016	-1.92	-0.52	0.55	-0.45	0.31	n/a	2.01	1.61	0.00	-1.55	0.78	-2.50	0.13	-0.64	-0.50	0.23	-0.49
2017	-1.47	-0.31	0.11	0.39	0.31	0.53	-0.66	-0.69	0.42	1.36	0.90	-0.15	-0.78	-1.35	-0.62	-0.10	-2.01
2018	0.02	-0.42	0.32	-0.09	0.25	0.65	0.20	0.37	-0.07	-0.82	-0.05	-1.28	-0.84	0.13	-0.84	0.29	-2.09
2019	-1.30	-0.46	n/a	-0.48	1.10	-0.16	-1.10	-0.96	0.76	1.11	0.76	n/a	n/a	n/a	-0.39	0.33	-1.57

The spotlight charts in Tables 4-4 and 4-5 provide valuable information on conditions experienced by the two stocks over time, but the volume of information in the tables is high and diverse, and is thus challenging to interpret. The CCIEA team and HC members will be developing approaches to refine this first iteration; that refinement will involve statistical analysis of tributary-specific variation and multivariate tools to reduce indicator redundancy and increase predictability (potentially building on the approach of Burke et al. 2013, and similar to analyses shown above in Figure 4-5). In the meantime, a simple way to assimilate and visualize the information in Tables 4-4 and 4-5 is with time-series plots of standardized average indicator scores for the freshwater and marine life stages of the two stocks, which highlight the fluctuation in habitat conditions over the past 37 brood years (Figure 4-6). Since the mid-1990s, both freshwater and marine habitat conditions have apparently declined for Sacramento River stocks, but these patterns are less clear for Klamath River stocks. While the combination of poor freshwater and marine habitat conditions has occurred previously, they have tended to trend in opposition. However, at least two of the three critical brood years defined in the rebuilding plans were characterized by below-average freshwater and marine conditions for Sacramento River stocks. In years subsequent to the rebuilding plans, freshwater conditions improved for Sacramento River populations, while freshwater conditions for Klamath River populations were close to the average for 1983–2019. Marine conditions have declined for both Sacramento and Klamath River populations since the rebuilding period.

PFMC has a long history of engaging with partner agencies to advocate for improved habitat conditions for the Sacramento and Klamath River fall Chinook salmon runs. While many possible management “dials” exist for improving habitat, few can easily be tracked annually. For both stocks, river flow is highly managed through hydropower, and flows at particular stages

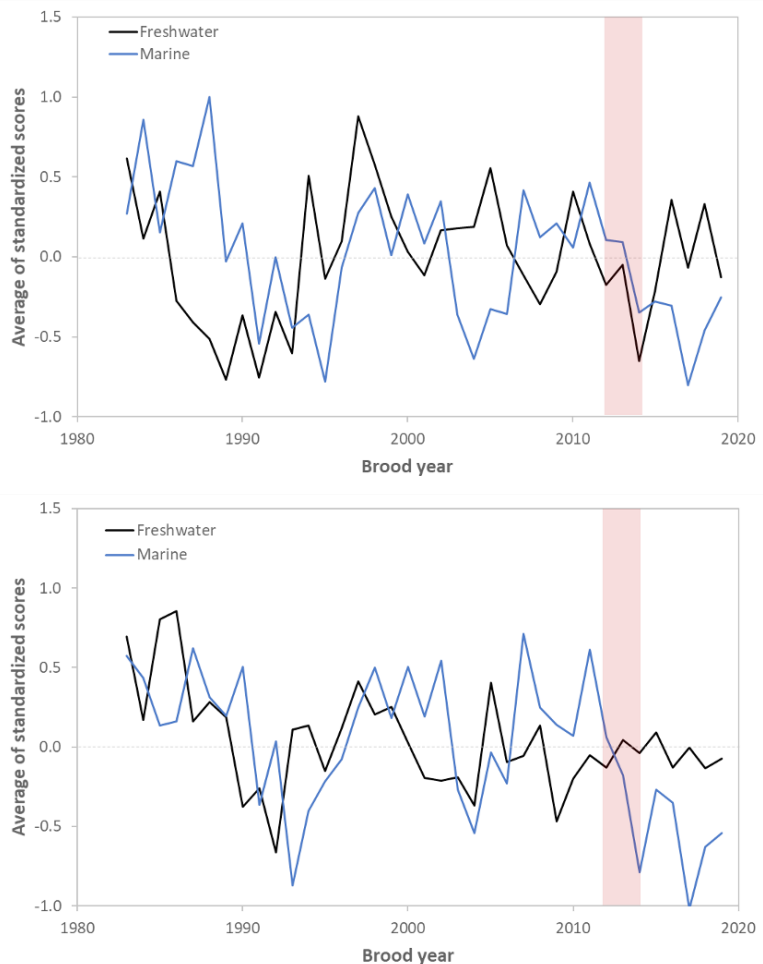


Figure 4-6. Average of standardized freshwater and marine habitat condition indicators for brood years 1983–2019 for the Sacramento River (top) and Klamath River (bottom) fall runs. The rebuilding plan was defined for brood years 2012–14 (red bar). Plots developed and provided by C. Greene (NMFS/NWFSC) and S. Munsch (NMFS/NWFSC, Ocean Associates, Inc.).

can influence water temperature. These indicators have shown evidence for long-term change as well as recent variability during brood years highlighted by the rebuilding plan and years thereafter. In particular, temperature conditions for the Sacramento River (during spawning and spring rearing) and flow conditions for the Klamath River (all types except maximum flushing flows) continue to remain at relatively low status, suggesting that improved flow management can have positive improvements for populations (Munsch et al. 2020). The CCIEA team will continue to work with HC, STT, and SSC as necessary to continue to present and refine these indicators for these two important stocks.

4.2 Groundfish Stock Abundance, Community Structure, and Distribution

The CCIEA team regularly presents the status of groundfish biomass and fishing pressure based on the most recent stock assessments. Except for Pacific hake, there were no groundfish assessment updates in 2020, so indices for the status of groundfish biomass and fishing pressure are essentially unchanged from last year’s report, in which we reported that no assessed stocks were considered to be in an overfished status—although yelloweye rockfish (*Sebastes ruberrimus*) are still in the process of rebuilding toward their target reference point—and nearly all groundfish were experiencing sustainable harvest pressure below their respective overfishing proxies (Harvey et al. 2020). We will update this information in next year’s report following the upcoming groundfish assessment cycle in 2021.

Changes in abundance and spatial distribution of groundfish may affect fishing opportunities in different locations. We are analyzing data from a U.S. West Coast groundfish survey to determine if groundfish stock availability is changing at different spatial and temporal scales. Here we focus on twelve key groundfish stocks and how relative availability of their biomass has changed over time for several U.S. West Coast ports (Figure 4-7). The approach follows that of Selden et al. (2020). In brief, we used data from the Northwest Fisheries Science Center’s annual West Coast Groundfish Bottom Trawl Survey (2003–19) and vector autoregressive spatio-temporal (VAST) modeling (Thorson 2019) to estimate spatial distribution of species-specific biomass (“location biomass”), and the center of gravity (CoG) of the location biomass. We then calculated an “Availability Index” for each port by summing the location biomass within a radius from that port (Figure 4-7) based on the 75th quantile of the distance travelled from port to harvest any of the species analyzed in Selden et al. (2020), weighted by catch, as measured by trawl logbooks from 1981–2015. We analyzed species that make up a large component of landings for vessels using bottom trawl gear along the U.S. West Coast, or that have broader management interest (e.g., shortbelly rockfish [*Sebastes jordani*], which have been an important bycatch species in recent midwater trawl fisheries).

The Availability Index for most of the selected species was highest for the northern ports, particularly Astoria, Oregon (Figure 4-7). This pattern is due in part to distribution of stock biomass. In addition, vessels from Astoria utilize a larger area on average than those from most other ports; the shelf and upper slope are wider near Astoria than in regions adjacent to other ports, as well (Figure 2-7). Estimated availability for big skate (*Beringraja binoculata*), petrale sole (*Eopsetta jordani*), and sablefish increased from approximately 2010 onwards for Astoria, doubling in availability for big skate and sablefish and increasing

sixfold for petrale sole, before dropping back to earlier levels (Figure 4-8). The Availability Index of lingcod (*Ophiodon elongatus*) increased rapidly for Bellingham, Washington, and Astoria from 2009 to 2013 but then declined steeply from 2014 to 2019. In contrast, availability of canary rockfish (*Sebastes pinniger*), yellowtail rockfish (*S. flavidus*), and shortspine thornyhead (*Sebastolobus alascanus*) to northern ports also increased after approximately 2010, but did not decrease in availability later in the time series. Overall, individual species tended to show some synchrony in availability coastwide, although variation at southern ports was generally muted compared to the two northern ports (shortbelly rockfish being the exception). However, for some species, there were within-region differences. For example, estimated availability of arrowtooth flounder (*Atheresthes stomas*) spiked sharply for Bellingham in 2016, but not for other northern ports. Similarly, estimated availability of darkblotched rockfish (*Sebastes crameri*) spiked off Coos Bay, Oregon, in 2013, but not off other northern ports.

Variation in center of gravity (Figure 4-9) was only directional for short periods of five-to-ten years. However, shifts in the CoG could be considerable, up to 2–3° of latitude. CoG variability was highest for big skate, lingcod, sablefish, and shortbelly rockfish. Sablefish CoG initially shifted south and remained stable for several years. Sablefish CoG then shifted north until 2018, and then returned to ~lat 41°N, where it was in 2003. Lingcod, shortbelly rockfish, and big skate showed similar patterns. Even arrowtooth flounder, which showed a slight long-term southward shift in CoG, shifted back north in 2019 to a similar latitude as in 2003. Thus there is as yet no evidence of unidirectional latitudinal or longitudinal shifts of groundfish during this time series; e.g., the types of climate-driven unidirectional shifts that have been observed or predicted for groundfish in other systems (e.g., Nye et al. 2009, Morley et al. 2018), but analysis of longer time periods or larger spatial extents (e.g., from the U.S. West Coast to the Gulf of Alaska) might be informative.

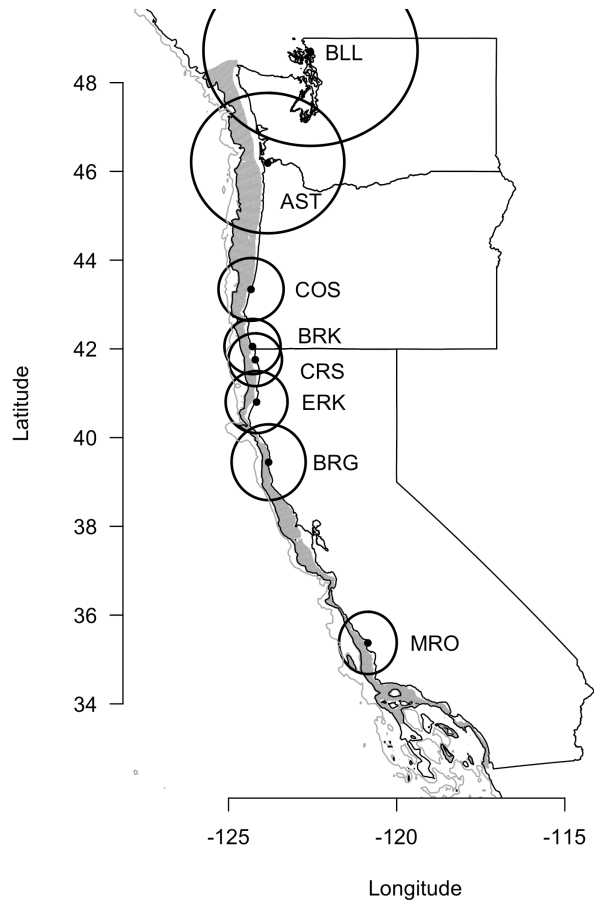


Figure 4-7. Locations of ports used in the availability analysis. The radii of the black circles centered on each port represent the areas within which groundfish availability is estimated (see text). Ports are Bellingham Bay (BLL), Astoria (AST), Charleston (Coos Bay, COS), Brookings (BRK), Crescent City (CRS), Eureka (ERK), Fort Bragg (BRG), and Morro Bay (MRO). Shaded area is inside the 600-m depth contour; gray line is the 1,200-m depth contour. Groundfish biomass availability index provided by B. Selden (Wellesley College) and N. Tolimieri (NMFS/NWFSC), with data derived from the West Coast Groundfish Bottom Trawl Survey.

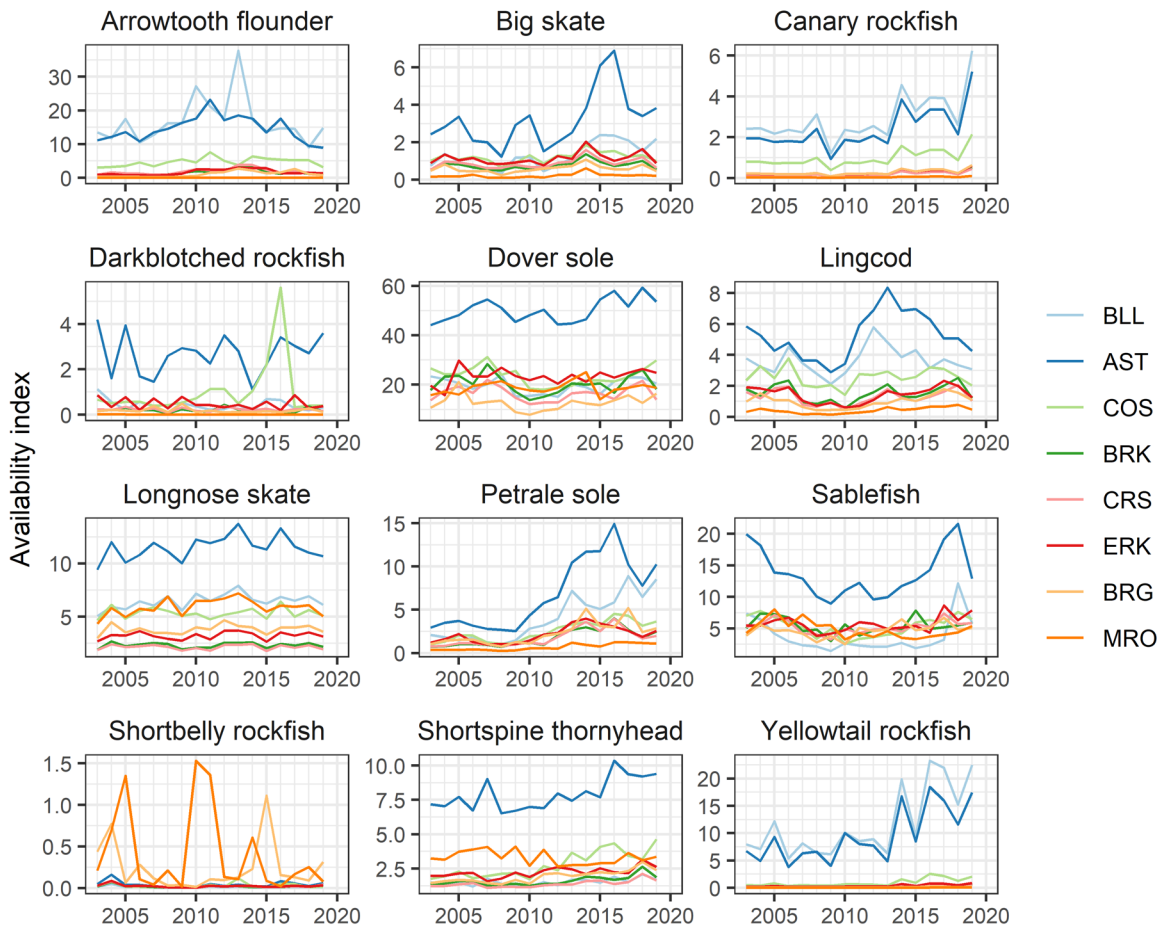


Figure 4-8. Availability Index of biomass for selected species to ports along the U.S. West Coast, 2003–19. Ports are: Bellingham Bay (BLL), Astoria (AST), Charleston (Coos Bay, COS), Brookings (BRK), Crescent City (CRS), Eureka (ERK), Fort Bragg (BRG), and Morro Bay (MRO). Groundfish biomass availability index provided by B. Selden (Wellesley College) and N. Tolimieri (NMFS/NWFSC), with data derived from the West Coast Groundfish Bottom Trawl Survey.

We will continue to track these changes in distribution and abundance as potential indicators of environmentally driven changes in groundfish stocks, as indicators of fishing opportunities for ports, and to inform decisions regarding allocation of fishing effort and catch. Future work to understand the relative roles of climate, recruitment, stock size, fisheries removal, and other factors will help us to clarify observed variability in centers of gravity of key groundfish stocks.

4.3 Highly Migratory Species

Several highly migratory species (HMS) targeted by U.S. West Coast fisheries have had recent updates to their assessments, including information on stock biomass and recruitment. For those recently assessed stocks, we here present quad plots summarizing recent short-term averages and trends of biomass and recruitment; time series and summaries of stock condition for these stocks, as well as stocks that have not been recently assessed (e.g., swordfish [*Xiphias gladius*], blue marlin [*Makaira mazara*], and skipjack [*Katsuwonus pelamis*]), are presented in Appendix J of Harvey et al. (2021).

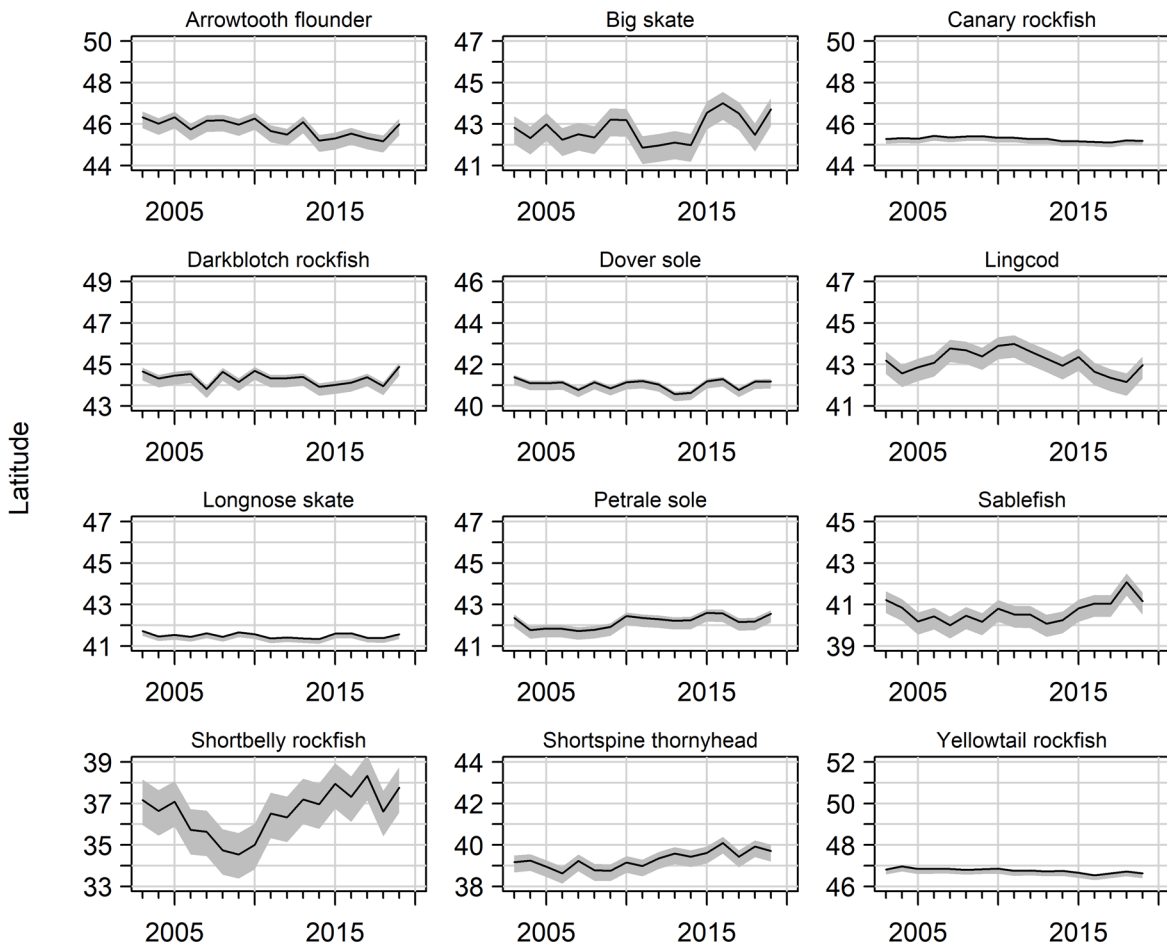


Figure 4-9. Center of gravity for 12 species of groundfish, 2003–19, calculated using VAST modeling and the West Coast Groundfish Bottom Trawl Survey. Note, y-axes differ but the range (6° lat) is constant among plots. Envelope is ± 1 SD. Groundfish biomass availability index provided by B. Selden (Wellesley College) and N. Tolimieri (NMFS/NWFSC) with data derived from the West Coast Groundfish Bottom Trawl Survey.

Biomasses of recently assessed HMS stocks appeared to be below average relative to the full assessment periods, and biomass trends ranged from weakly negative to weakly positive (Figure 4-10 left; see also Harvey et al. 2021, Appendix J). Of the stocks shown, bluefin tuna (*Thunnus orientalis*) are the most likely to be in an overfished status, though that is likely due to fishing pressure outside of the California Current (Harvey et al. 2021, Appendix J). HMS recruitment estimates from recent assessments are within ± 1 SD of long-term averages, and two stocks (albacore [*T. alalunga*] and yellowfin tuna [*T. albacares*]) experienced apparent increases in recruitment during the most recent five years (Figure 4-10, right), although these estimates should be interpreted cautiously given their high uncertainty (Harvey et al. 2021, Appendix J). The relationships between these indicators and different attributes of population condition (e.g., target and limit reference points) are complicated and differ by species, as summarized in Harvey et al. (2021, Appendix J); for example, bigeye tuna (*Thunnus obesus*) estimates are drawn from 44 separate reference models that broadly group into two outlooks, one relatively “optimistic” and one relatively “pessimistic.” We will continue to improve on HMS indicators in future reports.

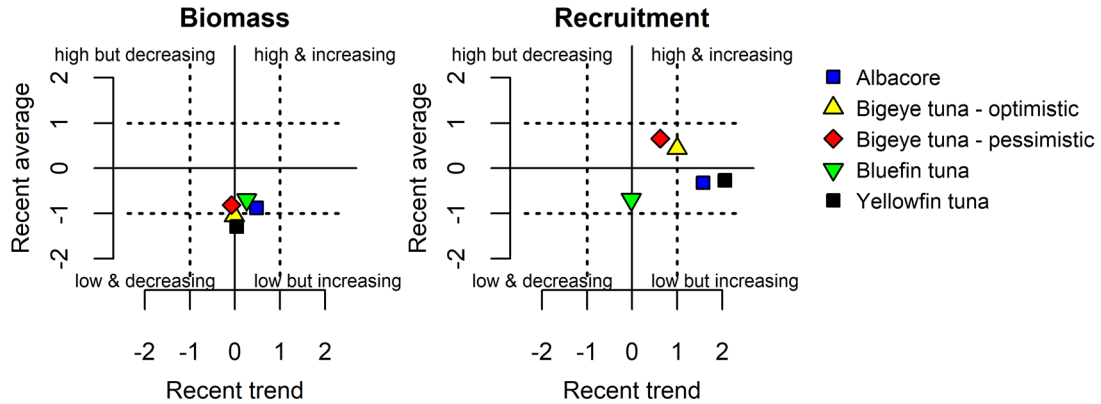


Figure 4-10. Recent trend and average of spawning biomass and recruitment for highly migratory species in the California Current from recent stock assessments: bluefin tuna (2018), albacore (2019), bigeye tuna (2019), and yellowfin tuna (2020). Lines, colors, and symbols as in Fig. 1-3c. Highly migratory species data provided by B. Muhling (NMFS/SWFSC). Data derived from stock assessment reports for the International Scientific Committee for Tuna and Tuna-like Species in the North Pacific Ocean (ISC)* or the Inter-American Tropical Tuna Commission (IATTC).[†]
 * http://isc.fra.go.jp/reports/stock_assessments.html
[†] <https://www.iattc.org/PublicationsENG.htm>

5 Marine Mammals and Seabirds

Sharon Melin, Morgan Ball, Elizabeth Jaime, Mary Hunsicker, Dan Lawson, Lauren Saez, Thomas P. Good, Rozy Bathrick, Jessie Beck, Cheryl Horton, Jaime Jahncke, Mike Johns, Kirsten Lindquist, Rachael Orben, Jessica Porquez, Jan Roletto, Pete Warzybok, and Chris J. Harvey

5.1 Marine Mammals

5.1.1 Sea lion production

California sea lions are permanent residents of the CCE, breeding in the California Channel Islands and feeding throughout the CCE in coastal and offshore habitats. Their condition is also an indicator of availability (a combination of abundance and distribution) and composition of the coastal pelagic prey community for nursing California sea lions foraging from the northern Channel Islands to Monterey Bay throughout the year (Melin et al. 2012). Nursing California sea lions are central place foragers for 11 months of the year, traveling to and from the breeding colonies in the Channel Islands, where their pups reside, to foraging areas within 200 km of the colonies. Consequently, they sample the coastal pelagic forage community throughout the year and their diet and resultant reproductive success, measured by pup metrics, depends on the availability of that forage community.

Two indices are particularly sensitive measures of prey availability to California sea lions: pup production and pup growth during the period of maternal nutritional dependence. These indicators represent different aspects of reproductive success, which relies on successful foraging by reproductive females. As such, the indicators are indirect qualitative measures of the forage available to reproductive females and do not provide specific forage community information. The annual number of pup births is an index of successful pregnancies, which depend on the nutritional condition of the female—which in turn depends on the quality and quantity of prey available during the gestation period. Higher numbers of pup births indicate that females consumed a diet that provided sufficient quantity and nutrition to support the energetic cost of gestation. Pup condition and growth depend on milk intake. The more milk consumed, the better the condition and growth rate. The amount of food consumed by a female on a foraging trip determines the amount of milk she has to deliver to a pup when she returns. Better pup condition and higher growth rates indicate abundant prey for nursing females during the lactation period.

In 2020, NOAA scientists were able to conduct counts of sea lion pups via aerial surveys. The 2020 cohort was the fourth consecutive year of above-average pup

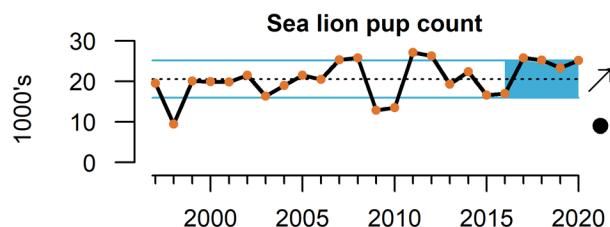


Figure 5-1. California sea lion pup counts on San Miguel Island for the 1997–2020 cohorts. Lines, colors, and symbols as in Fig. 1-3a. California sea lion data provided by S. Melin (NMFS/AFSC), with additional data collection and interpretation by E. Jaime (NMFS/AFSC) and M. Ball (Wildlands Conservation Science).

counts (Figure 5-1), and continued the positive trend since the relatively low counts in 2015–16. The relatively high pup count in 2020 implies abundant and high-quality prey for adult female sea lions in their foraging area (rectangle in Figure 1-4a), and is consistent with the estimates of high anchovy abundance derived from the limited sampling of forage communities of the Central and Southern CCE in 2020 (Figures 3-5 and 3-6).

We usually report sea lion pup growth from fall and winter, but researchers could not conduct in situ assessments of pup growth or condition in 2020 due to COVID-19 restrictions. However, based on an analysis relating sea lion pup growth to PDO, conditions in 2020 are consistent with normal to above-normal pup growth. Following approaches described by Samhuri et al. (2017), we are using generalized additive models (GAM) to identify the presence of nonlinear and threshold dynamics in pressure–response relationships in the CCE, with a focus on the response of key species and processes to basin- and regional-scale climate variables. In this case, we analyzed California sea lion pup growth as a function of PDO, which is an index of SST in the northeastern Pacific Ocean (see Figure 2-1 and related text). Pup growth was greatest when the PDO index was negative, indicative of the index region being in a cold phase, while pup growth estimates quickly declined as the PDO index became positive (indicative of a warm phase) and increased beyond a threshold value of ~ 0.4 (Figure 5-2). The same approach also found a negative relationship between pup growth and coastal SST in the Southern and Central regions of the CCE. The PDO from August 2020 to early winter of 2021 has been negative (i.e., well to the left of the threshold PDO value in Figure 5-2), consistent with average or potentially above-average growth conditions for the 2020 cohort of pups at San Miguel Island.

Some PFMC advisory bodies have expressed concerns that sea lion pup counts and growth may be less effective indicators when the population is close to carrying capacity, which it was in the 2010s: according to population modeling work by Laake et al. (2018), the San Miguel Island colony at that time had an estimated carrying capacity of $\sim 275,000$ animals (including pups), while annual population estimates between 2006 and 2014 ranged from 242,000 to 306,000 animals. Advisory bodies were concerned that changes in pup count or growth could be due to density-dependent mechanisms within the sea lion population, rather than to changes in the prey community. However, a linear mixed effects model of California sea lion pup growth that includes environmental variables, sea

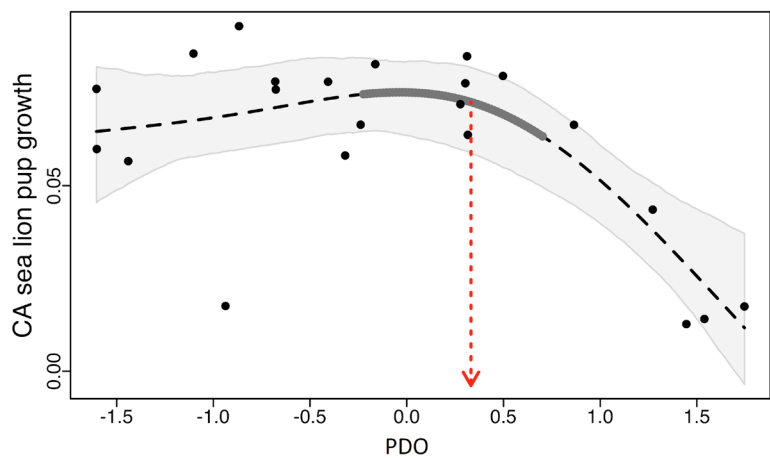


Figure 5-2. California sea lion pup overwinter growth rate (kg/d) in relation to fall–winter PDO. Points represent observed data, dashed black line represents generalized additive model fit, gray envelope = 95% confidence interval, red arrow indicates best estimate of the threshold value of PDO above which pup growth declines rapidly, and heavy black line indicates 95% confidence interval of threshold value. Data plot provided by M. Hunsicker (NMFS/NWFSC).

lion abundance, fish abundance and nursing female diet revealed that the abundance of California sea lions was not a significant factor in annual variability of pup growth rates (Melin et al. in preparation). The model also did not detect a declining trend in pup growth as the population size increased, which might occur if competition among nursing females for limited forage was affecting the ability of females to support the energetic demands of their pups. Elevated SST explained the greatest amount of variability for pup growth rates in the models: an increase of 1°C in SST resulted in a 7% decline in the population growth rate, even when the population was much smaller (<100,000 animals) in the 1980s (Laake et al. 2018). The reverse effect was not apparent when SST decreased by 1°C. These analyses indicate that pup count and pup growth are not compromised as indicators by population size, but rather reflect the dynamic relationship between environmental conditions and California sea lion reproduction. We believe the key underlying mechanism is that elevated SST affects the distribution and abundance of the California sea lion prey community, reducing access to food for nursing females until they cannot support the energetic demands of pregnancy (resulting in fewer births) or lactation (resulting in slower pup growth).

5.1.2 Whale entanglement

The number of whale entanglements reported along the U.S. West Coast increased in 2014 and even more over the next several years, particularly for humpback whales (*Megaptera novaeangliae*). While ~50% of entanglement reports cannot be attributed to a specific gear type, Dungeness crab fishing gear was the most common source identified during this period. The dynamics of entanglement risk and reporting are complex, affected by shifts in oceanographic conditions and prey fields, changes in whale populations, changes in distribution and timing of fishing effort, and increased public awareness leading to improved reporting (Santora et al. 2020). Pelagic habitat compression, as illustrated in Figure 2-8, may be further exacerbating interactions between whales and other ecosystem components (Santora et al. 2020).

There were 17 confirmed entanglement reports on the U.S. West Coast in 2020, again higher than any year prior to 2014—although fewer confirmed reports were received than in any year since 2013 (Figure 5-3; see also NOAA 2020). It is important to note that COVID-19 caused reduced reporting capability, with fewer vessels available to assist with sighting and documentation, which may be responsible for some of the decrease in confirmed entanglement reports. As in previous years, the majority of confirmed reports (10) were of entangled humpback whales, followed by gray whales (*Eschrichtius robustus*; six confirmed reports) and one sperm whale (*Physeter macrocephalus*). There were no confirmed reports of entangled blue whales (*Balaenoptera musculus*). Also as in previous years, the majority of reports in 2020 were in California, though entanglements were known to include gear from all three U.S. West Coast states and from commercial and recreational Dungeness crab, commercial rock crab, and gillnet fisheries. No confirmed entanglements occurred in sablefish fixed gear. Significant actions were taken in 2020 to address the increased entanglement risk (NOAA 2020), including closures and delays of Dungeness crab seasons in California and late-season reductions of allowable Dungeness crab gear and new line-marking requirements in Washington. In 2021, Oregon will implement newly adopted regulations that restrict depths and amount of Dungeness crab gear that can be fished. While these actions are expected to reduce entanglement risks, other factors will continue to present obstacles to risk reduction: exposure of whales to derelict gear, whales foraging in nearshore waters during certain ecosystem conditions, and growth of some whale populations.

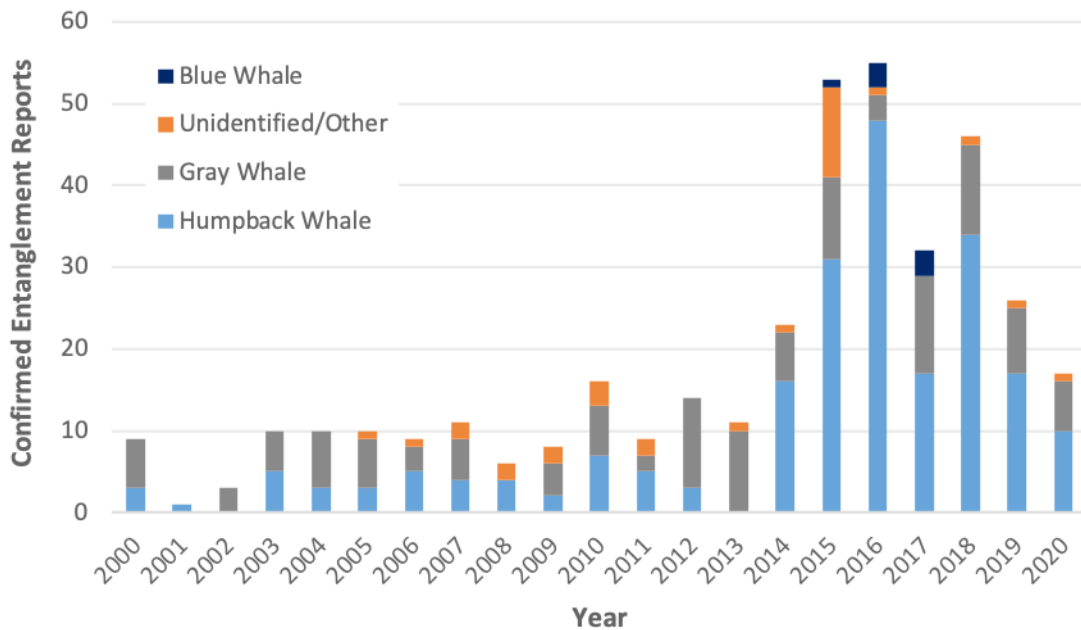


Figure 5-3. Confirmed numbers of whales (by species) reported as entangled in fishing gear and other sources along the U.S. West Coast, 2000–20. Whale entanglement data provided by D. Lawson and L. Saez (NMFS/WCR).

5.2 Seabirds

Seabird indicators (productivity, diet, mortality, and at-sea densities) constitute a portfolio of metrics that reflect population health and condition of seabirds as well as links to lower trophic levels and other conditions in the CCE. To highlight the status of different seabird guilds and relationships to their marine environment, we monitor multiple focal species throughout the CCE. The species we report on in the sections below represent a breadth of foraging strategies, life histories, and spatial ranges. Seabird data collection efforts in 2020 were curtailed in many cases due to COVID-19 precautions and restrictions. However, the data that were collected indicated that 2020 saw better conditions for seabirds in much of the CCE than many recent years. Several species experienced average to above-average fledgling production at colonies off California and Oregon, and there were no reports of mass seabird mortalities and strandings along U.S. West Coast beaches.

5.2.1 Seabird population productivity

Seabird population productivity, as measured through indicators of reproductive success, tracks marine environmental conditions and often reflects forage production near breeding colonies. Here we present standardized anomalies of fledgling production per pair of breeding adults for five focal species on Southeast Farallon Island (SEFI) in the central region of the CCE. The five species represent a range of feeding habits while on colonies:

1. Rhinoceros auklets (*Cerorhinca monocerata*) forage primarily on pelagic fishes in shallow waters over the continental shelf, generally within 50 km of colonies, and they return to the colony after dusk to deliver multiple whole fish to their chicks.

2. Common murres forage primarily on pelagic fishes in deeper waters over the shelf and near the shelf break, generally within 80 km of colonies, and they return to the colony during daylight hours to deliver single whole fish to their chicks.
3. Cassin's auklets (*Ptychoramphus aleuticus*) forage primarily on zooplankton in shallow water over the shelf break, generally within 30 km of colonies; they forage by day and night and return to the colony at night to feed chicks.
4. Brandt's cormorants (*Phalacrocorax penicillatus*) forage primarily on pelagic and benthic fishes in waters over the shelf, generally within 20 km of breeding colonies, and they return to the colony during the day to deliver regurgitated fish to their chicks.
5. Pigeon guillemots (*Cepphus columba*) forage primarily on small benthic and pelagic fish over the shelf, generally within 10 km of colonies, and they return to the colony during the day to deliver a single fish to their chicks.

Seabird colonies on SEFI off central California experienced mixed productivity in 2020 (Figure 5-4). Several species experienced improved fledgling production relative to 2019. Cassin's auklets, which feed on krill, bounced back strongly in 2020, consistent with higher amounts of krill in their diets (see Section 5.2.2). Pigeon guillemots and rhinoceros auklets experienced near-average fledgling production in 2020, an increase from 2019. Common murre fledgling production was below average, but slightly improved from 2019. In contrast to these four species, Brandt's cormorants at SEFI have had average to above-average fledgling production every year from 2013 to 2020.

At Yaquina Head off central Oregon, productivity in 2020 was mixed for the three monitored seabirds (Figure 5-5). Brandt's cormorant fledgling production was above average, but disturbances from bald eagles (*Haliaeetus leucocephalus*) were observed during incubation; this was new for this species at this location, and may have brought chick production down from the higher values of the last two years. Common murres experienced extremely low fledgling production in 2020, following two years of relatively high production. This was due primarily to bald eagle predation on adult murres, high levels of colony disturbance, and the highest egg depredation rates ever observed at this site. In 2020, 15 eagles were observed simultaneously at Yaquina Head, the largest aggregation of eagles documented over the disturbance study period. Pelagic cormorant (*Phalacrocorax pelagicus*) fledgling production at Yaquina Head in 2020 was the highest recorded at this site.

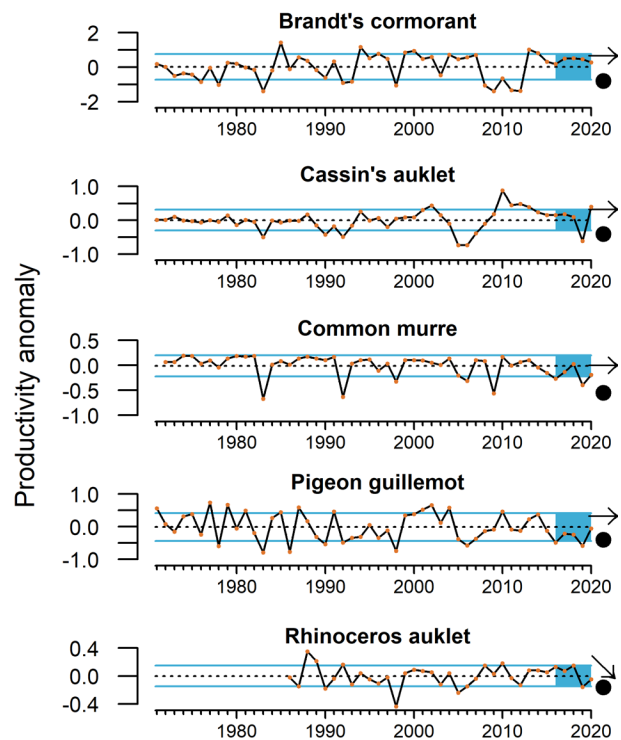


Figure 5-4. Standardized productivity anomalies (annual productivity, defined as the annual number of chicks fledged per pair of breeding adults, minus the long-term mean) for five seabird species breeding on SEFI through 2020. Lines and symbols as in Fig. 1-3a. Data provided by Point Blue Conservation Science (jjahncke@pointblue.org).

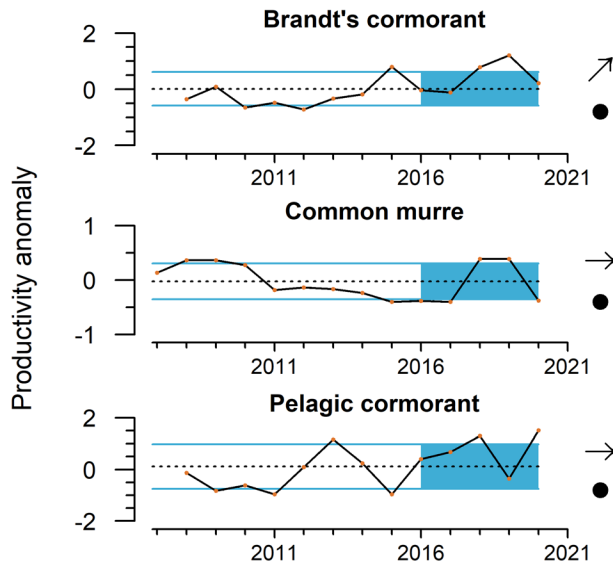


Figure 5-5. Standardized productivity anomalies (annual productivity, defined as the annual number of chicks fledged per pair of breeding adults, minus the long-term mean) for three seabird species breeding on Yaquina Head through 2020. Lines and symbols as in Fig. 1-3a. Data provided by Yaquina Head Seabird Colony Monitoring Project (rachael.orben@oregonstate.edu).

5.2.2 Seabird diets

Seabird diet composition during the breeding season tracks marine environmental conditions and often reflects production and availability of forage within different regions. Here, we present some seabird diet data that may shed light on foraging conditions along the U.S. West Coast in 2020. We are working with partner research organizations to better integrate diet information into our reporting.

At colonies off central California, there are diet data available for seabirds from SEFI, which is close to the region of the most intense upwelling in the CCE and thus a valuable source of information about ecosystem productivity and prey availability to higher trophic levels. Among piscivores, the past five years have shown increasing reliance on anchovy and decreasing reliance on juvenile rockfish. The proportions of anchovy in the diets of Brandt's cormorants and rhinoceros auklets provisioning chicks were above average in 2020 and showed significant positive short-term trends. The anchovy proportion was the highest ever recorded for Brandt's cormorants and the fourth-highest recorded for rhinoceros auklets at this location. The proportions of juvenile rockfish in these two species' diets have shown significant negative short-term trends, although the presence of rockfish was close to average for rhinoceros auklets in 2020 (Figure 5-6). For common murres, the proportions of anchovy were above average, while the proportions of rockfish and Pacific salmon were below average in 2020. Pigeon guillemots in 2020 had a below-average amount of rockfish in their diet. Juvenile rockfish did increase in the diets of rhinoceros auklets, common murres, and pigeon guillemots in 2020 relative to 2019 (Figure 5-6, right). For Cassin's auklets, which feed heavily on krill, the proportion of *Euphausia pacifica* in the diet was below average in 2020, while the proportion of *Thysanoessa spinifera* was just above average and showed a sharp increase from 2019 (Figure 5-6, bottom).

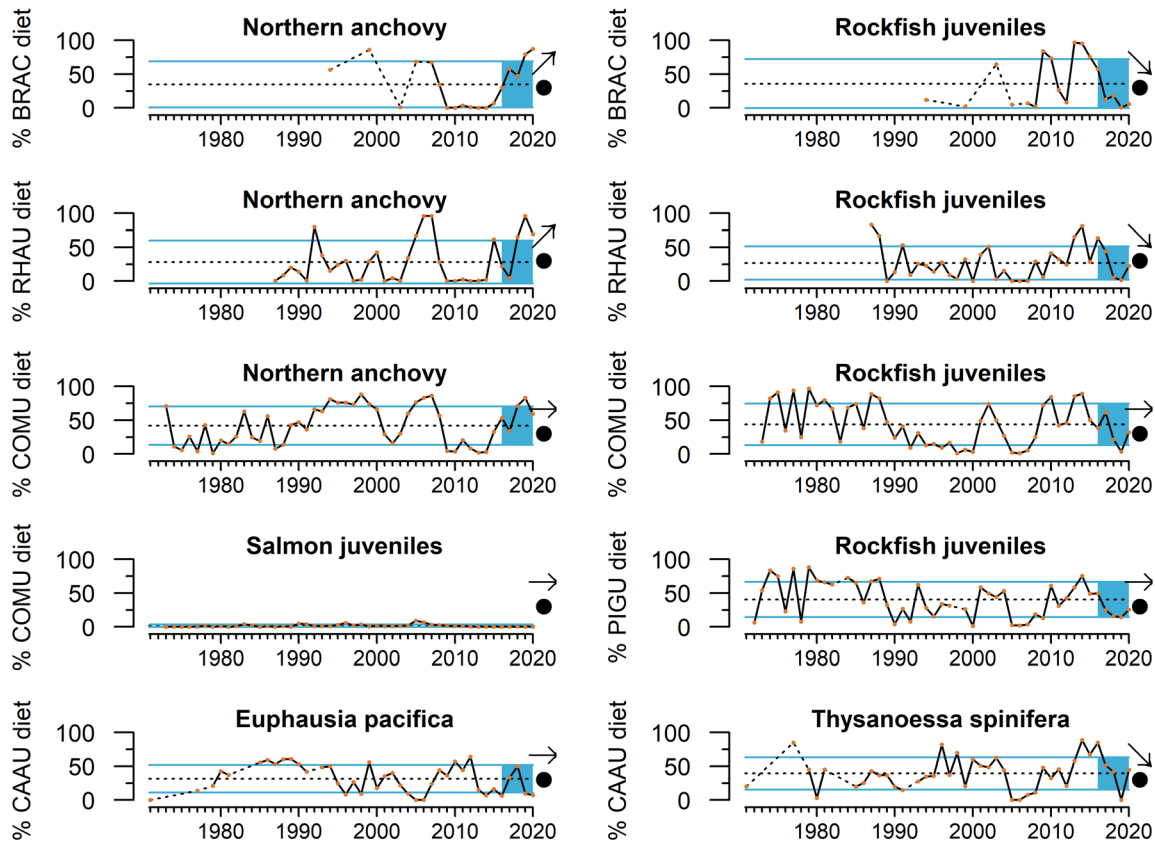


Figure 5-6. Southeast Farallon Island (SEFI) seabird diets through 2020. *BRAC* = Brandt’s cormorant; *CAAU* = Cassin’s auklet; *COMU* = common murre; *PIGU* = pigeon guillemot; *RHAU* = rhinoceros auklet. Lines, colors, and symbols as in Fig. 1-3a. Data provided by Point Blue Conservation Science (jjahncke@pointblue.org).

At Año Nuevo Island, the size of anchovy returned to rhinoceros auklet chicks in 2020 was slightly above the long-term average and has increased since 2014–16 (Figure 5-7). Researchers again expressed concern that while abundant and dominant in the observed diet, individual anchovy may have been too large to be ingested by rhinoceros auklet chicks; this may in turn have contributed to the below-average fledgling production of these and other birds in central California in 2020 (e.g., Figure 5-4). This may speak to the benefit of a more diverse diet that includes prey of different sizes.

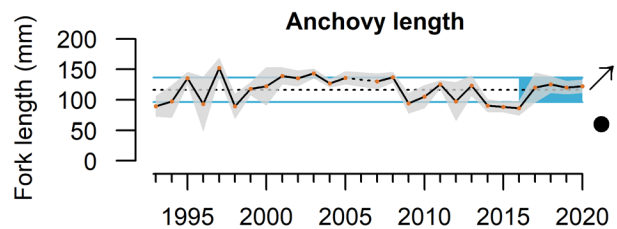


Figure 5-7. Fork length of northern anchovy brought to rhinoceros auklet chicks at Año Nuevo Island, 1993–2020. Error envelope shows ± 1 SD. Lines and symbols as in Fig. 1-3a. Data provided by Oikonos/Point Blue Conservation Science (jessie@oikonos.org).

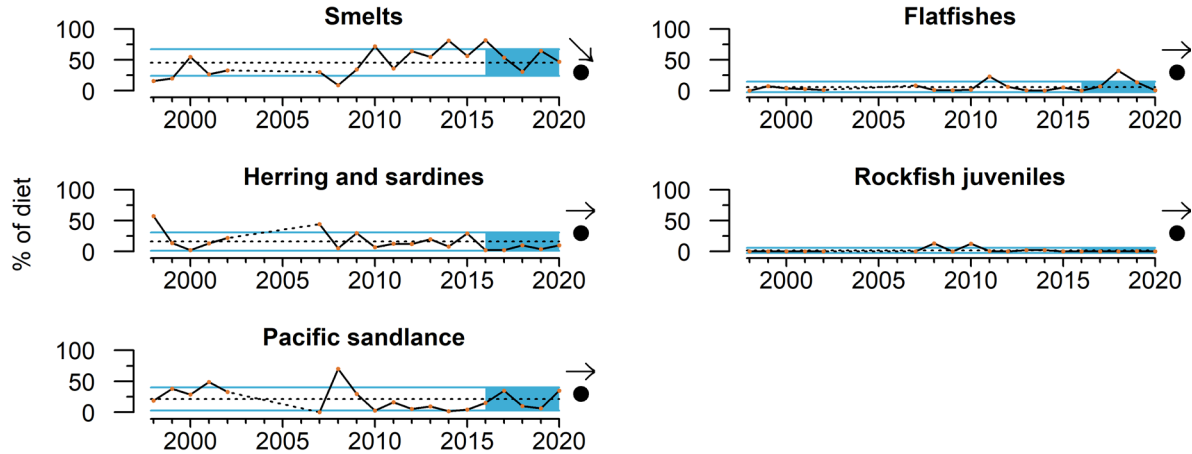


Figure 5-8. Common murre chick diets at Yaquina Head through 2020. Lines and symbols as in Fig. 1-3a. Data provided by the Yaquina Head Seabird Colony Monitoring Project (rachael.orben@oregonstate.edu).

In the Northern CCE, seabird diet observations were collected at Yaquina Head, Oregon, despite bald eagle disturbances and low common murre productivity. The proportion of osmerids (smelts) in the diet of common murres provisioning chicks at Yaquina Head was average in 2020, down from 2019, and is showing a short-term decline (Figure 5-8). The proportion of Pacific herring and sardine remained below average, as it has been since 2015. The proportion of Pacific sandlance (*Ammodytes personatus*) was above average in 2020, second only to smelts. The proportion of flatfishes was below average, down from a peak in 2018, and the proportion of rockfishes was below average in 2020 for the sixth straight year, and has been close to zero since 2011. The other monitored colony in the Northern CCE, a rhinoceros auklet colony on Destruction Island, Washington, was not sampled in 2020 due to COVID-19.

Collectively, these seabird diet indicators likely reflect both the variability of forage community composition and the plasticity or opportunistic nature of predator foraging and diet. While there have been shifts in dominant prey species over time, northern anchovy featured prominently in diets of multiple seabird predators in 2020, particularly in the central California Current, which likely tracks prey availability as indexed by forage indicators (high anchovy and low rockfish) in the Central CCE (Figure 3-5).

5.2.3 Seabird mortalities

Monitoring of dead beached birds provides information on the health of seabird populations, ecosystem health, and unusual mortality events. CCIEA reports from the anomalously warm and unproductive years of 2014–16 noted major seabird mortality events in each year. In 2020, seabird mortality monitoring effort by citizen scientists was greatly decreased due to the COVID-19 pandemic. Despite this, we feel some confidence in the qualitative patterns described below, because these citizen science networks tend to be aware of and responsive to unusual mortality events, and we have reason to believe that major wrecks would have been detected and that accounts would have been circulated via social or traditional media.

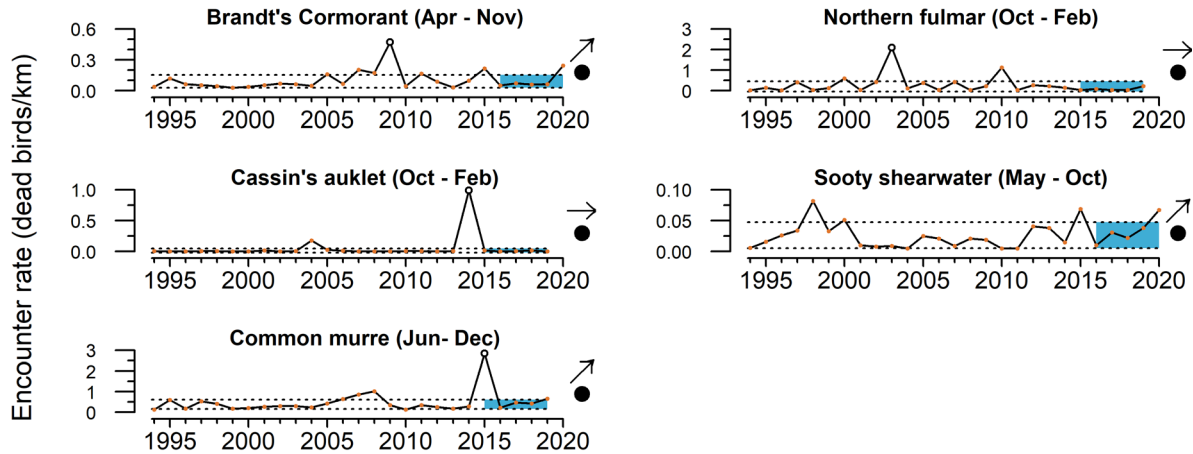


Figure 5-9. Encounter rate of bird carcasses on beaches in north-central California through 2020. The mean and trend of the last five years is evaluated versus the mean and SD of the full time series, but with the outliers removed. Open circles indicate outliers. Dotted lines indicate the upper and lower SD of the full time series with outliers removed. The blue box indicates the evaluation period and the upper and lower SD of the full time series with the outliers included. Annual data for Cassin's auklet and northern fulmar are calculated through February of the following year. Data provided by Beach Watch (<https://farallones.noaa.gov/science/beachwatch.html>).

This year's report does not include seabird mortality observations from the University of Washington-led Coastal Observation and Seabird Survey Team (COASST), which documents beach counts in the Northern CCE (Washington to Northern California). However, according to the [COASST website](#),¹³ there was an uptick in northern fulmar (*Fulmarus glacialis*) encounter rates in the COASST coverage area during the early spring of 2020.

In the Central CCE (Bodega Bay, California, to Point Año Nuevo, California), the BeachWatch program did observe upticks in encounter rates for two of the focal species in 2020 (Figure 5-9). The Brandt's cormorant encounter rate was >1 SD above average in 2020, but not high enough to be regarded as an unusual event. The Cassin's auklet encounter rate continued at low baseline levels in the 2019–20 winter (the most recent available data). The common murre encounter rate was above average in 2019 (the most recent available data), which continued an increasing recent trend; however, common murre encounter rates remain well below the peak from the wreck in 2015. The northern fulmar encounter rate was average in the 2019–20 winter (the most recent available data). The sooty shearwater encounter rate was >1 SD above average in 2020 and has a positive short-term trend, but the encounter rates in 2020 did not constitute a wreck. Due to COVID-19 effects, survey effort in 2020 was roughly 30% of a typical year.

The BeachCOMBERS program conducts surveys of beached seabirds on California beaches from Point Año Nuevo to Malibu, California, and we have previously reported on two survey regions: North (Point Año Nuevo to Lopez Point, California) and Central (Lopez Point to Rocky Point, California). BeachCOMBERS data have not been made available since our report last year, and are not shown here. After a program transition, data from 2020 will be available; however, due to COVID-19 restrictions, data collection was curtailed from April through August 2020.

¹³ <https://coasst.org/>

5.2.4 Seabird at-sea densities

Seabird densities on the water during the breeding season can track marine environmental conditions and may reflect regional production and availability of forage. Data from this indicator type can establish habitat use and may be used to detect and track seabird population movements or increases/declines as they relate to ecosystem change. Due to COVID-19-related impacts on spring pelagic community surveys, these data were not collected in 2020, and no plots are shown here.

6 Human Activities

Kelly Andrews, Marie Guldin, Ashley Vizek, Kayleigh A. Somers, Curt Whitmire, Erin Steiner, and Jerry Leonard

The CCIEA team compiles and regularly updates indicators of several of the human dimensions of the CCE, with particular focus on commercial and recreational fishing activities, nonfishing activities, and human wellbeing in coastal communities. Data on fishing and nonfishing activities come from a range of sources, particularly from state and federal agencies that manage such activities. Fishing activities indicators relate to total landed biomass, ex-vessel revenue, and some aspects of gear interactions with habitat. Nonfishing activities indicators focus on human activities that may directly or indirectly affect marine habitats, marine species, or fisheries.

6.1 Coastwide Landings and Revenue by Major Fisheries

Coastwide total landings have declined by 7–9% per year each year since 2017, largely tracking changes in hake, crab, and market squid (Figure 6-1). Total landings dropped by 7% in 2020 relative to 2019, and landings for six of nine major commercial landings groups declined in 2020 relative to 2019: salmon (–19%), non-hake groundfish (–19%), CPS finfish (–43%), hake (–9%), other species (–13%), and crab (–4%). Landings of shrimp (+46%), HMS (+6%), and market squid (+71%) fisheries increased in 2020 from 2019. Ocean conditions, wildfires, and COVID-related effects on supply and demand all likely contributed to the overall decrease in landings in 2020. COVID-related precautions and restrictions contributed to decreased demand for some species, particularly from restaurants and export markets. Additionally, COVID outbreaks on some Pacific hake (whiting) vessels may have reduced the fleet’s ability to harvest available quota (NMFS 2021).

Pacific hake made up 67% of all 2020 landings, and hake landings were at the highest levels of the time series during 2016–20. Commercial landings of salmon and CPS finfish over the last five years were >1 SD below the average of the time series. Groundfish (excluding hake) landings began to increase in 2017 from the low levels of catch over the previous ~16 years, but lost those increases in 2020. Market squid landings have been highly variable throughout the time series and were roughly 1 SD below average in 2020. Landings of crab and shrimp were close to average in 2020. HMS and other species landings have been consistently within ± 1 SD of time-series averages over the last 20+ years, though both are approaching lows for their respective time series. Additional information on state-by-state landings is available in Harvey et al. (2021), Appendix M.

Recreational landings data are complete at the coastwide level through 2020, with the important exception of recreational HMS landings data from California. In 2020, recreational landings (excluding salmon and Pacific halibut [*Hippoglossus stenolepis*]) were at their lowest levels of the time series and showed a decreasing trend since 2016 (Figure 6-2, left). The decline in coastwide recreational landings was driven by two primary factors: large decreases in albacore landings in Washington and Oregon in 2020, and a general decrease in landings of the top ten species in both California (six of top ten species

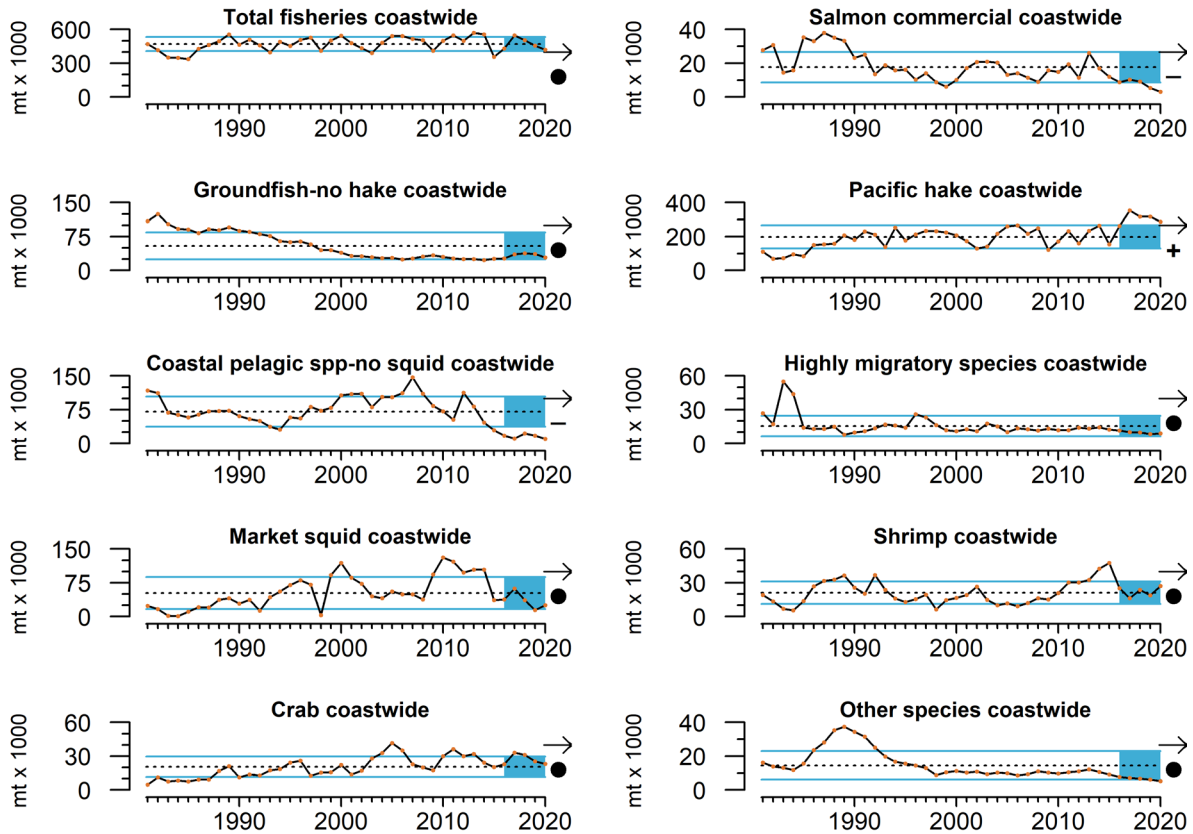


Figure 6-1. Annual landings of U.S. West Coast commercial fisheries, including total landings across all fisheries, 1981–2020. Lines, colors and symbols as in Fig. 1-3a. Data for commercial landings from PacFIN (<http://pacfin.psmfc.org>) and NORPAC (North Pacific Groundfish Observer Program).

decreased) and Washington (nine of top ten species decreased). As noted, recreational HMS landings data from 2020 were not yet available for California at the time of this report, and therefore all HMS data from California were excluded from this analysis to ensure consistency throughout the time series. Closures of popular marinas in Washington State and overall COVID-19 precautions and restrictions for personal and recreational charter activities likely contributed to these low levels in 2020. Relatively cool coastal waters off Oregon (see Figure 2-2) may also have contributed to poor recreational albacore catches. Recreational landings of Chinook and coho salmon at a coastwide level showed no recent trend from 2016–20 (Figure 6-2, right), but they were >1 SD below the time-series average and remained well below levels from the 1980s and early 1990s. State-by-state recreational landings are in Harvey et al. (2021), Appendix M.

Total revenue for U.S. West Coast commercial fisheries decreased from 2016–19, and was 12% lower in 2020 (\$437M) than in 2019 (\$498M; Figure 6-3). This pattern was driven primarily by decreases in revenue from crab, market squid, and groundfish (excluding hake) fisheries over this period. Revenue from crab has declined for the last three years, although five-year mean crab revenue was still >1 SD above the time-series average. Five-year mean revenue from Pacific hake landings was also >1 SD above the time-series average, whereas revenue from CPS finfish from 2016–20 was consistently >1 SD below the time-series

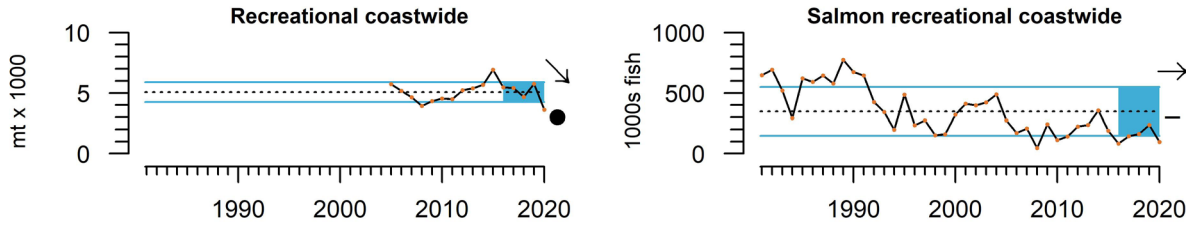


Figure 6-2. Annual landings of U.S. West Coast recreational fisheries, for all recreational fisheries and salmon, 1981–2020. Data from 2020 are incomplete (see text). Lines, colors and symbols as in Fig. 1-3a. Data for recreational landings from RecFIN (<http://www.recfin.org/>) and PFMCF (<https://www.pccouncil.org/salmon-management-documents/#safe>).

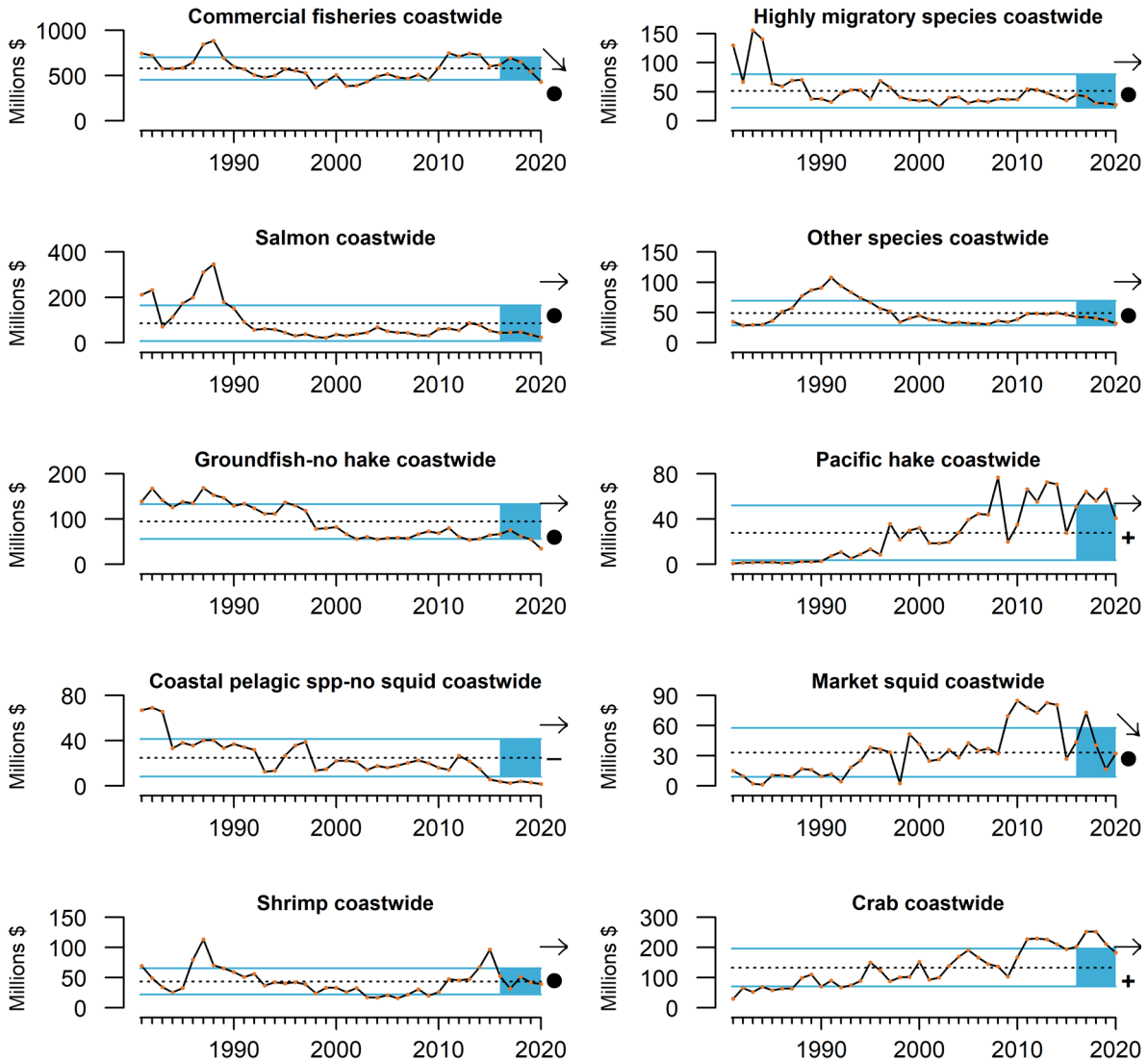


Figure 6-3. Annual revenue (ex-vessel value in 2020 dollars) of U.S. West Coast commercial fisheries (data from PacFIN), 1981–2020. Lines, colors, and symbols as in Fig. 1-3a. Pacific hake revenue includes shoreside and at-sea hake revenue values from PacFIN, NORPAC, and NMFS Office of Science and Technology.

average. Market squid revenue has declined substantially over the past five years. Revenues from other individual fisheries showed no recent trends and were within 1 SD of time-series averages, but revenue from salmon, groundfish (excluding hake), HMS, and other species were nearing the lowest levels of their respective time series. Ex-vessel revenue for eight of nine major target groups decreased in 2020 compared to 2019: CPS finfish (-45%), Pacific hake (-38%), non-hake groundfish (-36%), salmon (-20%), other species (-10%), crab (-7%), HMS (-10%), and shrimp (-1%). Market squid revenue increased in 2020 over 2019 (+91%). Ocean conditions, wildfires, compressed Dungeness crab fishing seasons, and COVID-related effects on supply and demand all likely contributed to the decrease in total revenue in 2020. In addition, vessels and processors may have experienced increased operating costs due to overcoming COVID outbreaks and implementing protective measures. Coastwide and state-level revenue data are presented in Harvey et al. (2021), Appendix M; note that total revenues in Figure 6-3 differ from total revenues in Harvey et al. (2021), because we have excluded bivalve shellfish revenues from Figure 6-3.

6.2 Bottom Trawl Contact with Seafloor

Benthic marine species, communities, and habitats can be affected by geological events (e.g., earthquakes, fractures, and slumping), oceanographic processes (internal waves, sedimentation, and currents), and human activities (bottom contact fishing, mining, energy-sector infrastructure, and dredging). Such disturbances can lead to mortality of vulnerable benthic species and disruption of food web processes. These effects may differ among types of seafloor habitat (hard, mixed, or soft sediments), and may be more dramatic in sensitive environments (e.g., seagrass, algal beds, coral and sponge reefs, or rocky substrates) than in soft sediments. The exploration of resources (e.g., oil, gas, and minerals), siting of energy-sector or aquaculture infrastructure, and marine fisheries often tend to operate within certain habitat types more than others, and long-term impacts of these activities may affect habitat integrity, biomass of key species, and the overall structure, function, and production of benthic communities. Thus, spatially explicit indicators are necessary to provide information for spatial management of specific human activities in relation to these resources.

Here we present updates to our ongoing estimates of seafloor contact by federally managed, limited entry bottom trawl gear, using the proxy of distance between start and end points of hauls. These indicators provide complementary data to inform management of specific human activities that affect seafloor habitat. These estimates may also be helpful in evaluating potential tradeoffs with future nonfishing activities along the U.S. West Coast, including offshore renewable energy development. Estimates of coastwide distances exposed to federally managed bottom trawl fishing gear from 1999–2019 were calculated based on set and haul-back locations. Data come from logbooks as reported to PacFIN and processed by NOAA's West Coast Groundfish Observer Program. Processing includes removing tows that appear to have errors in the logbook entries (e.g., set or haul-back location is on land, vessel speed necessary to make the tow was >5 knots, etc.).

We first present time series of the data at a coastwide scale and broken out by ecoregion (Northern, Central, Southern CCE), substrate (hard, mixed, soft), and depth zone (shelf, upper slope, lower slope). At the scale of the entire coast, estimated bottom trawl gear

contact with seafloor habitat from 2015–19 remained consistently at low levels relative to the available time series (Figure 6-4, top). During this period, the vast majority of estimated bottom trawl gear contact occurred in soft upper slope and soft shelf habitats (Figure 6-4, bottom). We estimate that the Northern CCE has seen the most bottom trawl fishing gear contact with seafloor habitat, with nearly four times more distance trawled than in the Central CCE and >40 times more than in the Southern CCE, where very little bottom trawling has occurred during the available time series. A shift in trawling effort from shelf to upper slope habitats was observed during the mid-2000s, which in part corresponded to depth-related spatial closures implemented by PFMC.

To examine finer-scale spatial variation in seafloor contact by bottom trawl gear in federally managed fisheries, we used the same logbook data to estimate distances trawled on a 2 × 2-km grid from 2002–19 (Figure 6-5). For each grid cell, we mapped: a) the 2019 total distance trawled, b) the 2019 departure (anomaly) from the long-term mean for each cell, and c) the most recent five-year trend in each cell. Note that the number of cells included in the five-year trend analysis is greater than in the 2019 anomaly analysis because there must be data from at least three vessels in a given cell for the period of analysis in order to conform to data confidentiality requirements.

Cumulative trawl distances within a given 2 × 2-km cell in 2019 were generally less than 50 km, though some cells (e.g., off of central Washington and just north of Cape Mendocino) had as much as 300 km of total trawling (Figure 6-5a). Distance trawled in 2019 was >1 SD above average (anomalously high relative to the available 2002–19 time series) in the red cells in Figure 6-5b, with notable concentrations off of central Washington, multiple bands off of central Oregon, and just north of Cape Mendocino. Distance trawled was >1 SD below average (anomalously low) in the dark blue cells in Figure 6-5b, with notable areas off of northern Washington, a stretch of trawlable bottom south of Cape Blanco, Oregon, into Northern California, and south of Cape Mendocino. Increasing trends from 2015–19 are shown in red in Figure 6-5c and indicate a short-term increase in trawl distance greater than 1 SD of the time-series average for a cell. Areas with increasing five-year trends are

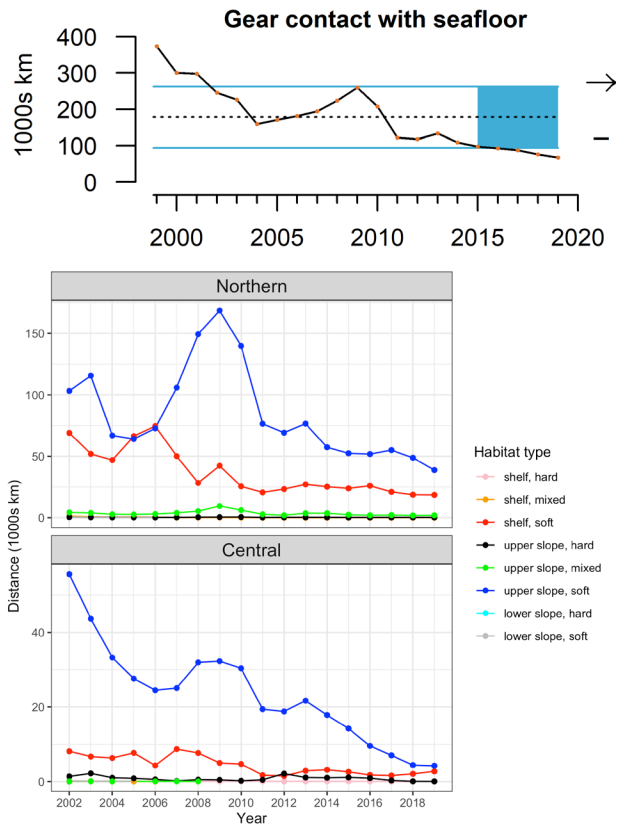


Figure 6-4. Distance (1,000s km) trawled by federally managed groundfish bottom trawl fisheries across the entire CCE (top: 1999–2019) and within each ecoregion (bottom: 2002–19). Lines, colors and symbols (top) as in Fig. 1-3a. Data for total distance trawled by federally managed bottom trawl fisheries provided by PacFIN and the NMFS/NWFSC West Coast Groundfish Observer Program.

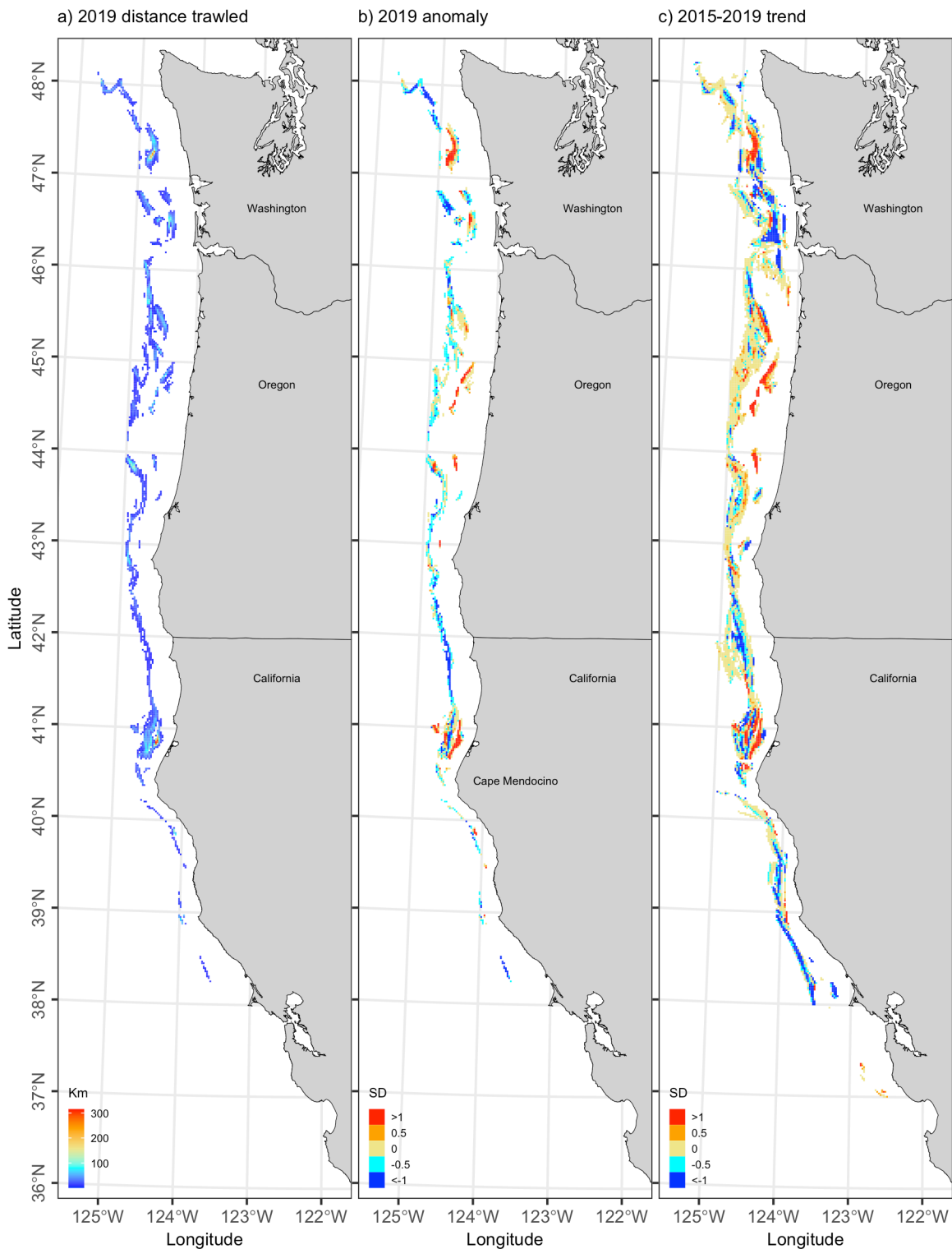


Figure 6-5. Spatial representation of seafloor contact by bottom trawl gear from federal groundfish fisheries, calculated from annual distances trawled within each 2×2 -km grid cell, 2002–19. a) Total distances trawled in 2019. b) Anomalies in 2019 relative to the long-term mean. c) Normalized trend values for most recent 5-yr period (2015–19). In b) and c), grid cell values >1 (red) or <-1 (blue) represent a cell in which the 2019 anomaly was at least 1 SD from the long-term mean of that cell, or a cell in which the 5-yr trend changed by at least 1 SD of the long-term mean of that cell during the time period. Data for total distance trawled by federally managed bottom trawl fisheries provided by PacFIN and the NMFS/NWFSC West Coast Groundfish Observer Program.

concentrated off of central Washington, northern and central Oregon, and north of Cape Mendocino. Decreasing trends from 2015–19 (dark blue: five-year trends that declined by at least 1 SD of the time-series average for a cell) occurred in many areas, with concentrations off of much of Washington, south of Cape Blanco, and south of Cape Mendocino (Figure 6-5c).

Because it highlights the variation of status and trends of trawling activity in specific areas across the CCE, the fine-scale spatial indicator of trawl distance (Figure 6-5) provides more information than the time series of the total coastwide distance trawled, which indicates that bottom trawl gear contact with the seafloor was at low levels and had no trend from 2015–19 (Figure 6-4, top). With new spatial closures and openings in the federally managed groundfish fishery beginning in 2020,¹⁴ this indicator will be of interest over the next several years, as bottom trawl fishing effort is likely to change. Subsequent efforts will also incorporate state-managed bottom trawl fisheries (e.g., for shrimp), fixed-gear fisheries, and other nonfishing human activities that could affect seafloor habitats. These spatial indicators should provide useful data to understand how fisheries might interact with other ocean-use sectors in the future (e.g., offshore renewable energy or aquaculture).

6.3 Aquaculture and Seafood Consumption

Aquaculture production is an indicator of seafood demand, and also may be related to some ecosystem benefits (e.g., water filtration by bivalves, nutrition, or income and employment) or impacts (e.g., habitat conversion, waste discharge, or nonindigenous species introductions). Shellfish aquaculture production in the CCE showed no trends and was within 1 SD of the time-series mean from 2015–19 (Figure 6-6, top), but production was near the upper limit of time-series observations, as it has been for nearly 15 years. Patterns for shellfish aquaculture are driven by production in Washington, which is home to >90% of U.S. West Coast shellfish production. Commercial finfish (Figure 6-6, bottom) aquaculture production in the CCE, which consists exclusively of Atlantic salmon (*Salmo salar*) raised in net pens in Washington marine waters, decreased over the last five years. Net-pen rearing of Atlantic salmon in Washington marine waters is scheduled to be phased out by 2022 due to regulatory changes. NOAA has recently announced that Southern California will be one of two new

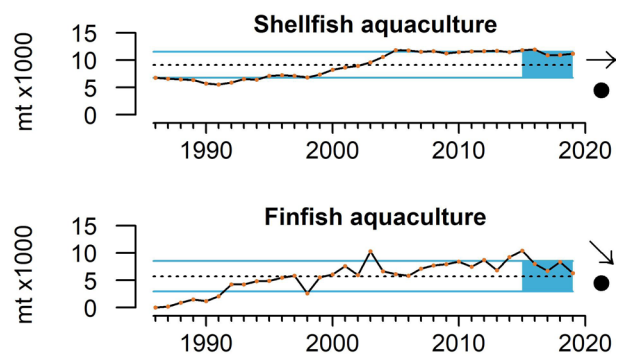


Figure 6-6. Aquaculture production of shellfish (clams, mussels, oysters) and finfish (Atlantic salmon) in CCE waters, 1986–2019. Lines, colors, and symbols as in Fig 1-3a. Shellfish production data retrieved and summed together from Washington Department of Fish and Wildlife’s Commercial Harvest Data Team (CHDT), Oregon Department of Agriculture, and California Department of Fish and Game. Finfish production data from CHDT.

¹⁴ <https://www.pccouncil.org/actions/amendment-28-pacific-coast-groundfish-essential-fish-habitat-rockfish-conservation-area-modifications-and-magnuson-act-discretionary-closures/>

Aquaculture Opportunity Areas, and siting analyses for the exact locations are underway. The siting analyses will identify suitable locations for offshore aquaculture production in federal waters, thus increasing the likelihood of new aquaculture in the CCE and increasing the importance of monitoring these human activity indicators alongside other indicators.

Data on total consumption of edible and nonedible fisheries products in the United States are available through 2019. Total consumption of fisheries products from 2015–19 was above the time-series average (Figure 6-7, top), continuing the overall upward trend generally observed since the early 1970s. Per-capita consumption was stable and remained near the upper end of the time-series range from 2015–19 (Figure 6-7, bottom). With increasing human populations and recommendations in U.S. dietary guidelines to increase seafood intake,¹⁵ total consumption of seafood products might be expected to increase in years to come. However, disruptions in food supply chains and markets caused by the COVID-19 pandemic in 2020 will affect U.S. seafood availability and consumption, and will likely be evident in this indicator time series in the future.

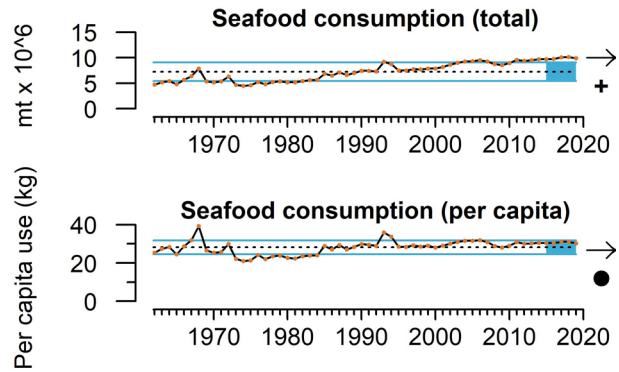


Figure 6-7. Total (millions metric tons) and per capita (kg) consumption of edible and nonedible fisheries products in the USA, 1962–2019. Lines, colors, and symbols as in Fig 1-3a. Data can be found in NOAA’s annual Fisheries of the United States reports (<https://www.fisheries.noaa.gov/resource/document/fisheries-united-states-2019-report>).

6.4 Nonfisheries Human Activities

6.4.1 Commercial shipping

Approximately 90% of world trade is carried by the international maritime shipping industry. The volume of cargo moved through U.S. ports increased 3% per year from 2000 to 2017 (U.S. Army Corps of Engineers [USACE], Waterborne Commerce Statistics Center¹⁶), and is expected to continue to increase at that rate through 2030 (Lloyd’s Register et al. 2013). Marine ecosystem impacts associated with commercial shipping include interactions between fishing and shipping vessels, ship strikes of protected species, carbon exhaust and pollution, and underwater noise—all of which affect the reproduction, recruitment, migration, behavior, and communication of target and protected species.

¹⁵ <https://health.gov/our-work/food-nutrition/previous-dietary-guidelines/2015#food-groups>

¹⁶ <https://www.iwr.usace.army.mil/About/Technical-Centers/WCSC-Waterborne-Commerce-Statistics-Center/>

Commercial shipping activity is measured by summing the total distances traveled within the CCE by vessels reported under “foreign waterborne” traffic to the U.S. Army Corps of Engineers. “Domestic coastwise” traffic is not included in this calculation, because their trips make up only 10% of distances traveled, have no effect on the overall status and trend, and are more difficult to update in a timely manner than the “foreign waterborne” data. Commercial shipping activity in the CCE was stable and near the lower bounds of the time series from 2015–19 (Figure 6-8).

This contrasts drastically with global estimates of shipping activity, which increased nearly 400% over the last 20 years and are projected to increase nearly 250% between 2010 and 2030 (Lloyd’s Register et al. 2013). Regional differences, lagging economic conditions, and different data sources may be responsible for the observed differences. For example, most maritime shipping activity indicators are based on cargo volume and value of goods, and thus capture different attributes of the industry than we show here (distances traveled). We consider vessel activity, as indicated by distance traveled, to be more relevant to CCE biota and human activities than the volume or value of the cargo on board.

Changes in major trading routes and vessel characteristics (e.g., vessel length and cargo capacity) may also be responsible for the observed differences between global indicators and estimates for the CCE.

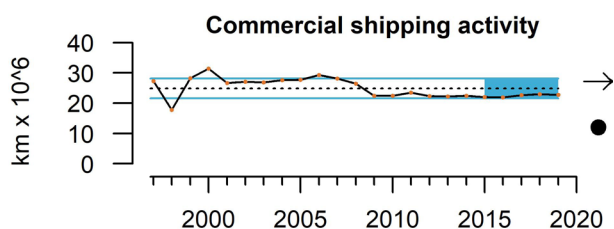


Figure 6-8. Distance transited by foreign commercial shipping vessels in the CCE, 1997–2019. Lines, colors, and symbols as in Fig. 1-3a. Foreign vessel entrance and clearance data from the USACE Waterborne Commerce Statistics Center.

6.4.2 Oil and gas activity

Oil and natural gas are extracted in offshore drilling in the CCE, with all active leases located in Southern California in the region of Point Conception and landward of the Channel Islands. Risks posed by offshore oil and gas activities include the release of hydrocarbons, smothering of benthos, sediment anoxia, benthic habitat loss, and the use of explosives. Petroleum products consist of thousands of chemical compounds such as polycyclic aromatic hydrocarbons (PAHs), which may impact marine fish health and reproduction. The effects of the physical presence of oil rigs on fish stocks are less conclusive, as rig structures may be aggregation points or provide habitat benefits.

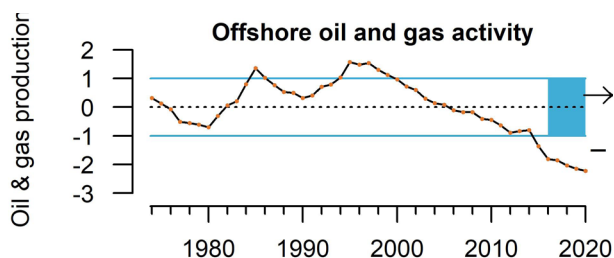


Figure 6-9. Standardized index of the sum of oil and gas production from offshore wells in California, 1974–2020. Lines, colors, and symbols as in Fig. 1-3a. State offshore oil production data come from annual reports and online data of the California State Department of Conservation’s Division of Oil, Gas, and Geothermal Resources,* federal offshore oil production data from the Bureau of Safety and Environmental Enforcement,† and state/federal offshore natural gas production data from the U.S. Energy Information Administration.‡

* https://www.conservation.ca.gov/calgem/pubs_stats/annual_reports/Pages/annual_reports.aspx

† <https://www.data.bsee.gov/Main/PacificProduction.aspx>

‡ https://www.eia.gov/dnav/ng/ng_prod_sum_dc_rcatf_mmcf_a.htm

Offshore oil and gas activity in the CCE in 2016–20 was well below the time-series average (Figure 6-9). Offshore oil and gas production in the CCE has been decreasing steadily since the mid-1990s.

6.4.3 Nutrient loading

Nutrient input into coastal waters occurs through natural cycling of materials, as well as through loadings derived from human activities. Nutrient loading is a leading cause of contamination, eutrophication, and related impacts in streams, lakes, wetlands, estuaries, and groundwater throughout the United States. Nutrient input data into all CCE waters have not been updated since 2012, and are thus not presented here.

7 Human Wellbeing

Karma Norman, Amanda Phillips, Cameron Speir, Jameal Samhour, Mary Fisher, Daniel Holland, Stephen Kasperski, and Chris J. Harvey

Human wellbeing is inextricably linked to the marine, coastal, and upland environments of the CCE. These relationships depend on qualities of both the biophysical environment and the human social system. The marine ecosystem of the California Current supports human wellbeing through fisheries sustenance and income, aesthetic and recreational opportunities, and a variety of economically and socially discernible contributions. Human wellbeing may be measured at the individual, community, and societal levels, and includes many component elements, some of which have been described and addressed within the output of a CCIEA-originated Social Wellbeing in Marine Management (SWIMM) working group (Breslow et al. 2017).

7.1 Community Social Vulnerability

Community-scale measures of social vulnerability are a way of partially assessing human wellbeing at the community level. Coastal community vulnerability indices are generalized socioeconomic vulnerability metrics for communities. The Community Social Vulnerability Index (CSVI) is derived from a factor analysis approach applied to social vulnerability data, and resultant factors then provide measures for categories of social vulnerability (demographics, personal disruption, poverty, housing characteristics, housing disruption, labor force structure, natural resource labor force, etc.; Jepson and Colburn 2013). The CCIEA team has been monitoring CSVI in U.S. West Coast communities that are highly dependent upon fishing. Fishery *dependence* can be expressed by two terms, or by a composite of both: engagement and reliance. *Engagement* refers to the total extent of fishing activity in a community, whereas *reliance* is the per capita engagement of a community. The commercial fishing engagement index is based on an analysis of variables reflecting commercial fishing engagement in 1,140 communities (e.g., fishery landings, revenues, permits, and processing). The commercial fishing reliance index applies the same factor analysis approach to these variables on a per capita basis. Thus, in two communities with equal engagement, the community with the smaller population would have a higher reliance on its fisheries activities.

Figure 7-1 plots CSVI against per capita commercial fishery reliance for 2018 (the most-recent available CSVI data) in the five communities with the highest reliance on commercial fishing in each of five regions: Washington, Oregon, and Northern, Central, and Southern California (five communities per region). Of note are communities that are above and to the right of the dashed lines, which indicate above-average levels of social vulnerability (horizontal dashed line) and commercial fishing reliance (vertical dashed line) from among all U.S. West Coast communities. Multiple ports in Washington (La Push, Westport, Taholah, Bay Center) and Oregon (Port Orford, Winchester Bay) are in the upper-right portion of the plot, and two others (Crescent City, California, and Quilcene, Washington) are close to that region of the plot. Communities that are outliers in both indices may be especially socially

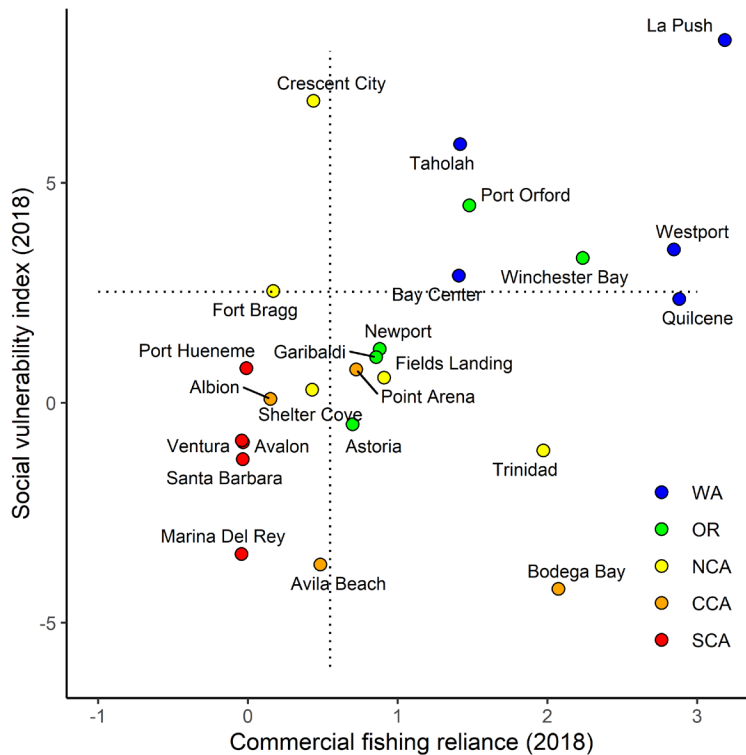


Figure 7-1. Commercial fishing reliance and social vulnerability scores as of 2018, plotted for 25 communities from WA, OR, and Northern (NCA), Central (CCA), and Southern California (SCA). The top 5 highest-scoring communities for commercial fishing reliance were selected from each region. Black dotted lines denote 1 SD above the mean for communities with landings data. CSVI and fishery reliance data provided by K. Norman (NMFS/NWFSC) and A. Phillips (PSMFC), with data derived from the U.S. Census Bureau’s American Community Survey (ACS; <https://www.census.gov/programs-surveys/acs/>) and PacFIN (<http://pacfin.psmfc.org>), respectively.

vulnerable to downturns in commercial fishing. We note, however, that commercial fishing reliance can be volatile, and communities may move left along the x-axis during years with reduced landings. The communities may thus appear to be less dependent on commercial fishing when in fact they have actually just experienced a difficult year; thus, these results should be interpreted with care, and we will work to improve this analysis in the future.

Figure 7-2 plots CSVI against total commercial fishing engagement in 2018 in the five communities with the highest engagement in commercial fishing in each of five regions. Again, communities above and to the right of the dashed lines are at least 1 SD above the coastwide averages of both indices. Of note are fishing-oriented communities like Westport, Crescent City, Port Orford, and Shelton (Washington), which have relatively high commercial fishing engagement results and also a high CSVI composite result.

This is an emerging area of work, and, as we have discussed in past reports, these data are difficult to ground-truth and require further study to understand the importance of these relationships. We also lack data for many communities altogether, including many tribal communities. Further, we lack data to regularly conduct similar analyses of CSVI relative to recreational fishing reliance and engagement. An effort to examine communities that may be particularly affected by ecosystem shifts, with respect to the Magnuson–Stevens Act’s National Standard 8 (NS-8; USOFR 2016), is ongoing.

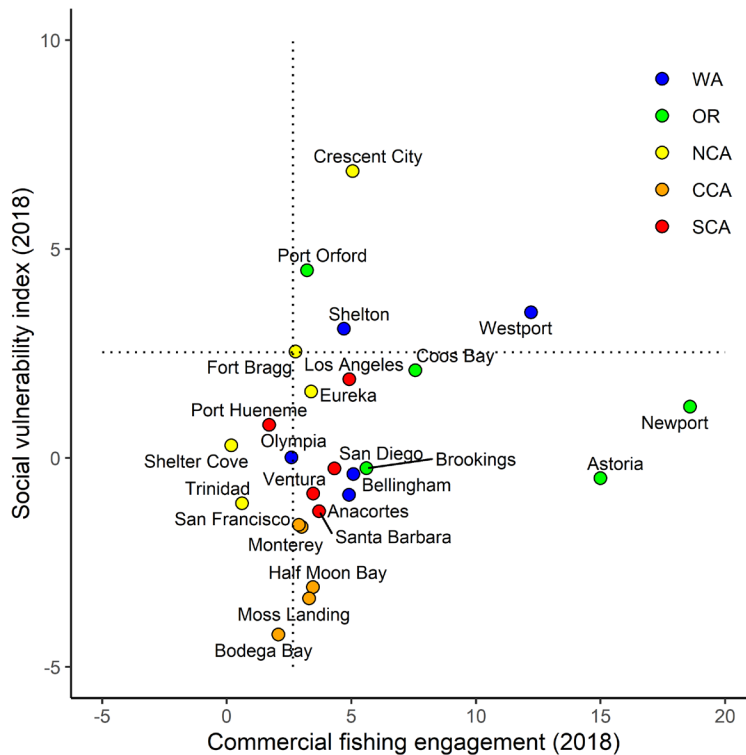


Figure 7-2. Commercial fishing engagement and social vulnerability scores as of 2018, plotted for 25 communities from WA, OR, and Northern (NCA), Central (CCA), and Southern California (SCA). The top 5 highest-scoring communities for commercial fishing engagement were selected from each region. Black dotted lines denote 1 SD above the mean for communities with landings data. CSVI and fishery engagement data provided by K. Norman (NMFS/NWFSC) and A. Phillips (PSMFC), with data derived from the U.S. Census Bureau’s American Community Survey (ACS; <https://www.census.gov/programs-surveys/acs/>) and PacFIN (<http://pacfin.psmfc.org>), respectively.

7.2 Fishing Revenue Diversification

Catches and prices from many fisheries exhibit high interannual variability—leading to high variability in fishers’ revenue—but variability can be reduced by diversifying fishing activities across multiple fisheries or regions (Kasperski and Holland 2013). It should be noted that there may be good reasons for individuals to specialize, including reduced costs or greater efficiency; thus, while diversification may reduce income variation, it does not necessarily promote higher average profitability. We use the effective Shannon index (ESI) to measure diversification among 28,000 fishing vessels off the U.S. West Coast and Alaska. The index has an intuitive meaning: ESI = 1 when all revenues are from a single species group and region, ESI = 2 when fishery revenues are spread evenly across two fisheries, and so on. It increases both as revenues are spread across *more* fisheries and as revenues are spread *more evenly* across fisheries.

In 2019 (the most recent year analyzed), revenue diversification of the fleet of 28,000 vessels that fished the U.S. West Coast and Alaska was less diverse on average than at any time in the preceding 38 years, and this was true for most home states, revenue categories, and size classes (Figure 7-3). Diversification rates for most categories of vessels fishing on the U.S. West Coast have been trending down for several years, but there were slight increases in 2019 for several categories of vessels with U.S. West Coast landings. California,

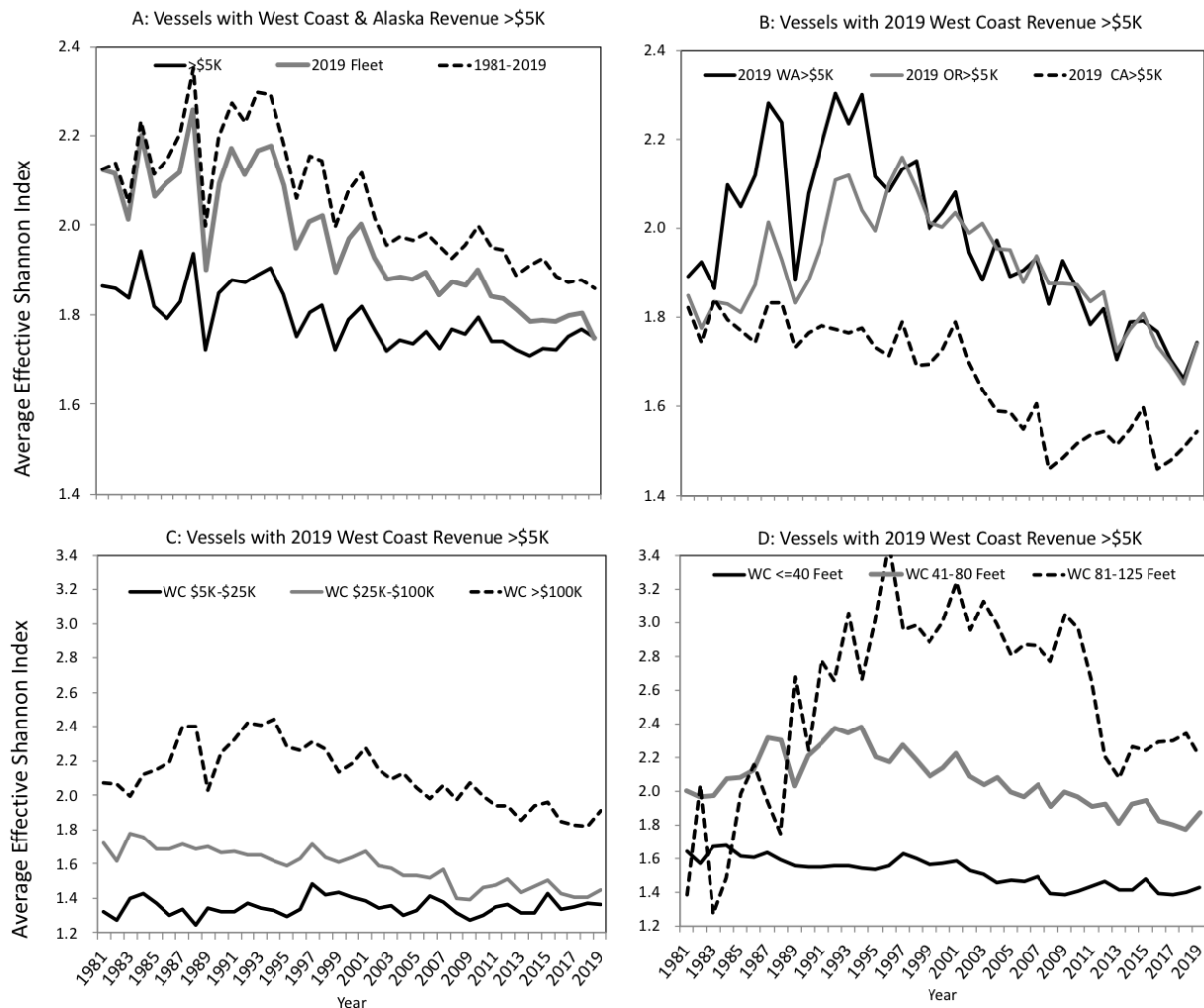


Figure 7-3. Average diversification for U.S. West Coast and Alaskan fishing vessels with over \$5K in average revenues (top left) and for vessels in the 2019 U.S. West Coast fleet with over \$5K in average revenues, grouped by state (top right), average gross revenue class (bottom left), and vessel length class (bottom right). Fishery diversification estimates provided by D. Holland (NMFS/NWFSC) and S. Kasperski (NMFS/AFSC).

Oregon, and Washington fleets all saw small increases in average diversification in 2019. The long-term declines are due both to entry and exit of vessels and changes for individual vessels. Less-diversified vessels have been more likely to exit; vessels that remain have become less diversified, at least since the mid-1990s; and newer entrants generally have been less diversified than earlier entrants. Within the average trends are wide ranges of diversification levels and strategies, and some vessels remain highly diversified. Increased diversification from one year to the next may not always indicate an improvement. For example, if a class of vessels was heavily dependent on a single fishery with highly variable revenues (e.g., Dungeness crab), a decline in that fishery might force vessels into other fisheries, causing average diversification to increase.

As is true with individual vessels, the variability of landed value at the port level is reduced with greater diversification of landings. Diversification of fishing revenue has declined over the last several decades for some ports (Figure 7-4); examples include Seattle and most but not all ports in southern Oregon and California. However, a few ports have become more

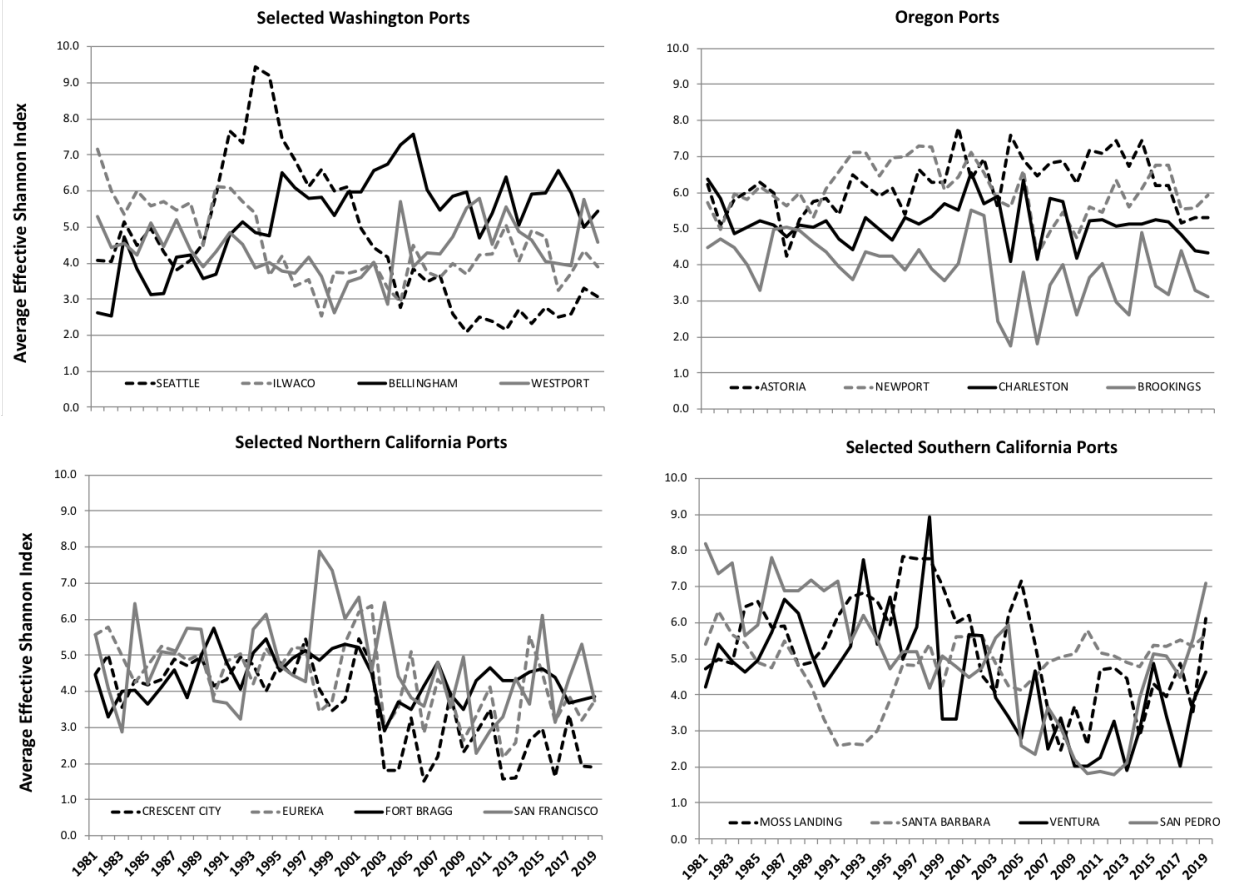


Figure 7-4. Trends in fishery revenue diversification in major U.S. West Coast ports by state/region: WA, OR, NCA, and SCA, 1981–2019. Fishery diversification estimates provided by D. Holland, NMFS/NWFSC, and S. Kasperski, NMFS/AFSC.

diversified, including Bellingham and Westport (Washington). Diversification in Astoria had been increasing, but decreased in recent years, while Brookings (Oregon) has had an erratic trend. Diversification scores are highly variable year-to-year for some ports, particularly those in southern Oregon (Brookings) and Northern California (Crescent City, Eureka) that depend heavily on the Dungeness crab fishery, which has highly variable landings.

7.3 Revenue Consolidation

At the request of PFMC’s Ecosystem Advisory Subpanel, we are working to develop indicators relevant to NS-8 of the Magnuson–Stevens Act (USOFR 2016). NS-8 states that:

Conservation and management measures shall, consistent with the conservation requirements of this Act (including the prevention of overfishing and rebuilding of overfished stocks), take into account the importance of fishery resources to fishing communities by utilizing economic and social data that meet the requirement of paragraph (2), in order to (a) provide for the sustained participation of such communities, and (b) to the extent practicable, minimize adverse economic impacts on such communities.

Paragraph (2), a.k.a. NS-2, states that “Conservation and management measures shall be based upon the best scientific information available.”

In last year’s report (Harvey et al. 2020), we presented a simple exploratory analysis of ex-vessel fishery revenue consolidation in U.S. West Coast ports, as an initial means of indicating if fishery access opportunities are changing within and across ports and/or FMPs. Following further discussions with PFMC’s SSC–Ecosystem Subcommittee, we updated our approach to use the Theil index (Theil 1967) as a measure of geographic concentration of fishery revenue. Though the Theil index typically measures economic inequality, it may be developed and applied in varying contexts. The Theil index is a single annual measure of geographic concentration of revenue for a particular fishery or group of fisheries, providing an estimate of the difference between observed revenue concentrations and what they would be if they were distributed uniformly across port groups (Speir and Lee 2021).

We calculated the annual Theil index from 1981–2019 for: a) all U.S. West Coast commercial fisheries combined, b) eight broad fishery management groups, and c) at the level of individual species within those fishery management groups. The eight management groups are: All Commercial Fisheries, Coastal Pelagic Species, Salmon, Groundfish, Highly Migratory Species, Crabs, Shrimps and Prawns, and Other Species. We used the Theil index to estimate revenue concentration at the level of the port groups established with the Input–Output Model for Pacific Coast fisheries (IO-PAC; Leonard and Watson 2011). The IO-PAC approach aggregates 97 fisheries landing locations into 21 port groups over the 1981–2019 time period.

For each management group, we plotted Theil index values as annual deviations from the time-series averages (Figure 7-5, top and middle); thus, positive values indicate revenue concentration greater than the long-term average, and negative values indicate revenue concentration closer to equality across the port groups. Port group-level revenue concentration summed across all commercial fisheries (Figure 7-5, top left) shows small deviations and little variability over time, suggesting that total aggregated revenue has not exhibited high levels or extended trends of geographic concentration. This is further shown in bubble maps (Figure 7-5, bottom), where the sizes of the bubbles, representing inflation-adjusted total commercial fishery revenue in each port group, are fairly consistent over time. Separate fishery management groups show clearer patterns of temporal variability, extended trends of decreasing or increasing concentration, or both (Figure 7-5, top and middle). For example, Theil index values for groundfish have been gradually increasing over time (Figure 7-5, top right), as groundfish landings have become more concentrated in Northern CCE ports. In contrast, the Theil index for HMS revenues presents a U-shaped trend (Figure 7-5, middle left), as HMS landings were highly concentrated early in the time series, became more equally distributed from 1981–2002, and then became more concentrated again from 2002–19. CPS, salmon, and shrimp show high short-term or decadal variability.

We examined Theil index trends of HMS at the level of key individual target species to better understand the spatial and temporal patterns of revenue concentration in HMS as a whole (Figure 7-5, middle left). Species-level Theil index values suggested that shifts in HMS revenue concentration are largely due to changes in revenue distribution of two important species: swordfish and albacore (Figure 7-6). Landings revenues for swordfish and albacore were mapped to U.S. West Coast ports by decade (Figure 7-6, top), and expressed as species-

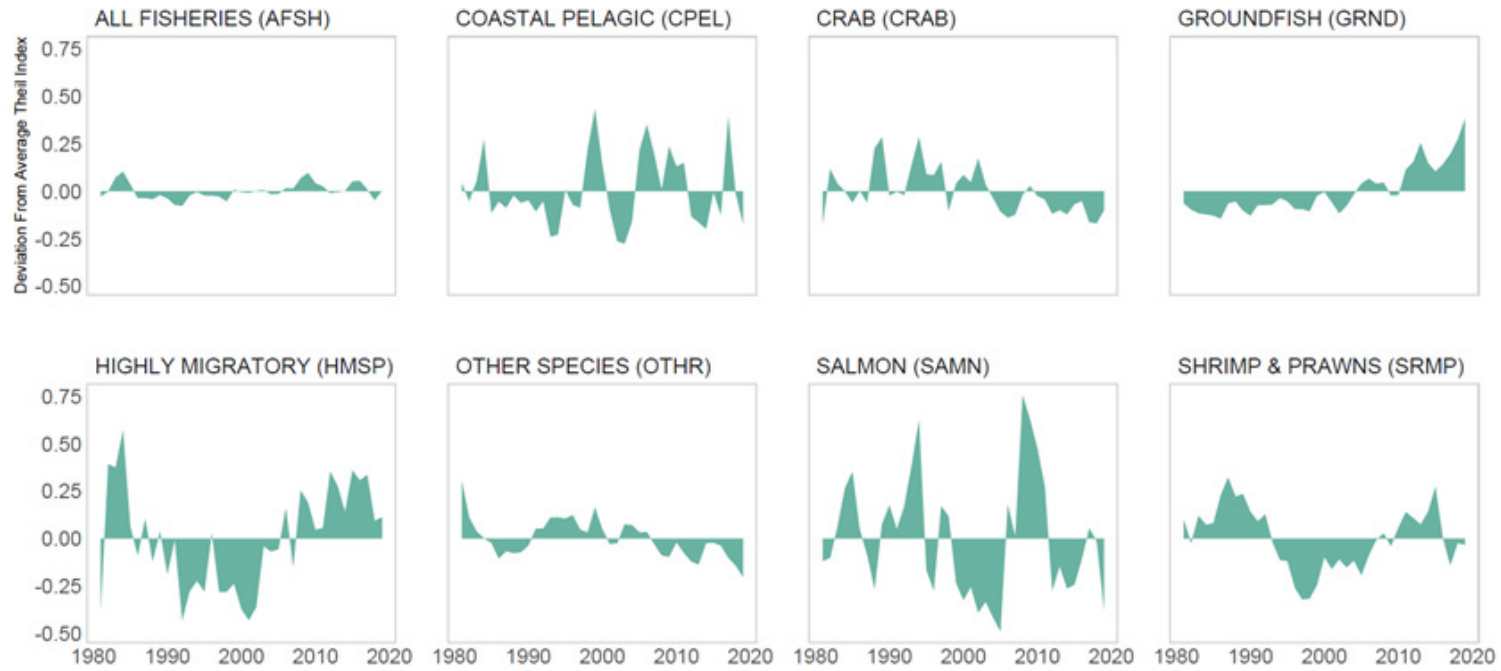
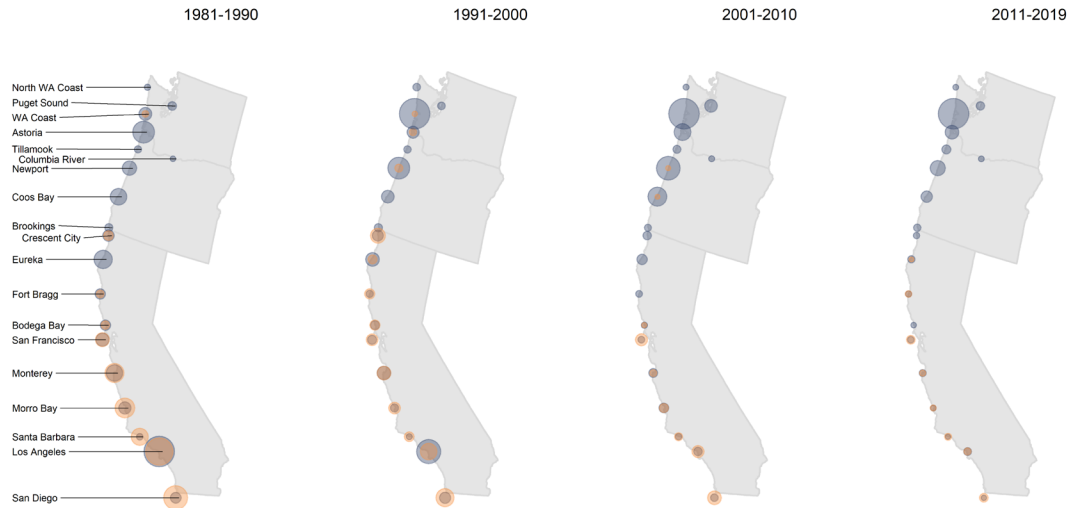
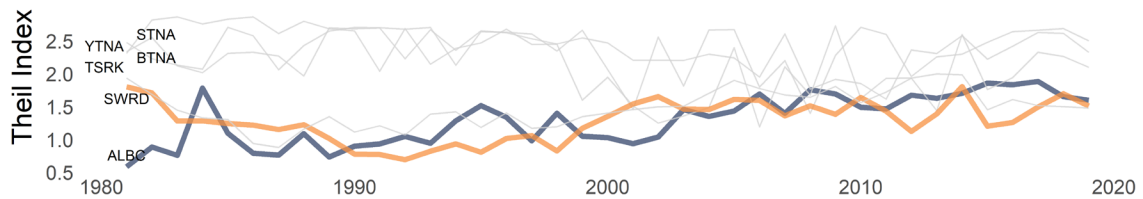


Figure 7-5. Top and middle: Theil index anomalies for all U.S. West Coast commercial fisheries plus 7 individual management groups. Positive values indicate above-average revenue concentration in a smaller number of port groups. Bottom: Maps of 21 port groups, with bubbles proportional to Theil index values for all fisheries revenue in a given port group for each 5-yr time period. See text for details. Theil index and annual commercial fishery revenue data provided by K. Norman (NMFS/NWFSC) and A. Phillips (PSMFC), with data derived from PacFIN (<http://pacfin.psmfc.org>).

Average Landings Revenue of Albacore and Swordfish



Theil Index for Highly Migratory Species



Revenue Share of Albacore and Swordfish in the Highly Migratory Species Fishery

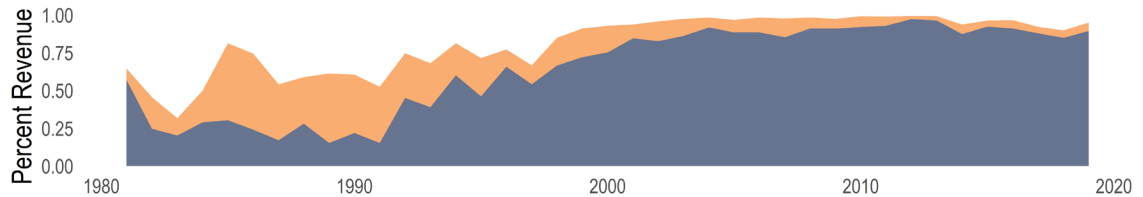


Figure 7-6. Top: Port group-specific revenue by decade for landings of albacore (blue) and swordfish (orange). Bubbles are proportional to average annual revenue for each port group in a decade. Middle: Annual Theil index measures for HMS components.* Increasing Theil index values indicating increasing revenue concentration in a smaller number of port groups. Bottom: Annual percent share of total coastwide HMS revenue derived from albacore (blue) and swordfish (orange), 1980–2019. Theil index and annual commercial fishery revenue data provided by K. Norman (NMFS/NWFSC) and A. Phillips (PSMFC), with data derived from PacFIN (<http://pacfin.psmfc.org>).

* ALBC = albacore (blue line), SWRD = swordfish (orange line), BTNA = bluefin tuna, STNA = skipjack tuna, TSRK = thresher shark, and YTNA = yellowfin tuna.

level Theil indices along with the rest of the HMS suite of major target species (Figure 7-6, middle). Swordfish revenues—a major fraction of HMS revenues in the early part of the time series, concentrated in southern port groups—were replaced in more recent years by albacore revenues, which have come to dominate the HMS category (Figure 7-6, bottom). The Theil index for aggregate HMS has generally increased over the past decade as the revenue share of albacore increased within the management group. Accordingly, greater geographic concentration of HMS revenues has corresponded with a shift in revenues to more northern ports, where albacore landings have recently been concentrated (Figure 7-6, top).

We will continue to develop these analyses for all fishery groups, in consultation with PFMC advisory bodies. We have made no effort yet to attribute changes in revenue concentration with management actions, environmental changes, food web changes, or changes within coastal communities. It is therefore premature to conclude that this is an effective indicator in the context of NS-8, or what changes in the index mean in terms of potential PFMC considerations. We also note that by pooling coastal communities into IO-PAC port groups, we are aggregating many communities at coarser scales than are appropriate for NS-8 considerations, which are attuned to individual communities rather than port groups. Community-scale estimation of the Theil index is possible, and we should anticipate different qualitative and quantitative outcomes than those presented here if the scale is refined to the community level. Community-scale estimation will increase the complexity of data analysis, presentation, and visualization, which will be an important discussion point between the CCIEA team and PFMC if we continue to present this metric.

7.4 Fishery Participation Networks

As fishers diversify their harvest portfolios, they create links between fisheries, even when ecological links between the harvested species are weak or absent. This creates networks of alternative sources of income, which can be described on a variety of spatial and temporal scales. Fishery participation networks (e.g., Fisher et al. 2021) offer one way to represent this information visually, with different fisheries depicted as “nodes” in the network; pairs of nodes can then be connected by lines (“edges”) that integrate information about vessels participating in both fisheries. The degree of connectivity within a fishery participation network reflects alternative sources of income within the portfolio of fisheries in the community. Networks can be constructed in a variety of ways and across different spatial and temporal scales, and can be examined before and after events such as environmental or management changes to discern differences in network structure (Anderson et al. 2017, Fuller et al. 2017, Addicott et al. 2018, Beaudreau et al. 2019, Kroetz et al. 2019, Fisher et al. 2021, Frawley et al. 2021). Fishery participation networks may therefore add levels of detail or context to other analyses such as CSVI (Figures 7-1 and 7-2), diversification indices (Figures 7-3 and 7-4), and Theil indices (Figures 7-5 and 7-6). As such, fishery participation networks offer one way to respond to requests from PFMC’s Ecosystem Advisory Subpanel and Ecosystem Workgroup for deeper characterization of the social and economic conditions in U.S. West Coast fishing communities, and information relevant to the implementation of NS-8 under the Magnuson–Stevens Act.

Here we present U.S. West Coast fishery participation networks derived from landings receipts from November 2019 through October 2020 and aggregated at the scale of IO-PAC port groups in Washington (Figure 7-7), Oregon (Figure 7-8), Northern and Central California (Figure 7-9), and Southern California (Figure 7-10). (All IO-PAC port groups are illustrated in these figures except for Other Coastal WA and Unknown Ports.) Networks consist of one to eight fisheries nodes, with 0–28 links between the fisheries within each network. Nodes are classified based on the species groupings used in the diversification index time series (as in Section 7.2; derived from Kasperski and Holland 2013). Following Fuller et al. (2017) and Fisher et al. (2021), node size represents the median contribution of a fishery to each vessel’s total annual revenue, scaled according to the amount of revenue generated by that fishery in each port group—therefore, node sizes are not comparable across port groups, only within them. The edges connecting pairs of nodes indicate that vessels participate in both fisheries, and the widths of these edges scale with the number of vessels exhibiting this behavior, as well as the total amount and evenness of revenue generation from each pair of fisheries. To maintain confidentiality, we include only fisheries with at least three vessels participating in a port group. Furthermore, for a fishery to be included in a port group’s network, the fishery must contribute to at least a median of 10% of the annual revenue of associated vessels. Vessels are represented in all port groups for which their landings meet these conditions.

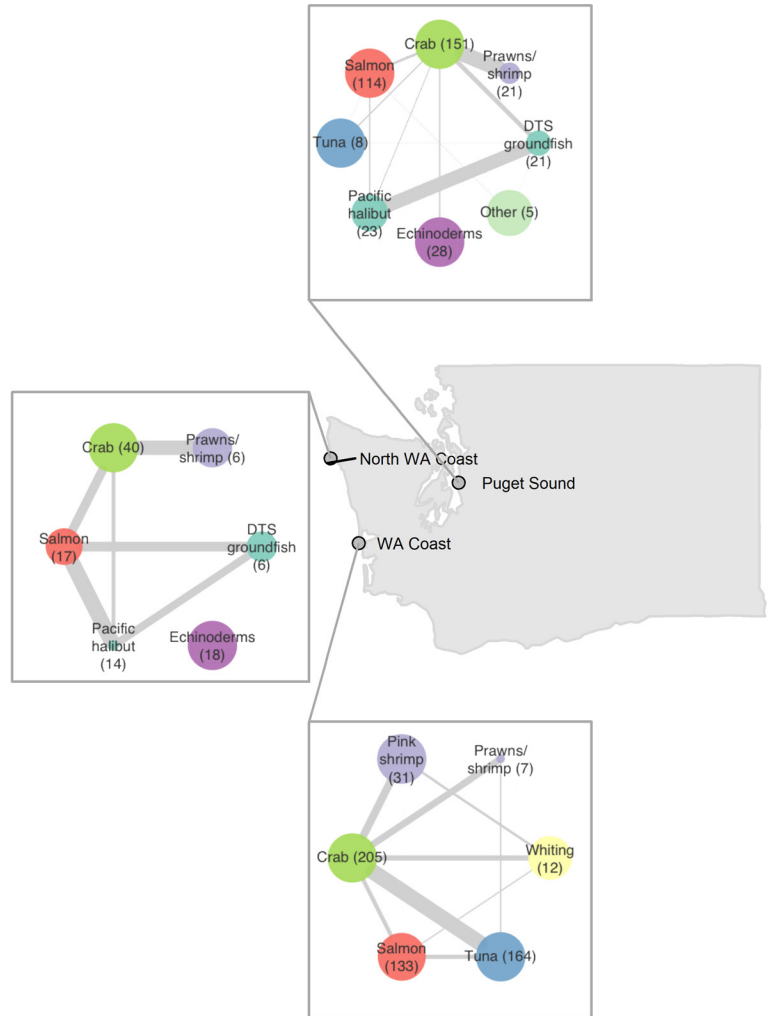


Figure 7-7. Fishery participation networks for IO-PAC port groups in WA based on Nov 2019–Oct 2020 landings receipts. Node size is proportional to the median contribution of a fishery to annual vessel-level revenue; numbers in parentheses are the number of vessels participating in a node. The thickness of lines (“edges”) is proportional to the number of vessels participating in the pair of fisheries connected by the edges and the evenness of revenue generation from each pair of fisheries. Fishery participation network data and analyses provided by J. Samhouri (NMFS/NWFSC), M. Fisher (UW), and A. Phillips (PSMFC), with data derived from PacFIN (<http://pacfin.psmfc.org>).

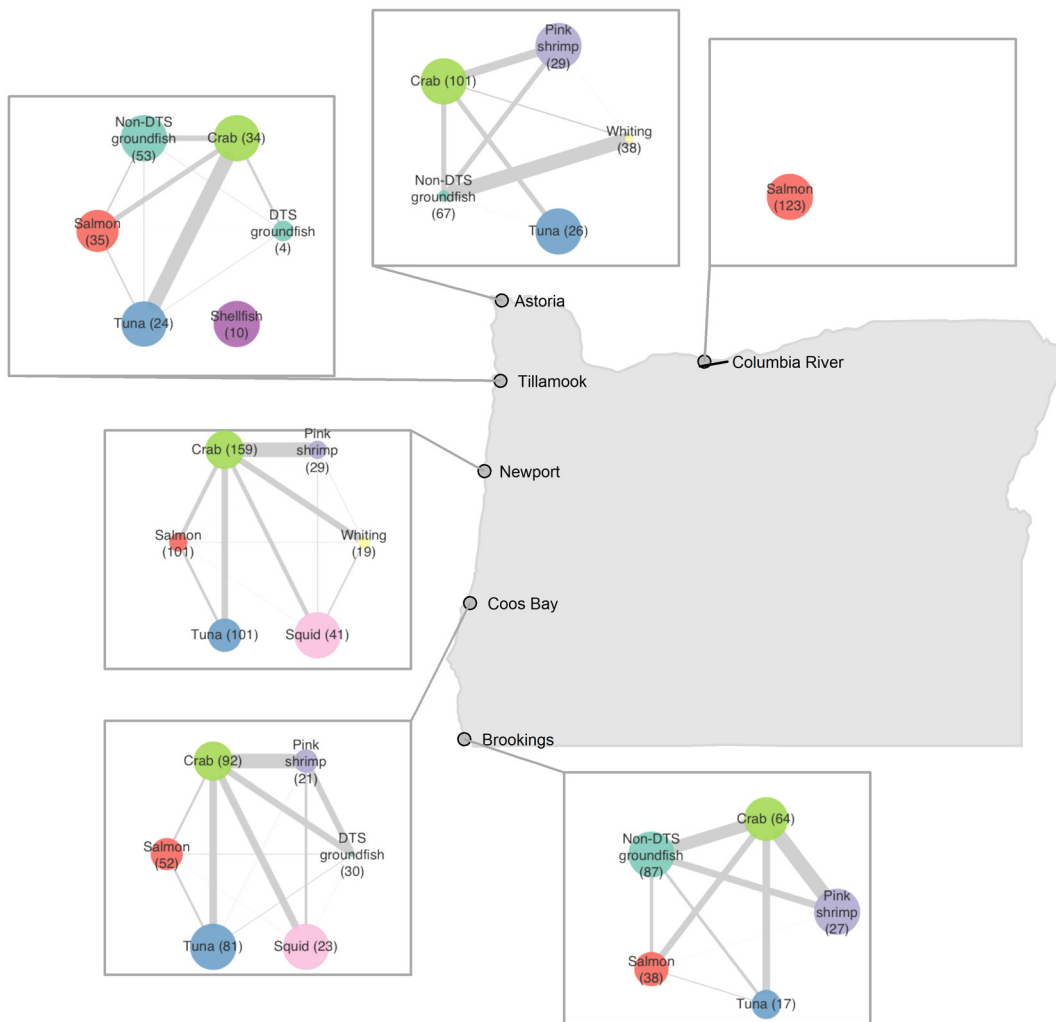


Figure 7-8. Fishery participation networks for IO-PAC port groups in OR based on Nov 2019–Oct 2020 landings receipts. Node size is proportional to the median contribution of a fishery to annual vessel-level revenue; numbers in parentheses are the number of vessels participating in a node. The thickness of lines (“edges”) is proportional to the number of vessels participating in the pair of fisheries connected by the edges and the evenness of revenue generation from each pair of fisheries. Fishery participation network data and analyses provided by J. Samhuri (NMFS/NWFSC), M. Fisher (UW), and A. Phillips (PSMFC), with data derived from PacFIN (<http://pacfin.psmfc.org>).

Some fisheries, like crab and groundfish, are represented at nearly all port groups, while others, like squid, are represented at fewer. In each network, nearly all fisheries are connected to at least one other fishery, indicating that most vessels participate in multiple fisheries over the course of a year. (Echinoderms in the North Washington Coast port group are an exception; Figure 7-7). Notably, many PFMC-managed fisheries connect to fisheries under state jurisdictions. The prime example from Washington (Figure 7-7) south to Morro Bay (Figure 7-10) is the crab fishery, which accounts for a large proportion of fishing revenue (large node size) and is highly connected to other fisheries that generate less revenue in each port group. The crab, salmon, and groundfish nodes involve consistently heavy levels of cross-fishery participation across port groups (Figures 7-7–7-10). In the three southernmost port groups (Santa Barbara, Los Angeles, and San Diego; Figure 7-10), echinoderms and shellfish generate the majority of revenue, but, compared to crab in the northern ports, there is less connectivity between these fisheries and others in the same port groups.

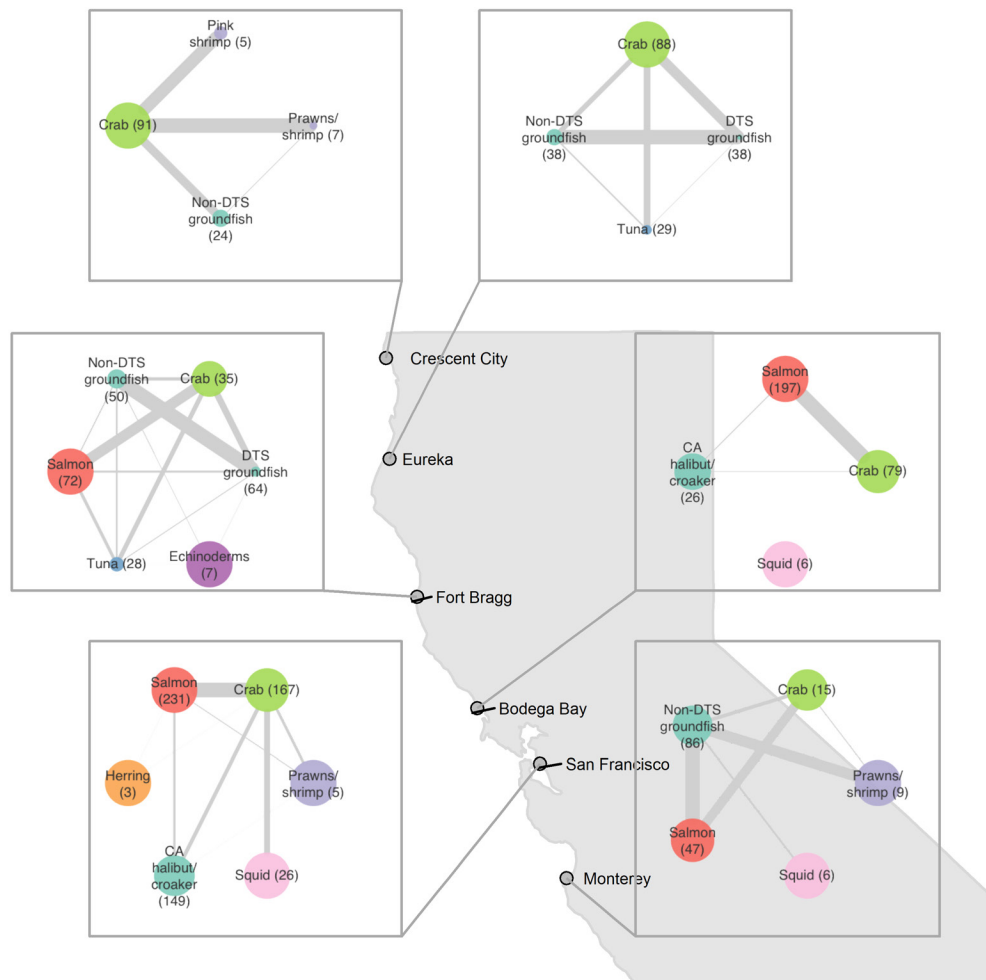


Figure 7-9. Fishery participation networks for IO-PAC port groups in NCA and CCA based on Nov 2019–Oct 2020 landings receipts. Node size is proportional to the median contribution of a fishery to annual vessel-level revenue; numbers in parentheses are the number of vessels participating in a node. The thickness of lines (“edges”) is proportional to the number of vessels participating in the pair of fisheries connected by the edges and the evenness of revenue generation from each pair of fisheries. Fishery participation network data and analyses provided by J. Samhuri (NMFS/NWFSC), M. Fisher (UW), and A. Phillips (PSMFC), with data derived from PacFIN (<http://pacfin.psmfc.org>).

Differences in the make-up of port group networks in part reflect differences in the ecology of adjacent coastal habitats and waters, and in part the legacy of management, market, and other factors that vary geographically. The networks demonstrate that individual fisheries do not operate in vacuums, just as species do not, and part of an ecosystem approach to fisheries management is to consider species and fisheries as interactive entities rather than in piecemeal fashion. Thus, these networks may provide context for understanding and interpreting indicators of human activities and wellbeing presented in these reports. Further, tracking changes in the networks themselves may support PFMC’s Climate and Communities Initiative and other activities by providing insight into how fishing communities are changing and potentially adapting to external forces such as changing stock availabilities, climate, regulations, and economic and social systems. The networks presented here, along with those for the years 2004–19, can be viewed on Github: https://github.com/jameals/ccia_networks/tree/main/data/networks/participation.

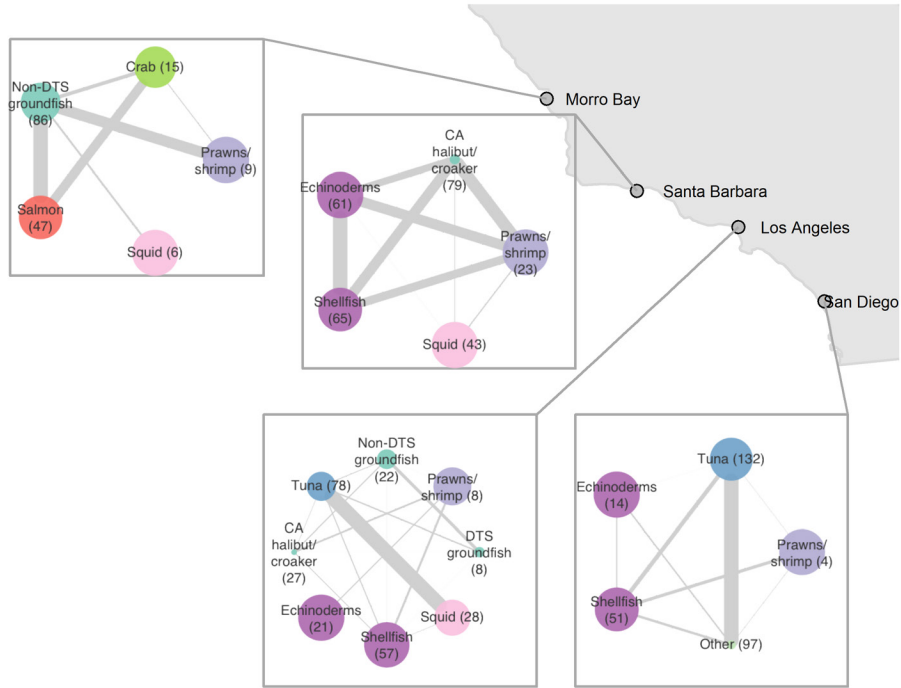


Figure 7-10. Fishery participation networks for IO-PAC port groups in SCA based on Nov 2019–Oct 2020 landings receipts. Node size is proportional to the median contribution of a fishery to annual vessel-level revenue; numbers in parentheses are the number of vessels participating in a node. The thickness of lines (“edges”) is proportional to the number of vessels participating in the pair of fisheries connected by the edges and the evenness of revenue generation from each pair of fisheries. Fishery participation network data and analyses provided by J. Samhouri (NMFS/NWFSC), M. Fisher (UW), and A. Phillips (PSMFC), with data derived from PacFIN (<http://pacfin.psmfc.org>).

8 Synthesis

Newell (Toby) Garfield and Chris J. Harvey

Accurately summarizing the status of the CCE in 2020 will be a challenge, now and going forward, due to the negative impacts of COVID-19: fisheries that depend on California Current stocks were badly disrupted, research effort was cut or delayed, and fewer eyes from the fishing, management, research, and public sectors were on the water to develop a collective sense of the state of the system.

Despite the challenges imposed by the COVID-19 pandemic, the tremendous efforts of field and lab researchers, data analysts, modelers, vessel crews, and citizen scientists generated a diversity of ecosystem indicators and indices. These metrics enable us to deduce the state of the California Current ecosystem in 2020. Some gaps were not possible to fill, but on the whole a picture emerged of a marine ecosystem that has returned closer to average or median conditions after the anomalously warm conditions that occurred in 2013–19. While 2020 once again witnessed a large marine heatwave in the northeastern Pacific Ocean, the second largest in the record (Figures 2-4–2-6), this feature had only limited intrusion into the CCE during the late summer and early fall; it was likely held offshore partly by average to above-average upwelling (Figure 2-7) and the expanded area of cool coastal waters (Figure 2-8). In addition, two of the three large-scale climate indices, ONI and PDO, went negative, another indication of conditions supporting higher marine productivity, while the NPGO indicated less North Pacific gyre water entering the system, generally consistent with lower productivity (Figure 2-1). All of these indices are derived from either satellite data or numerical models and thus were available for analyses despite COVID-19 disruptions. In addition, the development of a U.S. West Coast glider array provided supplementary subsurface data along standard sampling lines.

The ecological research surveys that were able to be conducted provided evidence of a return to average or above-average productivity for many key species in 2020. Such findings included a nutritious cool-water copepod assemblage off of Oregon (Figure 3-1); increased krill size (Figure 3-2); and continued high abundance of northern anchovy (Figures 3-5 and 3-6). Aerial counts of sea lion pups (Figure 5-1) and monitoring of fledgling success on seabird nesting areas (Figures 5-4 and 5-5) provided evidence of improvement of the availability of forage species as well as the success of top predators. Some of these results are continuations of past years' dynamics, such as the now years-long resurgence of the anchovy population. Others may have benefited from shifts in climate and ocean conditions that occurred in 2020, including the transition to La Niña and negative PDO conditions that are often associated with cooler and more productive years in the CCE. The strength and timing of local upwelling/relaxation events, particularly off Central California (Figure 2-7), may have helped boost productivity. We await to see if La Niña, negative PDO, and positive upwelling will persist further into 2021.

The past year was not without concerning physical and ecological signals. We continue to see regions of warm water, offshore in the form of heatwaves, and alongshore, particularly in the Southern CCE and to a lesser extent the Central CCE. Harmful algal blooms were an issue in all three coastal states (Figure 3-3), and the Southern California Bight experienced

an unprecedented and harmful bloom of the dinoflagellate *L. polyedra*. Pyrosomes, which are generally associated with warmer, unproductive waters, remained abundant off Central California, and whale entanglements in fixed fishing gear also remained above levels observed prior to 2014 (Figure 5-3). Salmon outlooks for 2021, which are a legacy of past years' conditions, remain a source of concern (Tables 4-1–4-5; Figures 4-5 and 4-6). Freshwater and terrestrial systems critical to anadromous species and to human wellbeing experienced poor snowpack (Figures 2-14 and 2-15), early melt, continued drought, and traumatic wildfires in many parts of the system in 2020. The ecological impact of the huge increase in wildfires has yet to be determined; however, it is safe to assume there will be lingering impacts in freshwater systems, and the outlook for 2021 is for continued widespread and severe-to-extreme drought in most of the CCE region.¹⁷

Finally in 2020, fishing communities went through the unprecedented stress test of the COVID-19 pandemic, which affected landings, revenues, operations, domestic markets, and exports for many fisheries, and added a new layer of uncertainty to the fishing profession. Landings and revenues were down nearly across the board (Figures 6-1–6-3), at a time in which U.S. West Coast fisheries on average have relatively undiversified revenue portfolios (Figure 7-3) and may thus be less resilient to downturns. As with any ecosystem shock, this one will reverberate, and its full effects will take time to understand. Future research will be needed to distinguish COVID-19 impacts on U.S. West Coast fisheries from other sources of fishery variability—both from expected forms of variability such as changes in ecosystem productivity, target species availability, regulations, and market fluctuations, and from episodes such as wildfires that disrupted product transportation or human safety in many parts of the West in 2020.



¹⁷ <https://www.cpc.ncep.noaa.gov/products/Drought>

References

- Abell, R., M. L. Thieme, C. Revenga, M. Bryer, M. Kottelat, N. Bogutskaya, B. Coad, N. Mandrak, S. C. Balderas, W. Bussing, M. L. J. Stiassny, P. Skelton, G. R. Allen, P. Unmack, A. Naseka, R. Ng, N. Sindorf, J. Robertson, E. Armijo, J. V. Higgins, T. J. Heibel, E. Wikramanayake, D. Olson, H. L. Lopez, R. E. Reis, J. G. Lundberg, M. H. S. Perez, and P. Petry. 2008. Freshwater ecoregions of the world: A new map of biogeographic units for freshwater biodiversity conservation. *BioScience* 58:403–414.
- Addicott, E. T., K. Kroetz, M. N. Reimer, J. N. Sanchirico, D. K. Lew, and J. Huetteman. 2018. Identifying the potential for cross-fishery spillovers: A network analysis of Alaskan permitting patterns. *Canadian Journal of Fisheries and Aquatic Sciences* 76:56–68.
- Alexander, J. D., S. L. Hallett, R. W. Stocking, L. Xue, and J. L. Bartholomew. 2014. Host and parasite populations after a ten year flood: *Manayunkia speciosa* and *Ceratonova* (syn *Ceratomyxa*) *shasta* in the Klamath River. *Northwest Science* 88:219–233.
- Anderson, S. C., E. J. Ward, A. O. Shelton, M. D. Adkison, A. H. Beaudreau, R. E. Brenner, A. C. Haynie, J. C. Shriver, J. T. Watson, and B. C. Williams. 2017. Benefits and risks of diversification for individual fishers. *Proceedings of the National Academy of Sciences* 114:10797–10802.
- Barton, A., B. Hales, G. G. Waldbusser, C. Langdon, and R. A. Feely. 2012. The Pacific oyster, *Crassostrea gigas*, shows negative correlation to naturally elevated carbon dioxide levels: Implications for near-term ocean acidification effects. *Limnology and Oceanography* 57:698–710.
- Beaudreau, A. H., E. J. Ward, R. E. Brenner, A. O. Shelton, J. T. Watson, J. C. Womack, S. C. Anderson, A. C. Haynie, K. N. Marshall, and B. C. Williams. 2019. Thirty years of change and the future of Alaskan fisheries: Shifts in fishing participation and diversification in response to environmental, regulatory and economic pressures. *Fish and Fisheries* 20:601–619.
- Bednaršek, N., R. A. Feely, J. C. P. Reum, B. Peterson, J. Menkel, S. R. Alin, and B. Hales. 2014. *Limacina helicina* shell dissolution as an indicator of declining habitat suitability owing to ocean acidification in the California Current Ecosystem. *Proceedings of the Royal Society B—Biological Sciences* 281:20140123.
- Bradford, M. J., and J. S. Heinonen. 2008. Low flows, instream flow needs and fish ecology in small streams. *Canadian Water Resources Journal* 33:165–180.
- Breslow, S. J., M. Allen, D. Holstein, B. Sojka, R. Barnea, X. Basurto, C. Carothers, S. Charnley, S. Coulthard, N. Dolsak, J. Donatuto, C. Garcia-Quijano, C. C. Hicks, A. Levine, M. B. Mascia, K. Norman, M. Poe, T. Satterfield, K. St. Martin, and P. Levin. 2017. Evaluating indicators of human well-being for ecosystem-based management. *Ecosystem Health and Sustainability* 3:1–18.
- Brodeur, R. D., T. D. Auth, and A. J. Phillips. 2019. Major shifts in pelagic micronekton and macrozooplankton community structure in an upwelling ecosystem related to an unprecedented marine heatwave. *Frontiers in Marine Science* 6:212.
- Brodeur, R. D., J. P. Fisher, R. L. Emmett, C. A. Morgan, and E. Casillas. 2005. Species composition and community structure of pelagic nekton off Oregon and Washington under variable oceanographic conditions. *Marine Ecology Progress Series* 298:41–57.
- Browman, H., P. Cury, R. Hilborn, S. Jennings, H. Lotze, P. Mace, S. Murawski, D. Pauly, M. Sissenwine, K. Stergiou, and D. Zeller. 2004. Perspectives on ecosystem-based approaches to the management of marine resources. *Marine Ecology Progress Series* 274:269–303.
- Burke, B. J., W. T. Peterson, B. R. Beckman, C. Morgan, E. A. Daly, and M. Litz. 2013. Multivariate models of adult Pacific salmon returns. *PLOS One* 8:e54134.

- Chan, F., J. A. Barth, J. Lubchenco, A. Kirincich, H. Weeks, W. T. Peterson, and B. A. Menge. 2008. Emergence of anoxia in the California current large marine ecosystem. *Science* 319:920.
- DeVries, P. 1997. Riverine salmonid egg burial depths: Review of published data and implications for scour studies. *Canadian Journal of Fisheries and Aquatic Sciences* 54:1685–1698.
- Dyson, K., and D. D. Huppert. 2010. Regional economic impacts of razor clam beach closures due to harmful algal blooms (HABs) on the Pacific coast of Washington. *Harmful Algae* 9:264–271.
- EPAP (Ecosystem Principles Advisory Panel). 1999. Ecosystem-based fishery management: A report to Congress by the Ecosystem Principles Advisory Panel. National Marine Fisheries Service, Washington, D.C.
- Feely, R. A., R. R. Okazaki, W. J. Cai, N. Bednarsek, S. R. Alin, R. H. Byrne, and A. Fassbender. 2018. The combined effects of acidification and hypoxia on pH and aragonite saturation in the coastal waters of the California current ecosystem and the northern Gulf of Mexico. *Continental Shelf Research* 152:50–60.
- Feely, R. A., C. L. Sabine, J. M. Hernandez-Ayon, D. Ianson, and B. Hales. 2008. Evidence for upwelling of corrosive “acidified” water onto the continental shelf. *Science* 320:1490–1492.
- Fisher, M. C., S. K. Moore, S. L. Jardine, J. R. Watson, and J. F. Samhuri. 2021. Climate shock effects and mediation in fisheries. *Proceedings of the National Academy of Sciences* 118:e2014379117.
- Fisher, J. L., W. T. Peterson, and R. R. Rykaczewski. 2015. The impact of El Niño events on the pelagic food chain in the northern California Current. *Global Change Biology* 21:4401–4414.
- FitzGerald, A. M., S. N. John, T. M. Apgar, N. J. Mantua, and B. T. Martin. 2021. Quantifying thermal exposure for migratory riverine species: Phenology of Chinook salmon populations predicts thermal stress. *Global Change Biology*, 27(3):536–549.
- Fluharty, D., M. Abbott, R. Davis, M. Donahue, S. Madsen, T. Quinn, J. Rice, and J. Sutinen. 2006. Evolving an ecosystem approach to science and management throughout NOAA and its partners: A report to the NOAA Science Advisory Board.
- Frawley, T. H., B. A. Muhling, S. Brodie, M. C. Fisher, D. Tommasi, G. Le Fol, E. L. Hazen, S. S. Stohs, E. M. Finkbeiner, and M. G. Jacox. 2021. Changes to the structure and function of an albacore fishery reveal shifting social–ecological realities for Pacific Northwest fishermen. *Fish and Fisheries* 22:280–297.
- Friedman, W. R., B. T. Martin, B. K. Wells, P. Warzybok, C. J. Michel, E. M. Danner, and S. T. Lindley. 2019. Modeling composite effects of marine and freshwater processes on migratory species. *Ecosphere* 10:e02743.
- Fuller, E. C., J. F. Samhuri, J. S. Stoll, S. A. Levin, and J. R. Watson. 2017. Characterizing fisheries connectivity in marine social–ecological systems. *ICES Journal of Marine Science* 74:2087–2096.
- Greene, C. M., D. W. Jensen, G. R. Pess, and E. A. Steel. 2005. Effects of environmental conditions during stream, estuary, and ocean residency on Chinook salmon return rates in the Skagit River, Washington. *Transactions of the American Fisheries Society* 134:1562–1581.
- Hall, J.E., C. M. Greene, O. Stefankiv, J. H. Anderson, B. Timpane-Padgham, T. J. Beechie, and G. R. Pess. 2018. Large river habitat complexity and productivity of Puget Sound Chinook salmon. *PLoS One* 13(11):e0205127.
- Harvey, C., N. Garfield, E. Hazen, and G. Williams, editors. 2014. *The California Current Integrated Ecosystem Assessment: Phase III report*. U.S. Department of Commerce, NOAA. Available: www.noaa.gov/iea/CCIEA-Report/index (July 2021).

- Harvey, C., N. Garfield, G. Williams, K. Andrews, C. Barceló, K. Barnas, S. Bograd, R. Brodeur, B. Burke, J. Cope, L. deWitt, J. Field, J. Fisher, C. Greene, T. Good, E. Hazen, D. Holland, M. Jacox, S. Kasperski, S. Kim, A. Leising, S. Melin, C. Morgan, S. Munsch, K. Norman, W. T. Peterson, M. Poe, J. Samhuri, I. Schroeder, W. Sydeman, J. Thayer, A. Thompson, N. Tolimieri, A. Varney, B. Wells, T. Williams, and J. Zamon. 2017. Ecosystem status report of the California Current for 2017: A summary of ecosystem indicators compiled by the California Current Integrated Ecosystem Assessment Team (CCIEA). U.S. Department of Commerce, NOAA Technical Memorandum NMFS-NWFSC-139.
- Harvey, C., N. Garfield, G. Williams, N. Tolimieri, K. Andrews, K. Barnas, E. Bjorkstedt, S. Bograd, J. Borchert, C. Braby, R. Brodeur, B. Burke, J. Cope, A. Coyne, D. Demer, L. deWitt, J. Field, J. Fisher, P. Frey, T. Good, C. Grant, C. Greene, E. Hazen, D. Holland, M. Hunter, K. Jacobson, M. Jacox, J. Jahncke, C. Juhasz, I. Kaplan, S. Kasperski, S. Kim, D. Lawson, A. Leising, A. Manderson, N. Mantua, S. Melin, R. Miller, S. Moore, C. Morgan, B. Muhling, S. Munsch, K. Norman, J. Parrish, A. Phillips, R. Robertson, D. Rudnick, K. Sakuma, J. Samhuri, J. Santora, I. Schroeder, S. Siedlecki, K. Somers, B. Stanton, K. Stierhoff, W. Sydeman, A. Thompson, D. Trong, P. Warzybok, C. Whitmire, B. Wells, M. Williams, T. Williams, J. Zamon, S. Zeman, V. Zubkousky-White, and J. Zwolinski. 2020. Ecosystem status report of the California Current for 2019-20: a summary of ecosystem indicators compiled by the California Current Integrated Ecosystem Assessment Team (CCIEA). U.S. Department of Commerce, NOAA Technical Memorandum NMFS-NWFSC-160.
- Harvey, C., T. Garfield, G. Williams, and N. Tolimieri, editors. 2021. California Current Integrated Ecosystem Assessment (CCIEA) California Current ecosystem status report, 2021, Report to the Pacific Fishery Management Council. Available: <https://www.pcouncil.org/documents/2021/02/i-1-a-iea-team-report-1.pdf/>; <https://www.pcouncil.org/documents/2021/02/i-1-a-iea-team-report-2.pdf/> (June 2021).
- Hobday, A. J., L. V. Alexander, S. E. Perkins, D. A. Smale, S. C. Straub, E. C. J. Oliver, J. A. Benthuisen, M. T. Burrows, M. G. Donat, M. Peng, N. J. Holbrook, P. J. Moore, H. A. Scannell, A. Sen Gupta, and T. Wernberg. 2016. A hierarchical approach to defining marine heatwaves. *Progress in Oceanography* 141:227–238.
- Hodgson, E. E., I. C. Kaplan, K. N. Marshall, J. Leonard, T. E. Essington, D. S. Busch, E. A. Fulton, C. J. Harvey, A. J. Hermann, and P. McElhany. 2018. Consequences of spatially variable ocean acidification in the California Current: Lower pH drives strongest declines in benthic species in southern regions while greatest economic impacts occur in northern regions. *Ecological Modelling* 383:106–117.
- Huang, B., C. Liu, V. Banzon, E. Freeman, G. Graham, B. Hankins, T. Smith, and H.-M. Zhang. 2021. Improvements of the daily optimum interpolation sea surface temperature (DOISST) version 2.1. *Journal of Climate* 34:2923–2939.
- Jacox, M. G., M. A. Alexander, S. J. Bograd, and J. D. Scott. 2020. Thermal displacement by marine heatwaves. *Nature* 584:82–86. DOI: 10.1038/s41586-020-2534-z
- Jacox, M. G., C. A. Edwards, E. L. Hazen, and S. J. Bograd. 2018. Coastal upwelling revisited: Ekman, Bakun, and improved upwelling indices for the US West Coast. *Journal of Geophysical Research—Oceans* 123:7332–7350.
- Jacox, M. G., E. L. Hazen, and S. J. Bograd. 2016. Optimal environmental conditions and anomalous ecosystem responses: Constraining bottom-up controls of phytoplankton biomass in the California Current System. *Scientific Reports* 6:27612.
- Jager, H. I., H. E. Cardwell, M. J. Sale, M. S. Bevelhimer, C. C. Coutant, and W. Van Winkle. 1997. Modelling the linkages between flow management and salmon recruitment in rivers. *Ecological Modelling* 103:171–191.

- Jeffries, K. M., S. G. Hinch, T. Sierocinski, T. D. Clark, E. J. Eliason, M. R. Donaldson, S. R. Li, P. Pavlidis, and K. M. Miller. 2012. Consequences of high temperatures and premature mortality on the transcriptome and blood physiology of wild adult sockeye salmon (*Oncorhynchus nerka*). *Ecology and Evolution* 2:1747–1764.
- Jepson, M., and L. L. Colburn. 2013. Development of social indicators of fishing community vulnerability and resilience in the U.S. Southeast and Northeast regions. U.S. Department of Commerce, NOAA Technical Memorandum NMFS-F/SPO-129.
- Jordan, M. S. 2012. Hydraulic predictors and seasonal distribution of *Manayunkia speciosa* density in the Klamath River, CA, with implications for ceratomyxosis, a disease of salmon and trout. MS thesis, Oregon State University.
- Kaplan, I. C., G. D. Williams, N. A. Bond, A. J. Hermann, and S. A. Siedlecki. 2016. Cloudy with a chance of sardines: Forecasting sardine distributions using regional climate models. *Fisheries Oceanography* 25:15–27.
- Kasperski, S., and D. S. Holland. 2013. Income diversification and risk for fishermen. *Proceedings of the National Academy of Sciences of the United States of America* 110:2076–2081.
- Keister, J. E., E. Di Lorenzo, C. A. Morgan, V. Combes, and W. T. Peterson. 2011. Zooplankton species composition is linked to ocean transport in the Northern California Current. *Global Change Biology* 17:2498–2511.
- Keller, A. A., J. R. Wallace, and R. D. Methot. 2017. The Northwest Fisheries Science Center’s West Coast Groundfish Bottom Trawl Survey: History, design and description. U.S. Department of Commerce, NOAA Technical Memorandum NMFS-NWFSC-136.
- Kershner, J., J. F. Samhuri, C. A. James, and P. S. Levin. 2011. Selecting indicator portfolios for marine species and food webs: A Puget Sound case study. *PLoS ONE* 6:e25248.
- Kroetz, K., M. N. Reimer, J. N. Sanchirico, D. K. Lew, and J. Huettelman. 2019. Defining the economic scope for ecosystem-based fishery management. *Proceedings of the National Academy of Sciences* 116:4188–4193.
- Laake, J. L., M. S. Lowry, R. L. DeLong, S. R. Melin, and J. V. Carretta. 2018. Population growth and status of California sea lions. *Journal of Wildlife Management* 82:583–595.
- Lasker, R. 1978. The relation between oceanographic conditions and larval anchovy food in the California Current: Identification of factors contributing to recruitment failure. *Rapports et procès-verbaux des réunions, Conseil Permanent International pour l’Exploration de la Mer* 173:212–230.
- Lefebvre, K. A., S. Bargu, T. Kieckhefer, and M. W. Silver. 2002. From sanddabs to blue whales: The pervasiveness of domoic acid. *Toxicon* 40:971–977.
- Leising, A. W. In revision. Marine heatwaves of the northeast Pacific from 1982–2020: A Blobtrospective. *Journal of Geophysical Research: Oceans*.
- Leonard, J., and P. Watson. 2011. Description of the input–output model for Pacific Coast fisheries. U.S. Department of Commerce, NOAA Technical Memorandum NMFS-NWFSC-111.
- Levin, P. S., M. J. Fogarty, G. C. Matlock, and M. Ernst. 2008. Integrated ecosystem assessments. U.S. Department of Commerce, NOAA Technical Memorandum, NMFS-NWFSC-92.
- Levin, P. S., M. J. Fogarty, S. A. Murawski, and D. Fluharty. 2009. Integrated ecosystem assessments: developing the scientific basis for ecosystem-based management of the ocean. *PLoS Biology* 7:23–28.
- Levin, P. S., and F. B. Schwing, editors. 2011. Technical background for an integrated ecosystem assessment of the California Current: Groundfish, salmon, green sturgeon, and ecosystem health. U.S. Department of Commerce, NOAA Technical Memorandum NMFS-NWFSC-109.

- Levin, P. S., B. K. Wells, and M. B. Sheer, editors. 2013. California Current Integrated Ecosystem Assessment: Phase II Report. Available: www.integratedecosystemassessment.noaa.gov/regions/california-current/cc-publications-reports/phaseIIreport2012 (July 2021).
- Levin, P. S., S. J. Breslow, C. J. Harvey, K. C. Norman, K. C., M. R. Poe, G. D. Williams, and M. L. Plummer. 2016. Conceptualization of social–ecological systems of the California current: An examination of interdisciplinary science supporting ecosystem-based management. *Coastal Management* 44(5):397–408.
- Limm, M. P., and M. P. Marchetti. 2009. Juvenile Chinook salmon (*Oncorhynchus tshawytscha*) growth in offchannel and main-channel habitats on the Sacramento River, CA, using otolith increment widths. *Environmental Biology of Fishes* 85:141–151.
- Lindgren, F., and H. Rue. 2015. Bayesian spatial modelling with R-INLA. *Journal of Statistical Software* 63:1–25.
- Link, J. 2017. A conversation about NMFS' Ecosystem-Based Fisheries Management Policy and Road Map. *Fisheries* 42:498–503.
- Lloyd's Register, QinetiQ, and University of Strathclyde. 2013. Global marine trends 2030. Available: www.lr.org/en-us/insights/global-marine-trends-2030/ (July 2021).
- Long, R., A. Charles, and R. Stephenson. 2015. Key principles of marine ecosystem-based management. *Marine Policy* 57:53–60.
- Marine, K. R., and J. J. Cech. 2004. Effects of high water temperature on growth, smoltification, and predator avoidance in Juvenile Sacramento River Chinook salmon. *North American Journal of Fisheries Management* 24:198–210.
- Marshall, K. N., I. C. Kaplan, E. E. Hodgson, A. Hermann, D. S. Busch, P. McElhany, T. E. Essington, C. J. Harvey, and E. A. Fulton. 2017. Risks of ocean acidification in the California Current food web and fisheries: Ecosystem model projections. *Global Change Biology* 23:1525–1539.
- McCabe, R. M., B. M. Hickey, R. M. Kudela, K. A. Lefebvre, N. G. Adams, B. D. Bill, F. M. D. Gulland, R. E. Thomson, W. P. Cochlan, and V. L. Trainer. 2016. An unprecedented coastwide toxic algal bloom linked to anomalous ocean conditions. *Geophysical Research Letters* 43:10366–10376.
- McClatchie, S. 2014. Regional fisheries oceanography of the California Current system. Springer, Dordrecht, Germany.
- McFadden, K., and C. Barnes. 2009. The implementation of an ecosystem approach to management within a federal government agency. *Marine Policy* 33:156–163.
- McKibben, S. M., W. Peterson, M. Wood, V. L. Trainer, M. Hunter, and A. E. White. 2017. Climatic regulation of the neurotoxin domoic acid. *Proceedings of the National Academy of Sciences* 114:239–244.
- Melin, S. R., A. J. Orr, J. D. Harris, J. L. Laake, and R. L. DeLong. 2012. California sea lions: An indicator for integrated ecosystem assessment of the California Current system. *California Cooperative Oceanic Fisheries Investigations Reports* 53:140–152.
- Miller, R. R., J. A. Santora, T. D. Auth, K. M. Sakuma, B. K. Wells, J. C. Field, and R. D. Brodeur. 2019. Distribution of pelagic thaliaceans, *Thetys vagina* and *Pyrosoma atlanticum*, during a period of mass occurrence within the California Current Large Marine Ecosystem. *CalCOFI Reports* 60:94–108.
- Miller, J. A., D. J. Teel, A. Baptista, and C. A. Morgan. 2013. Disentangling bottom-up and top-down effects on survival during early ocean residence in a population of Chinook salmon (*Oncorhynchus tshawytscha*). *Canadian Journal of Fisheries and Aquatic Sciences* 70:617–629.
- Moore, S. K., M. R. Cline, K. Blair, T. Klinger, A. Varney, and K. Norman. 2019. An index of fisheries closures due to harmful algal blooms and a framework for identifying vulnerable fishing communities on the US West Coast. *Marine Policy* 110:103543.

- Morgan, C., B. Beckman, L. Weitkamp, and K. L. Fresh. 2019. Recent ecosystem disturbance in the northern California Current. *Fisheries* 44:465–474.
- Morley, J. W., R. L. Selden, R. J. Latour, T. L. Frölicher, R. J. Seagraves, and M. L. Pinsky. 2018. Projecting shifts in thermal habitat for 686 species on the North American continental shelf. *PLoS ONE* 13:e0196127.
- Moser, H. G., and W. Watson. 2006. Ichthyoplankton. Pages 269–319 in: L. G. Allen, D. J. Pondella, and M. H. Horn, eds. *The ecology of marine fishes: California and adjacent waters*. University of California Press, Berkeley, California.
- Munsch, S., C. Greene, R. Johnson, W. Satterthwaite, H. Imaki, and P. Brandes. 2019. Warm, dry winters truncate timing and size distribution of seaward-migrating salmon across a large, regulated watershed. *Ecological Applications* 29:e01880.
- Munsch, S. H., C. M. Greene, R. C. Johnson, W. H. Satterthwaite, H. Imaki, P. L. Brandes, and M. R. O'Farrell. 2020. Science for integrative management of a diadromous fish stock: Interdependencies of fisheries, flow, and habitat restoration. *Canadian Journal of Fisheries and Aquatic Sciences* 77:1487–1504.
- Neveu, E., A. M. Moore, C. A. Edwards, J. Fiechter, P. Drake, W. J. Crawford, M. G. Jacox, and E. Nuss. 2016. An historical analysis of the California Current circulation using ROMS 4D-Var: System configuration and diagnostics. *Ocean Modelling* 99:133–151.
- NMFS (National Marine Fisheries Service). 2016. Fisheries of the United States, 2015. National Marine Fisheries Service, Silver Spring, Maryland. Available: www.st.nmfs.noaa.gov/Assets/commercial/fus/fus15/documents/FUS2015.pdf (July 2021).
- NMFS (National Marine Fisheries Service). 2021. West coast fisheries impacts from COVID-19. National Marine Fisheries Service, Silver Spring, Maryland.
- NOAA (National Oceanic and Atmospheric Administration). 2016. Ecosystem-based fisheries management policy of the National Marine Fisheries Service. National Oceanic and Atmospheric Administration, Silver Spring, Maryland. Available: www.fisheries.noaa.gov/resource/document/ecosystem-based-fisheries-management-policy (July 2021).
- NOAA (National Oceanic and Atmospheric Administration). 2020. 2019 West Coast whale entanglement summary. National Oceanic and Atmospheric Administration, Silver Spring, Maryland. Available: www.fisheries.noaa.gov/resource/document/2019-west-coast-whale-entanglement-summary (July 2021).
- Nye, J. A., J. S. Link, J. Hare, and W. J. Overholtz. 2009. Changing spatial distribution of fish stocks in relation to climate and population size on the Northeast United States continental shelf. *Marine Ecology Progress Series* 393:111–129.
- Perry, R. W., P. L. Brandes, J. R. Burau, A. P. Klimley, B. MacFarlane, C. Michel, and J.vR. Skalski. 2013. Sensitivity of survival to migration routes used by juvenile Chinook salmon to negotiate the Sacramento–San Joaquin River Delta. *Environmental Biology of Fishes* 96(2):381–392.
- Peterson, W. T., J. L. Fisher, J. O. Peterson, C. A. Morgan, B. J. Burke, and K. L. Fresh. 2014. Applied fisheries oceanography ecosystem indicators of ocean condition inform fisheries management in the California Current. *Oceanography* 27:80–89.
- PFMC (Pacific Fishery Management Council). 2013. Pacific Coast Fishery Ecosystem Plan for the U.S. portion of the California Current large marine ecosystem. Pacific Fishery Management Council, Portland, Oregon.
- PFMC (Pacific Fishery Management Council). 2016. Pacific Coast Salmon Fishery Management Plan for commercial and recreational salmon fisheries off the coasts of Washington, Oregon, and California as amended through Amendment 19. Pacific Fishery Management Council, Portland, Oregon.

- PFMC (Pacific Fishery Management Council). 2019a. Status of the Pacific Coast coastal pelagic species fishery and recommended acceptable biological catches. Stock assessment and fishery evaluation for 2018. Pacific Fishery Management Council, Portland, Oregon.
- PFMC (Pacific Fishery Management Council). 2019b. Salmon rebuilding plan for Sacramento River fall Chinook. Pacific Fishery Management Council, Portland, Oregon.
- PFMC (Pacific Fishery Management Council). 2019c. Salmon rebuilding plan for Klamath River fall Chinook. Pacific Fishery Management Council, Portland, Oregon.
- Ralston, S., K. M. Sakuma, and J. C. Field. 2013. Interannual variation in pelagic juvenile rockfish (*Sebastes* spp.) abundance—going with the flow. *Fisheries Oceanography* 22:288–308.
- Reis, G. J., J. K. Howard, and J. A. Rosenfield. 2019. Clarifying effects of environmental protections on freshwater flows to—and water exports from—the San Francisco Bay Estuary. *San Francisco Estuary and Watershed Science* 17(1).
- Richter, A., and S. A. Kolmes. 2005. Maximum temperature limits for Chinook, coho, and chum salmon, and steelhead trout in the Pacific Northwest. *Reviews in Fisheries Science* 13:23–49.
- Ritzman, J., A. Brodbeck, S. Brostrom, S. McGrew, S. Dreyer, T. Klinger, and S. K. Moore. 2018. Economic and sociocultural impacts of fisheries closures in two fishing-dependent communities following the massive 2015 US West Coast harmful algal bloom. *Harmful Algae* 80:35–45.
- Robertson, R. R., and E. P. Bjorkstedt. 2020. Climate-driven variability in *Euphausia pacifica* size distributions off northern California. *Progress in Oceanography* 188:102412.
- Roemmich, D., and J. McGowan. 1995. Climatic warming and the decline of zooplankton in the California Current. *Science* 267:1324–1326.
- Rudnick, D. L., K. D. Zaba, R. E. Todd, and R. E. Davis. 2017. A climatology using data from the California Underwater Glider Network—Dataset. *Scripps Institution of Oceanography*. DOI: 10.21238/S8SPRAY7292
- Sainsbury, K., P. Gullestad, and J. Rice. 2014. The use of national frameworks for sustainable development of marine fisheries and conservation, ecosystem-based management and integrated ocean management. Pages 301–316 in S. M. Garcia, J. Rice, and A. Charles, editors. *Governance of Marine Fisheries and Biodiversity Conservation: Interaction and Coevolution*. John Wiley & Sons, West Sussex, U.K.
- Sakuma, K. M., J. C. Field, N. J. Mantua, S. Ralston, B. B. Marinovic, and C. N. Carrion. 2016. Anomalous epipelagic micronekton assemblage patterns in the neritic waters of the California Current in spring 2015 during a period of extreme ocean conditions. *California Cooperative Oceanic Fisheries Investigations Reports* 57:163–183.
- Samhuri, J. F., A. J. Haupt, P. S. Levin, J. S. Link, and R. Shuford. 2014. Lessons learned from developing integrated ecosystem assessments to inform marine ecosystem-based management in the USA. *ICES Journal of Marine Science* 71(5):1205–1215.
- Samhuri, J. F., K. S. Andrews, G. Fay, C. J. Harvey, E. L. Hazen, S. M. Hennessey, K. Holsman, M. E. Hunsicker, S. I. Large, K. N. Marshall, and A. C. Stier. 2017. Defining ecosystem thresholds for human activities and environmental pressures in the California Current. *Ecosphere* 8:e01860.
- Santora, J. A., N. J. Mantua, I. D. Schroeder, J. C. Field, E. L. Hazen, S. J. Bograd, W. J. Sydeman, B. K. Wells, J. Calambokidis, L. Saez, D. Lawson, and K. A. Forney. 2020. Habitat compression and ecosystem shifts as potential links between marine heatwave and record whale entanglements. *Nature Communications* 11:536.
- Satterthwaite, W. H., S. M. Carlson, S. D. Allen-Moran, S. Vincenzi, S. J. Bograd, and B. K. Wells. 2014. Match–mismatch dynamics and the relationship between ocean-entry timing and relative ocean recoveries of Central Valley fall run Chinook salmon. *Marine Ecology Progress Series* 511:237–248.

- Selden, R. L., J. T. Thorson, J. F. Samhuri, S. J. Bograd, S. Brodie, G. Carroll, M. A. Haltuch, E. L. Hazen, K. K. Holsman, M. L. Pinsky, N. Tolimieri, and E. Willis-Norton. 2020. Coupled changes in biomass and distribution drive trends in availability of fish stocks to US West Coast ports. *ICES Journal of Marine Science* 77:188–199.
- Siedlecki, S. A., I. C. Kaplan, A. J. Hermann, T. T. Nguyen, N. A. Bond, J. A. Newton, G. D. Williams, W. T. Peterson, S. R. Alin, and R. A. Feely. 2016. Experiments with seasonal forecasts of ocean conditions for the northern region of the California Current upwelling system. *Scientific Reports* 6:27203.
- Slater, W., G. DePiper, J. Gove, C. Harvey, E. Hazen, S. Lucey, M. Karnauskas, S. Regan, E. Siddon, E. Yasumiishi, S. Zador, M. Brady, M. Ford, R. Griffis, R. Shuford, H. Townsend, T. O'Brien, J. Peterson, K. Osgood, and J. Link. 2017. Challenges, opportunities and future directions to advance NOAA Fisheries ecosystem status reports (ESRs): Report of the National ESR Workshop. U.S. Department of Commerce, NOAA Technical Memorandum NMFS-F/SPO-174.
- Speir, C., and M. Lee. 2021. Geographic distribution of commercial fishing landings and port consolidation following ITQ implementation. *Journal of Agricultural and Resource Economics* 46:152–169.
- Strange, J. S. 2012. Migration strategies of adult Chinook salmon runs in response to diverse environmental conditions in the Klamath River basin. *Transactions of the American Fisheries Society* 141:1622–1636.
- Sturrock, A. M., W. H. Satterthwaite, K. M. Cervantes-Yoshida, E. R. Huber, H. J. Sturrock, S. Nusslé, and S. M. Carlson. 2019. Eight decades of hatchery salmon releases in the California Central Valley: Factors influencing straying and resilience. *Fisheries* 44:433–444.
- Sykes, G. E., C. J. Johnson, and J. M. Shrimpton. 2009. Temperature and flow effects on migration timing of Chinook salmon smolts. *Transactions of the American Fisheries Society* 138:1252–1265.
- Theil, H. 1967. *Economics and information theory*. Rand McNally, Chicago.
- Thompson, A., C. Harvey, W. Sydeman, C. Barceló, S. Bograd, R. Brodeur, J. Fiechter, J. Field, N. Garfield, T. Good, E. Hazen, M. Hunsicker, K. Jacobson, M. Jacox, A. Leising, J. Lindsay, S. Melin, J. Santora, I. Schroeder, J. Thayer, B. Wells, and G. Williams. 2019a. Indicators of pelagic forage community shifts in the California Current large marine ecosystem, 1998–2016. *Ecological Indicators* 105:215–228.
- Thompson, A. R., I. D. Schroeder, S. J. Bograd, E. L. Hazen, M. G. Jacox, A. Leising, B. K. Wells, J. L. Largier, J. L. Fisher, K. Jacobson, S. Zeman, E. P. Bjorkstedt, R. R. Robertson, M. Kahru, R. Goericke, C. E. Peabody, T. R. Baumgartner, B. E. Lavaniegos, L. E. Miranda, E. Gomez-Ocampo, J. Gomez-Valdes, T. D. Auth, E. A. Daly, C. A. Morgan, B. J. Burke, J. C. Field, K. M. Sakuma, E. D. Weber, W. Watson, J. M. Porquez, J. Dolliver, D. E. Lyons, R. A. Orben, J. E. Zamon, P. Warzybok, J. Jahncke, J. A. Santora, S. A. Thompson, B. Hoover, W. Sydeman, and S. R. Melin. 2019b. State of the California Current 2018–19: A novel anchovy regime and a new marine heat wave? *California Cooperative Oceanic Fisheries Investigations Reports* 60:1–65.
- Thorson, J. T. 2019. Guidance for decisions using the Vector Autoregressive Spatio-Temporal (VAST) package in stock, ecosystem, habitat and climate assessments. *Fisheries Research* 210:143–161.
- True, K., A. Voss, and J. Foott. 2017. Myxosporean parasite (*Ceratonova shasta* and *Parvicapsula minibicornis*) prevalence of infection in Klamath River basin juvenile Chinook salmon, March–August 2017. U.S. Fish and Wildlife Service, California–Nevada Fish Health Center, Anderson, California.
- USOFR (U.S. Office of the Federal Register). 2016. 50 CFR Part 600: Magnuson–Stevens Act Provisions; National Standard Guidelines; Final Rule (RIN 0648-BB92). *Federal Register* 81:201(18 October 2016):71858–71904.
- Walther, Y. M., and C. Möllmann. 2014. Bringing integrated ecosystem assessments to real life: A scientific framework for ICES. *ICES Journal of Marine Science* 71:1183–1186.

- Waples, R. S. 1995. Evolutionarily significant units and the conservation of biological diversity under the Endangered Species Act. *Evolution and the Aquatic Ecosystem: Defining Unique Units in Population Conservation* 17:8–27.
- Wells, B. K., C. B. Grimes, J. G. Sneva, S. McPherson, and J. B. Waldvogel. 2008. Relationships between oceanic conditions and growth of Chinook salmon (*Oncorhynchus tshawytscha*) from California, Washington, and Alaska, USA. *Fisheries Oceanography* 17:101–125.
- Wilkerson, F. P., A. M. Lassiter, R. C. Dugdale, A. Marchi, and V. E. Hogue. 2006. The phytoplankton bloom response to wind events and upwelled nutrients during the CoOP WEST study. *Deep Sea Research Part II: Topical Studies in Oceanography* 53:3023–3048.
- Zimmerman, M. S., C. Kinsel, E. Beamer, E. J. Connor, and D. E. Pflug. 2015. Abundance, survival, and life history strategies of juvenile Chinook salmon in the Skagit River, Washington. *Transactions of the American Fisheries Society* 144:627–641.

Recently published by the Northwest Fisheries Science Center

NOAA Technical Memorandum NMFS-NWFSC-

- 169 Steiner, E., A. Vizek, M. Guldin, M. Krigbaum, and L. Pfeiffer. 2021.** Evaluating the Economic Performance of the U.S. West Coast Groundfish Trawl Catch Share Program. U.S. Department of Commerce, NOAA Technical Memorandum NMFS-NWFSC-169. <https://doi.org/10.25923/pzys-ay72>
- 168 Jacobsen, N. S., K. N. Marshall, A. M. Berger, C. J. Grandin, and I. G. Taylor. 2021.** Management Strategy Evaluation of Pacific Hake: Exploring the Robustness of the Current Harvest Policy to Spatial Stock Structure, Shifts in Fishery Selectivity, and Climate-Driven Distribution Shifts. U.S. Department of Commerce, NOAA Technical Memorandum NMFS-NWFSC-168. <https://doi.org/10.25923/x9f9-9b20>
- 167 Anderson, L., and R. Fonner. 2021.** Economic Survey of Recreational Steelhead Fishers in Washington: Methodology and Survey Results. U.S. Department of Commerce, NOAA Technical Memorandum NMFS-NWFSC-167. <https://doi.org/10.25923/gn14-f110>
- 166 Somers, K. A., J. E. Jannot, K. E. Richerson, V. J. Tuttle, N. B. Riley, and J. T. McVeigh. 2021.** Estimated Discard and Catch of Groundfish Species in U.S. West Coast Fisheries. U.S. Department of Commerce, NOAA Technical Memorandum NMFS-NWFSC-166. <https://doi.org/10.25923/z84a-w607>
- 165 Jannot, J. E., A. Wuest, T. P. Good, K. A. Somers, V. J. Tuttle, K. E. Richerson, R. S. Shama, and J. T. McVeigh. 2021.** Seabird Bycatch in U.S. West Coast Fisheries, 2002–18. U.S. Department of Commerce, NOAA Technical Memorandum NMFS-NWFSC-165. <https://doi.org/10.25923/78vk-v149>
- 164 Crozier, L. G., L. E. Wiesebron, B. J. Burke, D. Widener, and T. Marsh. 2021.** Reframing Steelhead Migration Behavior: A Population Perspective on Migration Rate and Survival Through the Columbia and Snake Rivers. U.S. Department of Commerce, NOAA Technical Memorandum NMFS-NWFSC-164. <https://doi.org/10.25923/dds5-jg64>
- 163 Jannot, J. E., K. E. Richerson, K. A. Somers, V. J. Tuttle, R. S. Shama, and J. T. McVeigh. 2021.** Pacific Halibut Bycatch in U.S. West Coast Groundfish Fisheries, 2002–19. U.S. Department of Commerce, NOAA Technical Memorandum NMFS-NWFSC-163. <https://doi.org/10.25923/8y03-z703>
- 162 Sol, S. Y., B. Anulacion, D. P. Lomax, P. Chittaro, P. Moran, G. M. Ylitalo, A. Hanson, C. Corbett, and L. L. Johnson. 2021.** Juvenile Salmon Ecology in Tidal Freshwater Wetlands in the Lower Columbia River Estuary. U.S. Department of Commerce, NOAA Technical Memorandum NMFS-NWFSC-162. <https://doi.org/10.25923/2bfz-ah24>
- 161 Clarke, M. E., E. L. Fruh, A. Powell, J. Anderson, J. C. Taylor, and C. E. Whitmire. 2020.** Autonomous Underwater Vehicle (AUV) Survey at The Footprint and Piggy Bank in the Southern California Bight, 2011. U.S. Department of Commerce, NOAA Technical Memorandum NMFS-NWFSC-161. <https://doi.org/10.25923/mfq8-6773>

NOAA Technical Memorandums NMFS-NWFSC are available from the NOAA Institutional Repository, <https://repository.library.noaa.gov>.



U.S. Secretary of Commerce
Gina M. Raimondo

Under Secretary of Commerce for
Oceans and Atmosphere
Dr. Richard W. Spinrad

Assistant Administrator for Fisheries
Janet Coit

September 2021

[fisheries.noaa.gov](https://www.fisheries.noaa.gov)

OFFICIAL BUSINESS

National Marine
Fisheries Service
Northwest Fisheries Science Center
2725 Montlake Boulevard East
Seattle, Washington 98112